

ENPH352:

Laboratory Techniques in Physics



Department of Physics and Astronomy
University of British Columbia,
Vancouver
6224 Agricultural Road
Vancouver, British Columbia
CANADA
V6T 1Z1

Created by Mario Beaudoin, Will Gunton, Tongkai Huang, Blair Jamieson, Aleksy Jones, Carl Michal, Darren Peets, Stefan A Reinsberg, and Chris Waltham, 2000-2018
Last updated 2020/01/07 22:47:26UTC

Session Specifics

Please see the course website for specific information on scheduling, marking schemes, late penalties and contact information.

Communications

One important aspect of this course is communications. To this end, each of your experiments will be presented to the instructors and your classmates. The first will be presented in the form of a scientific poster, the second will take the form of journal article, and the third in the form of a 15 minute talk. There will be details posted on the website, and we'll give more complete instructions in the course.

Contents

Contents	3
Safety Policy and Procedures	4
Introduction to the Lab	9
1 Thermal Noise	13
2 Servomechanism	17
3 Guided Microwaves	25
4 Gamma Ray Spectroscopy	31
5 Air Suspension Gyroscope	38
6 Alpha Particle Range in Air	44
7 Electromagnetic Skin Depth of Metals	49
8 NMR: Spin-Spin Coupling	52
9 Pulsed NMR	58
10 Lock-in Detection: High- T_c Superconductivity	70
11 Vacuum Systems	80
12 Fourier Transform Infrared Spectroscopy of Air and CO ₂	89
13 Absorption Band-edge Thermometry of Semiconductors	99
14 Optical Pumping of Rubidium	105
15 Water Waves	113
16 Acoustic Radiation	116
17 Acoustic Impedance	118

Department of Physics and Astronomy Safety Policy and Procedures

General Guidelines

Safety Statement

- Physics research presents a variety of technical situations involving a wide spectrum of potential hazards. Laboratory work, therefore, may involve tasks that are potentially hazardous.
- Faculty members and shop supervisors are responsible for safety in their laboratories/shops. They may delegate other qualified personnel to implement safety measures.

General Policy

- Do not perform hazardous experimental work in any research or teaching laboratory, day or night, when you are entirely alone. Make sure that someone is aware of your activity and is available to assist you in case of emergency.
- Make yourself familiar with potentially dangerous situations outlined in the safety check list below. Note: some work areas are unique hazardous situations are regulated by specific safety provisions which you should follow in addition to these guidelines.
- Members of the department are required to familiarize themselves with the Workplace Hazardous Material Information System (WHMIS) legislation and sign a statement to that effect.
- Safety Section on Legislation is located in the Physics Main Office which consists of resource material concerning Safety aspects of work, materials and procedures (resource person Bridget Hamilton). The Material Safety Data Sheets (MSDS) are located in the physics stores.
- The Physics Department Health and Safety Committee closely follows the University Policy PeA-11; provides advice and assistance on Safety matters and regularly carries out inspections of the Physics premises. Please refer to the bulletin board for the current members of the Physics Health and Safety Committee.
- All accidents must be reported to the Physics Administrative Assistant, and an accident report form must be filled out immediately.
- Students will not be issued keys until they have read the Department Safety Regulations as well as the WHMIS regulations, and have signed a statement that they will comply with these regulations. This also applies to new members of the Department.
- M.Sc. and Ph.D. theses will be accepted only after the candidates have signed a statement that they have disposed of hazardous chemicals in accordance with the safety regulations and are leaving their workplace in a safe condition.

- First Aid Kits are provided by the department and can be obtained from the Physics stores. Emergency telephone numbers are posted on the notice board and a copy can be obtained from stores for posting in your own laboratory.

Safety Checklist

Many accidents happen due to avoidable factors such as negligence, improper use of equipment and undue haste.

Evacuated or Pressurized Equipment

(See also “Cryogenic Liquids” below).

- Rotary pumps emitting oil mist should not be vented into the building.
- Pulley belts have to be properly guarded.
- Equipment containing mercury, especially pumps, gauges, etc. not in use should be safely stored. Mercury gauges and diffusion pumps should be fitted with receptacles to collect spills in the event of damage to equipment.
- Evacuated or pressurized vessels must be suitably shielded to protect personnel from implosions or explosions.
- Users of gas traps must acquaint themselves with the possible hazards (see Vacuum Hazards Departmental Safety Regulations – Appendix [Physics Main Office]).

Cryogenic Liquids

Cold fluids and solids can cause severe burns.

- Those using liquid helium must be authorized users (see list posted in Room 114), or be supervised by an authorized user.
- Cryostats must be protected by safety pressure-release valves.
- Glass dewars should be screened as far as possible to reduce risk of mechanical damage, and be protected against the hazards of implosion or explosion.
- Thermally insulated gloves and safety goggles or glasses must be worn when transferring cryogenic liquids.
- Liquid hydrogen systems can only be operated with the consent of the Department Head. (See “Liquid Hydrogen: Hazards & Precautions” – Safety Regulations). [Physics Main Office, Room 325]
- Users of cryogenic liquids must familiarize themselves with the information given in the Appendix entitled “Vacuum Hazards – Safety Regulations [Physics Main Office, Room 325]
- All students who need to obtain liquid nitrogen from the main liquid nitrogen storage tank outside Stores must obey the posted regulations and must be instructed in the proper procedures. The instructions will be arranged by the Technical Services Coordinator.

Gases

- Gas bottles must be secured to solid supports.
- Gas bottles must be kept in areas where fire and mechanical shock are at minimum risk.
- Gas cylinder regulators are serviced by Canadian Liquid Air. Do not dismantle. Do not use oil or solvents.
- Hazardous gases must not be vented inside the building.
- Hazardous gases must be disposed of after suitable pacification.
- Permission to use explosive gases must be obtained from the Department Head, and the Department Health and Safety Committee must also be advised.

High Voltage Equipment

- High voltage equipment must be mounted inside robust grounded metal enclosures.
- Instructions on shut-down procedures must be prominently displayed near the high voltage equipment and equipment must be fitted with a working safety interlock and working shut-down system.
- Make sure you are protected against dangers of accidental short circuits by wearing ear guards, goggles, etc.
- Filmchecks must be used to verify that there are no x-ray hazards.
- Checks for ozone and oxides of nitrogen must be carried out on a regular basis.

Sources of Optical and Emission Radiation

Lasers can cause severe eye damage; arc light can burn your skin.

- Arcs must be properly screened to prevent radiation burn.
- Combustion products should not be vented into the laboratories.
- Microwave diathermy units must be properly screened.
- High pressure arcs must be shielded to prevent explosion, radiation and release of poisonous gases (e.g. Quartz Halogen bulbs).
- Laser beams should be isolated from laboratory personnel – particularly important for high power infrared lasers and Q-spoiled giant pulse lasers.
- Radiation goggles must be worn for eye protection against exposure to ultraviolet rays (UV).

Fire Hazards

- All persons working in the laboratory must be familiar with the fire procedures.
- All exits, hallways, stairways and passages must be kept clear at all times and not be used as storage space.
- Devices left running unattended (especially overnight) must be fire-proof.
- Flammable liquids must be clearly labelled, stored in approved containers and limited to 1 litre for daily use. (See National Fire Code of Canada, 1963, on file in Physics Main Office, Room 325).
- Laboratories must be equipped with fire extinguishers appropriate to the hazardous materials used in the laboratory. Occupants of the laboratory must be familiar with the location and operation of the fire fighting equipment. Laboratory supervisors must advise the Health and Safety Committee of the need to upgrade or replace fire equipment.

Mechanical Hazards

Moving machinery can be dangerous.

- Unstable heavy objects must be firmly secured.
- Moving machine parts must be enclosed by suitable guards.
- Wheels and load bearing parts on trolleys, cranes, etc., must be checked for sufficient capacity when transporting heavy loads (e.g. magnets). The location and nature of such machinery must be reported to the Physics Health and Safety Committee.
- Goggles, face masks, gloves and other protective equipment must be available to all laboratory personnel using hazardous machinery such as lathes, millers, drill presses, etc.
- Walkways in laboratories must be kept clear of obstruction at all times.
- Equipment using fluids must be fitted with a conservation tray in the event of leakage.

Handling and Disposal Dangerous Substances

- Persons ordering chemicals and solvents must obtain MSDS for hazardous substances. Please refer to the WHMIS regulations.
- Make sure suitable storage space is available before ordering chemicals. Check with the appropriate codes for limits on quantities, compatibilities of substances and other requirements.
- Know the antidote and disposal methods before you use a hazardous chemical.
- Make sure antidotes for dangerous poisons and neutralizing agents for corrosive substances are kept close to where the dangerous materials are used.
- Make sure hazardous materials are labelled with permanent labels (see WHMIS) identifying the substance. Blank workplace labels are available from the Physics stores. It is required that labels also bear the owner's name and date of acquisition.

- Waste substances must be diagnosed of in accordance with the University regulations. Check with the Physics stores for the correct procedures. Arrangements can also be made with the Chemistry Department stores for disposal of these substances.
- Make sure the location of abnormally dangerous materials, and the name(s) of user(s) have been reported to the Physics Health and Safety Committee.

Radioactive Materials

- Radioactive materials must be operated in accordance with University Regulations, see Manual on Radiation Hazards Control. A copy of this report is on file in the Physics Main Office, Room 325. For the UBC Radiation Safety and Methodology Manual, see:
<http://riskmanagement.sites.olt.ubc.ca/files/2015/09/Radiation-Reference-Manual-2011.pdf>

Introduction to the Lab

What is Expected

The ENPH352 lab is designed to let students investigate concepts they have learned in their physics classes to date. The labs are all quite different and students have a choice as to which ones they want to do. Since this is a class for engineering students, some emphasis is placed upon learning various techniques. We expect you to demonstrate, through your reports, that you understand all aspects of the lab. Briefly explain the important concepts and summarize any relevant mathematics in a “Theory” section of your report.

In addition, we expect you to become confident in using computers. Many of the experiments collect data using LabView. Equipment and computer manuals are often located right at the bench, but if not, can be retrieved from the Lab Engineering Technician or Teaching Assistant. Don’t hesitate to get them out during a lab, but please remember to return them at the end of the day. For most labs, we expect a thorough computer-assisted analysis. Whenever possible, don’t just treat the programs or apparatus like a black box. Try to go through those you’re using to understand how they work, and write down what you learn. If you’re confused, just ask.

You should all have accounts on the Physics server. If you do not have one by the end of the second week, let the TA or professor know. You can access your Physics account from any terminal on campus and also from PCs with SSH software (such as those in the ENPH352 lab). You should also be able to use most webmail sites, to send your data to yourself. Do not expect to find USB ports on our computers.

Data should be graphed as it is taken, and final graphs should be done on a computer. Some of our computers have programs such as GNUplot or Mathematica installed. If you would rather use another scientific plotting program, feel free to do so. Beware of office software; excel-type chartjunk will be penalized.

Lab Notebooks

You should always write your data, observations, and calculations directly into your notebooks, and never onto scrap pieces of paper. If you are recording data and make a mistake, simply cross it out. If you make a big mistake and have an entire page of useless calculations, just draw a line through it and write OMIT and explain why you believe it’s flawed. Don’t tear out the page. If the data turn out to be of value after all (as often happens), they are easily resurrected. Remember, this is intended to be a working lab notebook. It will hopefully be relatively neat and fairly easy to follow, but it need not be perfect. We require you to record your data in pen, and white-out is forbidden. An engineer’s notebook is a legal document, and there can be no evidence of tampering. Use the unambiguous ISO date format (YYYY-MM-DD) for each entry.

You have a choice of keeping a paper notebook or an electronic notebook (a professional type with time stamps and history etc.).

If you choose paper you will need to have two softcover (yellow) lab notebooks so that you can hand in a completed lab while working on the next one.

The format and contents of your notebook are to be like a working engineer's or scientist's notebook. In it you will record all useful information about the work you have done — a brief statement of your objectives, your method for attaining them, your results in raw and reduced form (usually tabular), graphs arising from your results, your analysis and conclusions. Scientists and engineers aim at having their lab notebook communicate their work to their colleagues, supervisors, clients, and to themselves in the future when they must understand what they have done previously with as little reworking, re-analysis and confusion as possible. A good lab book can be photocopied and submitted to a client as a record of work in progress or as a preliminary version of the final report.

A working lab book evolves as your work progresses; you can move backward in the book to fill in details or augment explanations as you go, and forward to lay out a logical plan of work to be done, and how, and what mode of display of results you will use. You are strongly advised to plan and explore the experiment before the time you will actually do it. You can then come to the lab with your notebook already containing a plan of what you will do, and how. Your book could already contain tables laid out for data entry, algorithms specified for reducing the data, graph pages designed, and a checklist to ensure all experimental work has been done. If you record things in your book which you later decide to be wrong or otherwise to be ignored, that's OK — indicate this, and leave it there. Data and analysis in the logbook need to have a date associated with them, particularly if parts of the report are out of sequence.

The notebook is not a formal report. It is not glossy, typed or unnecessarily lengthy. For a client, or for completion of a research project, a well prepared final publication is necessary, but it is not necessary or done in this course. The notebook may have pasted into it graphs and other output from instruments and computers, or photocopies of valuable information from other sources. **We do not accept in your notebook any material cut, scanned, printed, or photocopied from this manual.** You may not refer to this lab manual at all, except in identifying the experiment. Your description of purpose, methods, theory, apparatus etc. must be self-contained and original, not a transcription of the manual.

To many of you the preceding discussion of notebook technique will have been an unnecessary repetition of what you already know from previous lab courses. Others may not find this so, and may wish to ask us for guidance in this technique. It is your responsibility to do so.

As with all undergraduate labs, you will do best if you arrive well prepared. Come in advance, look at the apparatus and study the manual(s). Being well prepared allows you to deal with the possibility of equipment malfunctions. If necessary, consult the available instruction manuals for the equipment beyond what is provided in this lab manual. The lab has a collection of books relating to experimental physics. And of course there is also the internet, but pay attention to the provenance of the material. In all cases: caveat emptor.

Data Analysis and Presentation of Results

An essential part of an engineering experiment is the presentation of the fully analyzed results in the form of a well prepared report for a client or prospective client (who is as likely to be within your own organization as external to it). Your lab workbook, if well done, may be considered as the preliminary state of such a report. Since time is money, engineers plan to record, analyze and display as immediately as possible the results and conclusions of the experiment. This immediate analysis and display has a second enormous virtue; it shows at once when an experiment is going wrong.

You are free to use any appropriate software tool to help in your analysis. There are several

PC-based data analysis programs on the PCs in the lab, and you are also encouraged to explore the (often more powerful) packages available on the UNIX system.

When grading the submitted lab notebooks, we will be looking, amongst other things, for:

- Entries should appear in chronological order, i.e. the order in which things were done. Do not leave spaces to be filled in later. At the end of each lab period, get your notebook initialled by your instructor or TA.
- Engineering level of presentation: orderly, easy to follow, clear and definite. Since this is a working notebook, it may well contain certain material you consider not to be taken into account. Please indicate this.
- Epitome of problem: Precise, clear statement of what is to be done in the experiment which follows. The theory or theoretical statements to be tested or established. No derivation of theory is required, only the relevant formula followed by a definition of the symbols. Also an outline of the measurements and procedures critical to the results.
- How it was done: Circuit diagrams, apparatus used, critical properties of the apparatus, relevant calibrations, settings and why they were chosen, and procedures used.
- Results obtained:
 - Unprocessed data. For large amounts of data, just give the location of the original data files and be prepared to produce them. Formulate a good scheme for naming files (e.g. including the date, your name/initials); the data file name should point to the page in your lab notebook that describes fully how the data was collected. Your lab notebook should point back to the data file name. Show summary graphs (properly labelled) of unprocessed data.
 - Reduced graphs etc. which reveal final results
 - Analysis of results — extracting the physical results from the data and an estimate of the errors
- In all labs (and homework 1) you will be required to produce publication quality graphs to display your data and communicate your results. It is difficult to generate such graphs in any spreadsheet-based application (such as Open Office, Excel, etc). Accordingly, you should use a scientific graphing program such as Gnuplot (free), Matlab, Igor, Origin, etc.
- Conclusion: including as an essential component: how did results bear on the second point.
- Abstract: We would like you get practice in the writing of proper scientific abstracts. The abstract should be the last thing you write in your book for each experiment. It should be a short, **self-contained** summary of the main results of the experiment. You can't possibly write a useful abstract until the experiments are finished, the data analyzed, and the conclusions drawn. There is plentiful advice on the web about how to do this; e.g. the AIP style manual.

Your lab book should be written at a level of completeness so that a reader who is knowledgeable in the physics of the experiment can understand what you are doing at every step. Everything you write should be written so that if you were to come back to this lab book two years from now, you would be able to use the results to write a formal report from it.

If your lab notebook is not complete, do not expect to receive a passing grade for that experiment. Consult the checklist on the course webpage before you start and before you hand your notebook in for marking.

Hints

Do not labour over something for hours. Try to figure it out yourself and if you can't, then ask for help.

You are expected to attend the lab during the allotted time for ENPH352, since the same room and equipment are used for the 4th year physics lab three afternoons a week. You **must** attend on weeks where you are to give a presentation and the week before where we will discuss and grade a draft of your presentation. However, if you do end up having 3 midterms and 6 assignments due in one week, we don't mind if you do your lab work at some other time the week before or after. You are not guaranteed access to the equipment or assistance outside your scheduled lab. If you do come in outside of the scheduled lab period, you *must* sign in and out at the front on the sheet provided. We keep track of who attends.

Challenging tasks

These are marked with a *, and we expect these tasks to cause a lot of head scratching; they will be best attempted if and when you have completed all other tasks and have time to think.

Plagiarism

While students are encouraged to talk with each other and help each other where appropriate, copying from current or pre-existing lab reports, marked or unmarked, is strictly prohibited. This is considered plagiarism, which UBC's Senate typically punishes with an 8-12 month suspension and a mark of zero in the course. The UBC Calendar discusses the evils of plagiarism at <http://students.ubc.ca/calendar/index.cfm?tree=3,54,111,959>.

N.B. We make frequent updates to the manuals; mostly changes are clarifications to experimental procedures occasioned by discussions with a current student. Always use the online version, and never trust any old copy left on computer desktops by previous students.

Finding Help

You can find the contact info of relevant TA's and professors written on the blackboard near the entrance to the laboratory, and on the course website at <http://phas.ubc.ca/~enph352/>.

Experiment 1

Thermal Noise

1.1 Purpose

1. To become familiar with the occurrence and characteristics of thermal noise.
2. To become familiar with calibration techniques.
3. To determine one of the fundamental constants in nature.

1.2 Theory

Due to the random thermal motion of the charge carriers in a material, a fluctuating potential will occur across the terminals of any device which has electrical resistance. This fluctuating potential, which is small but quite measurable, is called thermal noise or Johnson noise (after J.B. Johnson, who made the first studies of thermal noise in 1928). The mean value of the fluctuating potential is zero if averaged over a long period of time. However, the mean square value is finite and can be measured with a suitable detector.

Using general thermodynamic arguments and applying the principle of equipartition, Nyquist (1928) showed that for a pure resistance R the mean square of the noise voltage $\overline{V_n^2}$ in a frequency increment Δf about f is given by

$$\overline{V_n^2} = 4k_B T R p(f) \Delta f \quad (1.1)$$

$$p(f) = \frac{hf}{k_B T} \left\{ \frac{1}{e^{\frac{hf}{k_B T}} - 1} \right\} \quad (1.2)$$

where

$\overline{V_n^2}$ = mean square noise voltage in (volts)²

k_B = Boltzmann's constant

T = absolute temperature

R = resistance in ohms

$p(f)$ = Planck factor

Δf = bandwidth over which the measurement of $\overline{V_n^2}$ is made.

At the frequencies and temperatures encountered in this experiment $p(f)$ is very close to unity — why? — and we're left with the most common form of Nyquist's theorem:

$$\overline{V_n^2} = 4k_B T R \Delta f \quad (1.3)$$

where the noise power per unit bandwidth is independent of frequency. Noise with this type of constant power spectrum is often called "white noise."

Since the noise voltage $\sqrt{\overline{V_n^2}}$ is very small (4×10^{-7} V for $R=1000\Omega$, $T=300$ K and $\Delta f=10$ kHz), it must be amplified before it can be measured. For an amplifier whose power (V^2) gain, $G(f)$,

varies with frequency, the mean square noise voltage at the output of the amplifier, with a resistor R across the input, is

$$\overline{V_o^2} = 4k_B T R \int_0^\infty G(f) df \quad (1.4)$$

An array of three amplifiers is used in this experiment — a pre-amp, the main amplifier, and an RMS to DC converter/amplifier whose gain is controlled *indirectly* via the **INPUT RANGE CONTROL**. It is convenient at this point to collect the three gains into a single overall gain, $G(f)$. Although the various amplifiers will be treated from here on as a single black box, it's useful to know what exactly is being done to the signal, particularly if something goes wrong — since there are three separate amplifiers, there are three points where the signal can get clipped and three pieces of equipment that can overload.

Substituting into equation (1.4) and rearranging, we obtain an expression for k_B ,

$$k_B = \frac{V_{DC}^2}{4TR\gamma} \quad (1.5)$$

where V_{DC} is the output from the RMS/DC converter and γ is the gain bandwidth product, defined as:

$$\gamma = \int_0^\infty G(f) df \quad (1.6)$$

Since T can be easily measured, k_B can be determined by finding the relation between V_{DC}^2 and R , and by measuring γ . It should be emphasized that the above expression only applies if

1. the output of the system is linearly proportional to $\sqrt{\overline{V_n^2}}$ and
2. the reactive component of the resistor's impedance is negligible over the bandwidth of the amplifier.

This latter condition requires that the upper frequency cut-off not be too high, allowing the gain to approach zero before this effect kicks in.

The gain of the system at a given frequency is given by:

$$G(f) = \left(\frac{V_{out}}{V_{in}} \right)^2 \quad (1.7)$$

where V_{out} ($=V_{DC}$) is the voltage out of the RMS to DC converter given an RMS input voltage V_{in} . V_{out} can be easily measured, but since V_{in} is very small, it cannot be directly measured. It can, however, be calculated if one uses a calibrated attenuator.

1.3 Procedure

The electronic system used in this experiment consists of a pre-amplifier (small “brass” box) with a gain of ≈ 200 , connected to a main unit containing a power amplifier with adjustable gain, a filter used to set the pass band, followed by an RMS to DC converter, whose conversion gain can be set indirectly via the **INPUT RANGE CONTROL** lever.

The unit should be turned on and given at least 5-10 minutes to warm up before taking any data. While the amplifier is warming up you should familiarize yourself with the settings and be

sure you can answer the following questions before proceeding to the next step. The accuracy of this experiment depends on your knowledge of the amplifier and converter system and on your understanding of what you are trying to measure.

Connect the signal generator through an attenuator to the amplifier input and view the **AC MONITOR** on the oscilloscope. Set the attenuator to reduce the source voltage to a level enough above the noise level to be distinguishable from it, yet low enough that you don't overload the amplifier — typical settings are between 60 and 110 dB, depending on what you choose as an input voltage. Adjust the attenuator and try varying the frequency and amplitude of the signal generator. TRY NOT TO OVERLOAD THE AMPLIFIER.

What happens to the voltage response at high and low frequencies?

Why do you think it does this?

How linear is this amplifier?

What does it do with signals that are too large?

Try changing the settings and observe the results. What happens to the output when you change the bandwidth, gain and range?

When selecting the settings to be used for the actual experiment, you should recognize that the same settings are used for the whole lab. Therefore it is crucial that you choose appropriate settings. Spend some time testing the different settings keeping these requirements in mind:

- The signal must be amplified enough so that you can measure the noise voltages of the resistors
- You must be able to measure and integrate the complete gain curve (zero to infinity) using the available apparatus
- High frequencies should be avoided, since the load begins to have significant reactive components.

Task 1: Measurement of Noise Voltage

*****Warning:** Connecting the oscilloscope changes the data — only connect the scope for troubleshooting, never when taking data.

1. Connect the various resistances (ranging up to 10 k Ω) across the pre-amplifier input, and measure the noise level with the DMM connected across the **DC OUTPUT** of the amplifier.
2. Plot your V_{DC} vs. R data to get a relationship you can use when calculating k_B . Why did the voltmeter not read zero when R was zero?

Task 2: Measurement of $G(f)$

*****Warning:** The DC output will likely change when the **AC MONITOR** or signal generator is connected to the oscilloscope. If this happens, take data with the **AC MONITOR** disconnected and, to avoid clipping, just watch that the current doesn't exceed 80 μA on the analog dial meter.

1. To avoid reflections, BNC lines carrying variable-frequency AC require 50 Ω terminations, which are built into many (but not all) devices' BNC connections. You will need to make sure your lines are properly terminated. You can assume that the input impedance of the amplifier system is very high.

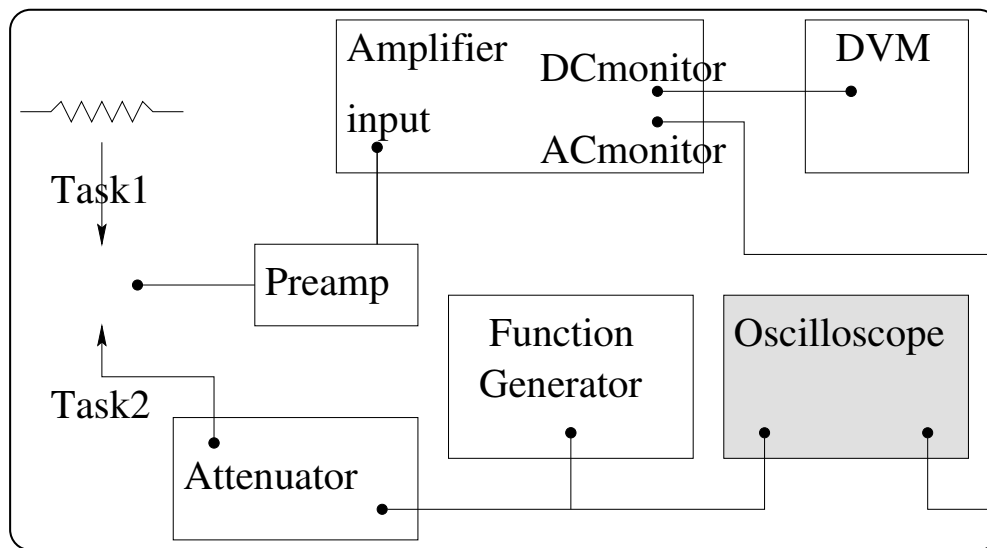


Figure 1.1: A block diagram of the thermal noise apparatus.

2. Making sure not to overload the amplifier or clip the signal, determine a value for $G(f)$ over the entire range of frequencies. Take enough data to resolve the shape of $G(f)$ so you can accurately determine γ .
3. Do some more-rigorous measurements of $G(f)$ at a few representative frequencies by fixing the frequency and attenuation and then plotting V_{out}^2 vs V_{in}^2 . Why is this method more rigorous?
4. Determine γ , and therefore a value for Boltzmann's constant, using the results from Task 1.
5. (Optional) As a good exercise you should also construct a Bode plot to see how closely the -3 dB drop from the peak gain relates to the frequency cutoff points.

Experiment 2

Servomechanism

2.1 Purpose

1. To construct and study a closed loop servo system.

2.2 Theory

In an automatic control system we are able, by means of transducers, to compare the actual output (shaft position, flow rate, etc.) with the output required. The system must be able, if there is a difference or error, to respond by modifying the signals sent to an actuator. Because this system feeds back information about the actual state for comparison with the desired state, it is called a closed-loop system. In this experiment you will be studying speed and position control, so the transducers used will be a tachogenerator and a rotary potentiometer. The actuator that you will be controlling is a motor. Most of your voltage supply and measuring needs will be met by an analogue-to-digital card, controlled under LabView.

A servomechanism is (usually) an electromechanical analogue of an amplifier (it can be operated by other than electrical means — e.g. fluidic servos and amplifiers). The analogy lies in the equations of motion governing the dynamics of such systems and the uses to which they are put.

The same equations apply to the electromechanical servo as to an electronic amplifier, and the same difficulties apply; large forward gains are required to minimize the error signal, but large forward gains coupled with requirements for high frequency response lead to instability of the system. The same analysis holds and the same cures are applied. Additional complexities arise in mechanical systems, where two types of friction are present: Coulomb (independent of speed) and viscous (proportional to speed). Viscous friction is analogous to ohmic resistance, but Coulomb friction is difficult to mimic — it's like the forward resistance of a diode.

2.3 Procedure

There is an extensive equipment manual/write-up available which describes various measurements that illustrate the properties of the servo system. The write up is wordy and covers far more work than you could possibly hope to do in the time available. However, you may wish to peruse it and try some of its exercises in order to help you with this lab.

Task 1 — Operational Amplifier

The operational amplifier is a high-gain, low-drift DC amplifier, and is designed to be independent of variations in the power supply voltage. The advantage of an amplifier with a very high gain, up to 10^6 , is that it can be used to perform mathematical operations with a high degree of accuracy. In this lab, two types of operational amplifier (OU150A and PA150C) are used.

1. OU150A is used as an adder or subtractor (inputs of opposite polarity) in this lab. Using the circuit shown in Fig. 2.1, verify that the OU150A with negative feedback has the property

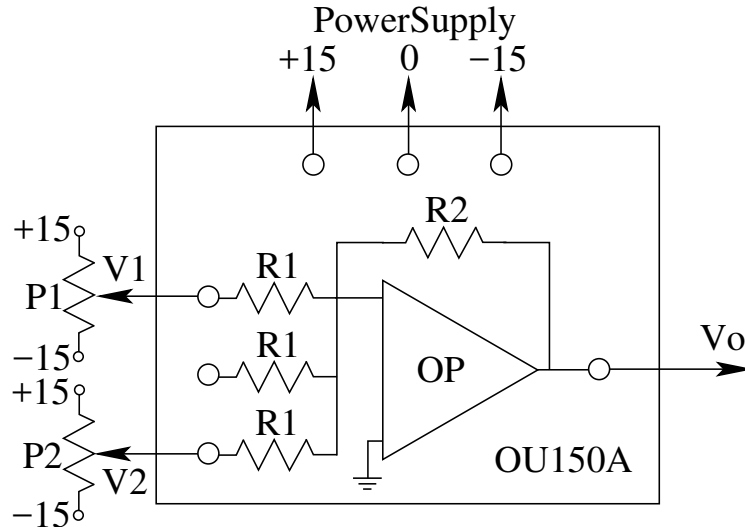


Figure 2.1: Use of the OU150A op amp. $R_1 = R_2 = 100\text{k}\Omega$.

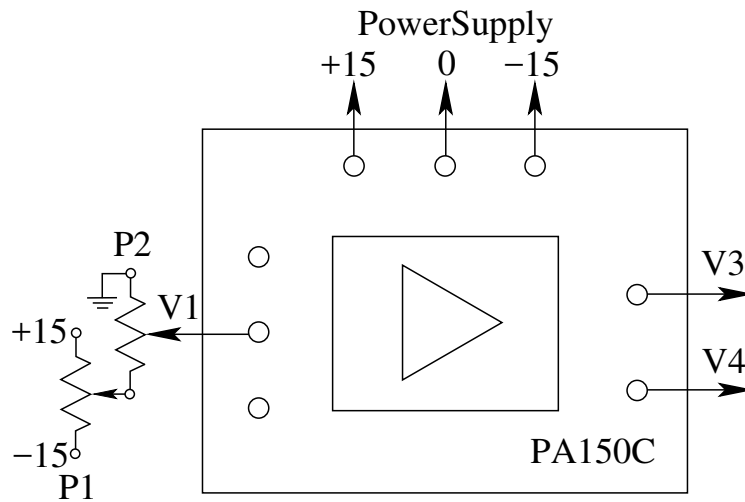


Figure 2.2: Use of the PA150C pre-amp.

that

$$V_o = -\frac{R_2}{R_1}(V_1 + V_2) = -(V_1 + V_2). \quad (2.1)$$

Applying different values of both positive and negative voltage for V_1 and V_2 , measure the output V_o . Plot a graph of the input voltage ($V_1 + V_2$) versus the output V_o . Determine the range of input (sum) voltages over which the OU150A responds linearly.

2. The output of the OU150A can be either positive or negative, but we cannot use this polarity to control the direction of motor rotation using the servo amplifier SA150D directly. The pre-amplifier PA150C solves this problem. Using the circuit shown in Fig. 2.2, graph V_3 , V_4 and $(V_3 - V_4)$ against input voltage V_1 . Calculate the gain of the PA150C, and determine its input voltage range. Double the input signal by connecting PA150C terminals 1 and 2 (this

means 1 and 4 on the box) — what is the output voltage now?

Task 2 — Tachometer Calibration

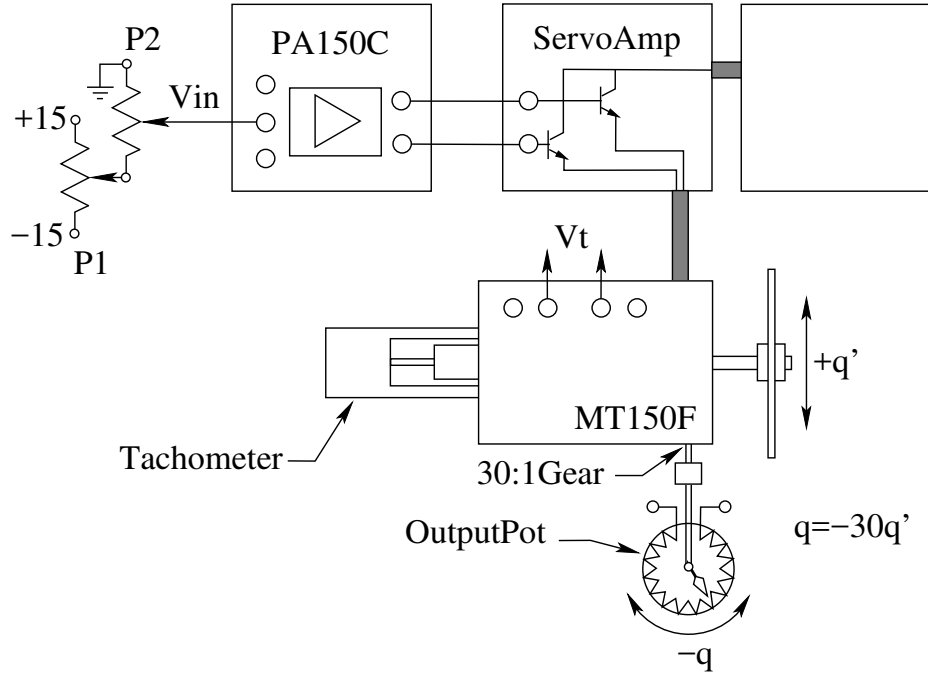


Figure 2.3: Setup for Task 2.

Set up the circuit shown in Fig. 2.3 (Power supply connections for +15, common, and -15 are not shown in this or subsequent diagrams).

The tachometer is a DC electrical generator which produces an output voltage V_t ,

$$V_t = k_t \frac{d\theta'}{dt} \quad (2.2)$$

where θ' is the angular position of the Output Pot, in radians.

1. Determine k_t by varying V_{in} (both polarities). Why does the motor stop when $|V_{in}|$ is less than a certain value?

Task 3 — Motor Transient Response

For any rotational system, we have a dynamic equation

$$I \frac{d^2\theta}{dt^2} = \tau, \quad (2.3)$$

where I is the moment of inertia of the system and τ is the torque acting on the system. As the input voltage on the motor is varied, the motor accelerates; consequently, its armature generates

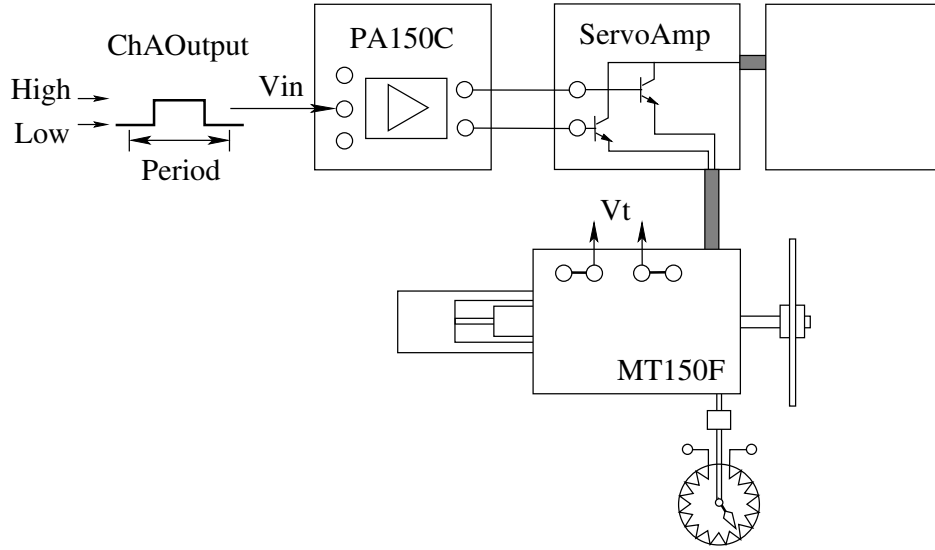


Figure 2.4: Setup for Task 3.

an increasing EMF V_e (which is proportional to the angular speed $\omega = \frac{d\theta}{dt}$) back to the motor. The total torque is proportional to the combination of input voltage and back EMF. Thus

$$\tau = k_1(V_{in} + V_e) = k_1 \left(V_{in} - k_2 \frac{d\theta}{dt} \right) \quad (2.4)$$

where k_1 and k_2 are constants. We can now rewrite the equation of motion as

$$\frac{d^2\theta}{dt^2} + c \frac{d\theta}{dt} = k_m V_{in}, \quad (2.5)$$

which has the solution

$$\frac{d\theta}{dt} = \frac{k_m V_{in}}{c} (1 - e^{-ct}) \quad (2.6)$$

and

$$\frac{d^2\theta}{dt^2} = k_m V_{in} e^{-ct} \quad (2.7)$$

in response to a step-like voltage of amplitude V_{in} applied at $t = 0$, with the motor initially at rest. From the above equations, we obtain

$$V_t = \frac{-k_t k_m V_{in}}{30c} (1 - e^{-ct}).$$

1. Set up the circuit in Fig. 2.4. Choose suitable high and low voltages, and an appropriate period for the ChA Output such that the speed of the servo motor will (nearly) stabilize at each input voltage.
2. Determine k_m and c graphically.

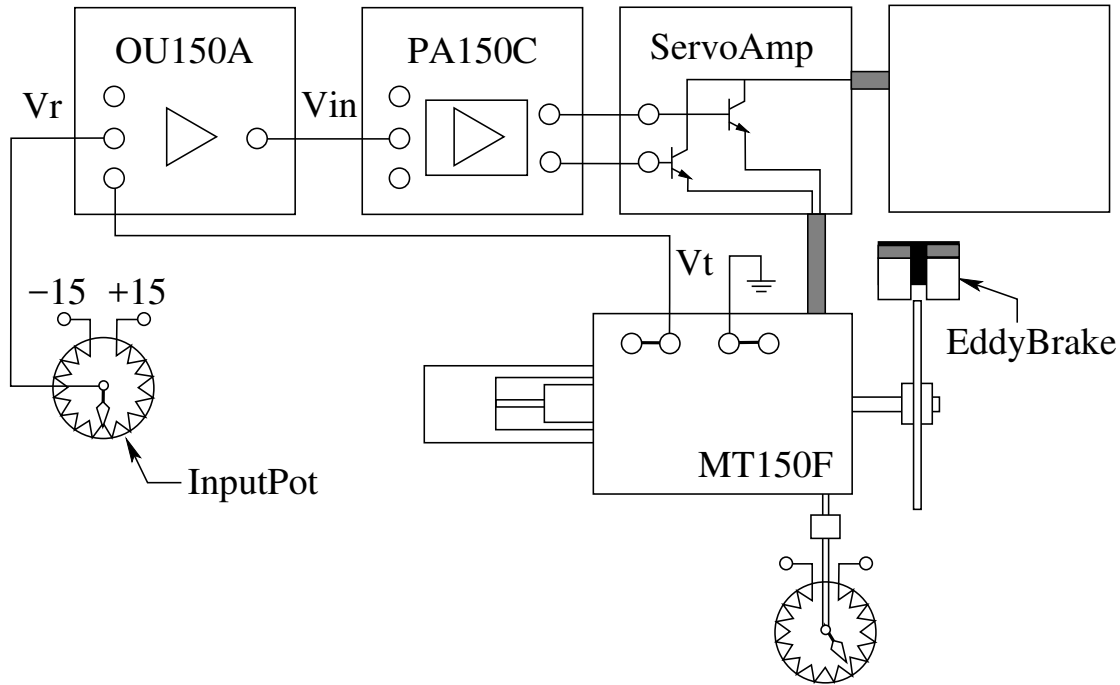


Figure 2.5: Setup for Task 4.

Task 4 — Closed Loop Speed Control

Set up the circuit shown in Fig. 2.5.

In this task, a signal proportional to the speed is fed back to the OU150A and compared with the required speed (reference voltage V_r). This produces an error signal to actuate the Servo Amplifier output, allowing the motor to maintain a more constant speed in the face of fluctuating loads than would be possible without feedback.

If $V_t < -V_r$, then $V_{in} > 0$ and power will be supplied to the motor to accelerate it, so as to bring $(V_t + V_r)$ closer to zero (reducing the “error” signal by negative feedback.) The speed of the motor will therefore be controlled by the setting of V_r , and will remain reasonably constant despite changes in the mechanical load the motor must drive.

1. Plot the relation between the reference voltage and motor speed.
2. Slowly apply the eddy brake and observe what happens to the error voltage.
3. What happens if you reverse the tachogenerator signal to the OU150A (i.e. swap the V_t and ground wires)? What sort of feedback would you call this?

Task 5 — Closed Loop Position Control

Set up the circuit shown in Fig. 2.6.

Here we utilize the error signal output of OU150A to control the position of the motor shaft as monitored by the Output Pot. Potentiometer P_1 is connected between the OU150A and PA150C to act as a gain control. The input of the PA150C will be

$$V_{in} = -(V_r + V_p)r_1. \quad (2.8)$$

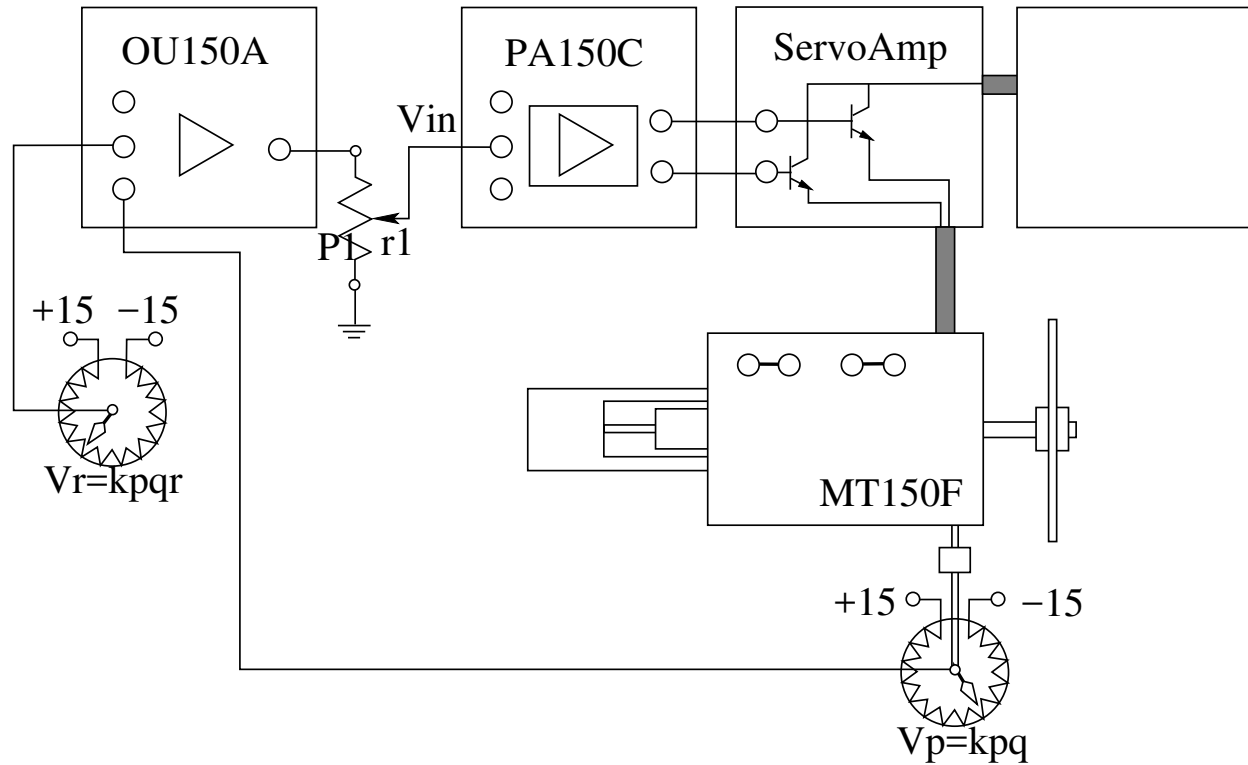


Figure 2.6: Setup for Task 5. Ratio r_1 scales OU150A signal from 0% to 100%.

The motor drive signal is given by the voltage difference between these two inputs. We can see that $V_{in} = 0$ if $V_p = -V_r$ or $\theta = -\theta_r$. If $\theta \neq -\theta_r$, the negative feedback will drive the motor to reduce $\theta + \theta_r$.

1. After setting up the circuit as in Fig. 2.6 (with the toggle switch on the PA150C in its center position), manually adjust the potentiometer P_1 , so that the Output Pot position is controlled by the Input Pot position.
2. Replace the signal from the Input Pot by a 2V peak-to-peak square wave from ChA. The period should be about 3-5 seconds. Vary the potentiometer P_1 and observe how the response varies.
3. Using the linear relationship between the voltage from the Output Pot and the angle of the shaft, determine a value for k_p . Find the solution to the equation of motion in terms of c , k_m , k_p , r_1 , and V_A , the amplitude of ChA's square wave.
4. Solve for the critical r_1 value. What type(s) of damping can you obtain in this setup? Measure and plot examples of this damping, and record the corresponding value r_1 from P_1 . How does the feedback parameter affect the steady-state position of the output shaft?

Task 6 — Closed Loop with Position and Velocity feedback

Assemble the system shown in Fig. 2.7.

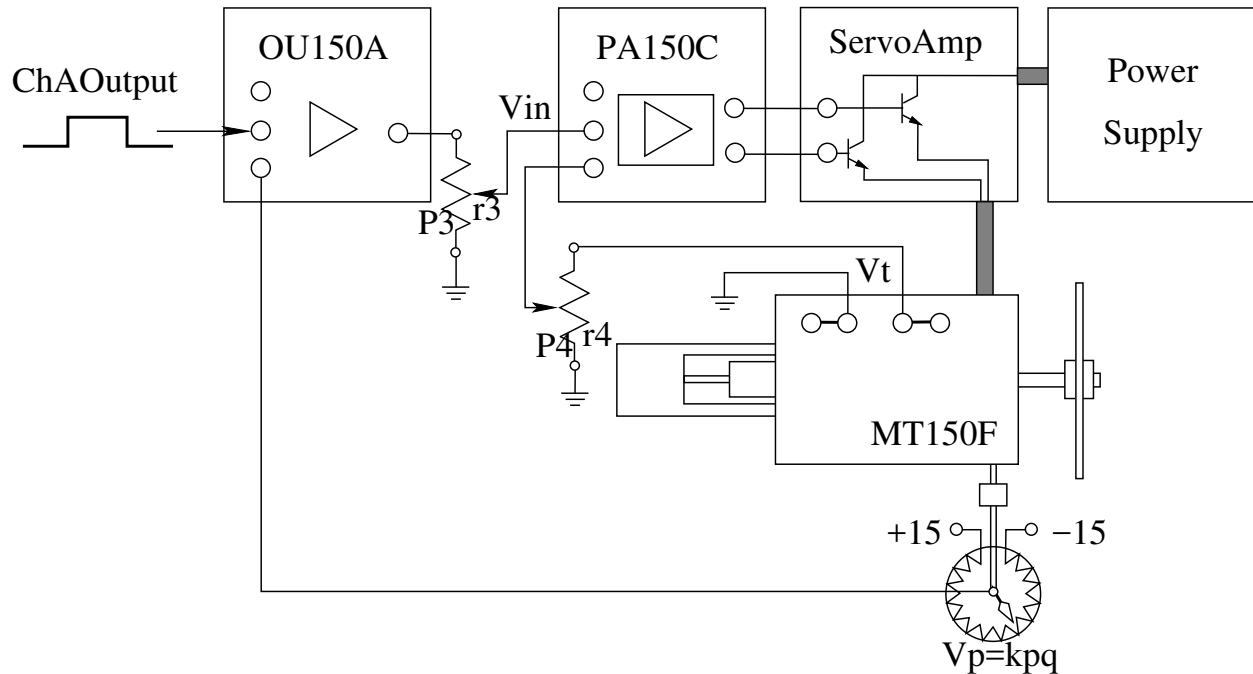


Figure 2.7: Setup for Task 6. r_4 scales the tachometer signal.

In Task 5 we saw that the positional control would be accurate only at high gain. However, the high gain caused overshooting and instability. The problem of overshoot is a result of the motor's speed carrying it past the point of alignment. To prevent this overshoot we can feed back a proportion of the derivative of the error signal, which we then subtract from the error signal, to produce a drive signal to the motor.

To demonstrate mathematically, the solution to the equation of motion in Task 5 contains an undamped transient term. The coefficient of this term should satisfy a certain condition to prevent overshoot. Adding a term in $\frac{d\theta}{dt}$ to the differential equation obtains this condition, which physically corresponds to connecting the tach voltage V_t through P_4 to the PA150C.

1. Choose appropriate high and low voltages for ChA Output, and observe how the angular position tracks the square wave applied.
2. Determine the equation of motion in terms of $k_m, k_p, k_t, c, r_3, r_4$, and V_A .
3. Using your values of k_m, k_p, k_t , and c , obtain the relation between r_3 and r_4 which produces critical damping.
4. Determine what values of r_3 and r_4 are associated with underdamped, overdamped and critically damped responses. Measure and plot an example of each type of damping.

2.4 References

1. "Control Mechanism", H.K. Skramstad and G.L. Landsman
2. "Servomechanisms", J.C. West

3. **“Feedback and Control Systems”**, Sydney Davis.

Experiment 3

Guided Microwaves

3.1 Purpose

1. To become familiar with microwave propagation in rectangular waveguides.
2. To become familiar with microwave generation and measurement techniques.

3.2 Theory

As the speed of electronics increases to the gigahertz region and beyond, conventional circuit analysis starts to break down due to the fact that the signals propagate at a finite speed throughout a circuit. This is due to the intrinsic relationship (Maxwell equations) between voltage and current signals on the one hand, and electromagnetic wave propagation on the other hand. One of the simplest and most direct ways of demonstrating propagation effects is by launching a gigahertz signal into a rectangular metal waveguide, and using a rectifying diode to monitor the voltage at different points along the guide. (How would the voltage vary along the guide if a kilohertz signal generator was connected to the guide?)

To analyze signal propagation along a given conducting channel (here we use a hollow rectangular metal waveguide, but we could equally well consider a coaxial cable or the more-common strip-line geometry), one has to specify the geometry and the material parameters. Usually the metallic components can be considered ideal conductors, and the dielectric components as ideal insulators with real dielectric constants. With this information, Maxwell's equations can be solved for the harmonic electromagnetic modes supported by this system in the frequency range of interest. The solutions for the ideal rectangular metal waveguide are particularly simple, especially if one only considers solutions with electric field vectors perpendicular to the axis of the guide (so called transverse electric modes, or TE modes). With reference to Fig. 3.1 for the geometry, the solution for the electric field takes the form

$$\begin{aligned} \vec{E}(x, y, z) = & \left[E_x^R \sin\left(\frac{n\pi}{b}z\right) \cos\left(\frac{m\pi}{a}x\right) \hat{x} + E_z^R \sin\left(\frac{m\pi}{a}x\right) \cos\left(\frac{n\pi}{b}z\right) \hat{z} \right] e^{-j\left(\omega t - \frac{2\pi y}{\lambda_g}\right)} \\ & + \left[E_x^L \sin\left(\frac{n\pi}{b}z\right) \cos\left(\frac{m\pi}{a}x\right) \hat{x} + E_z^L \sin\left(\frac{m\pi}{a}x\right) \cos\left(\frac{n\pi}{b}z\right) \hat{z} \right] e^{-j\left(\omega t + \frac{2\pi y}{\lambda_g}\right)} \end{aligned} \quad (3.1)$$

where

$$\left(\frac{1}{\lambda_g}\right)^2 = \left(\frac{1}{\lambda_0}\right)^2 - \left(\frac{n}{2b}\right)^2 - \left(\frac{m}{2a}\right)^2 \quad (3.2)$$

Here λ_g is the wavelength in the waveguide, $\lambda_0 = c/\nu$ is the wavelength in free space, and R and L refer to right and left propagating waves respectively. The x and z components of the field in each direction are not independent. The spectrum of allowed modes is discrete (due to the similarity of the free space wavelengths and the guide geometry) and they can be labelled by positive integer indices (m and n) that basically specify how many nodes the electric field amplitude exhibits along the two transverse axes (x and z in Fig. 3.1). One, but not both, of (m, n) , can be zero.

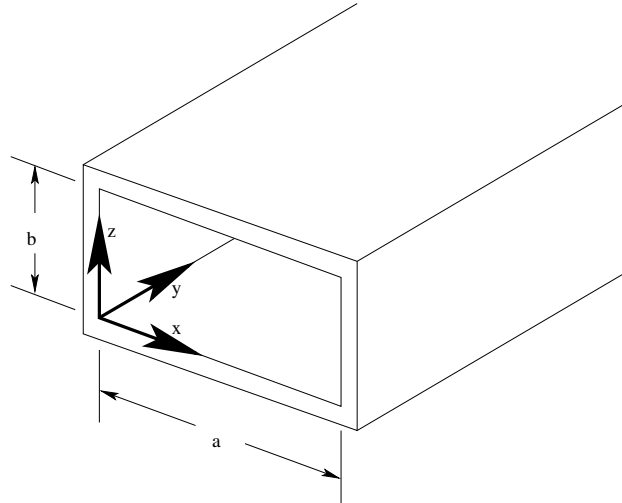


Figure 3.1: A waveguide.

From Eq. 3.2 it is clear that the solution propagates along the guide, unattenuated, if the square of the guide wavelength is real, but is exponentially attenuated, with no oscillatory behaviour along y at all, if the square of the guide wavelength is negative. For each mode m, n , therefore, there is a corresponding maximum wavelength (minimum frequency), beyond which electromagnetic waves will not propagate along the guide. This wavelength is called the cutoff wavelength, and is given by

$$\left(\frac{1}{\lambda_c}\right)^2 = \left(\frac{n}{2b}\right)^2 + \left(\frac{m}{2a}\right)^2 \quad (3.3)$$

Thus the propagation characteristics at a given frequency are completely determined by the dimensions of the guide, as contained in the expression for the cutoff wavelength.

The right and left propagating field amplitudes are determined by the nature of the microwave source, how it is coupled into the guide, and by what terminates the guide at the end opposite the signal launcher. In the present experiment, since $b < a$, the cutoff frequencies for all modes other than the first mode (TE_{10}) are higher than the frequencies available from the source, hence we only have to be concerned with the ratio $\zeta = E^L/E^R$. The overall magnitude is a function of the source and its coupling into the guide. The ratio ζ is by definition the reflection coefficient of the right propagating wave at the termination of the waveguide. As in conventional electronics, the reflection coefficient ζ is related to the impedance mismatch between (in this case) the guide itself and the load, Z_l :

$$\zeta = \frac{Z_l - Z_g}{Z_l + Z_g} \quad (3.4)$$

The guide impedance, Z_g can be obtained by solving Maxwell's equations for the magnetic field as well as the electric field, and the result for the TE_{10} mode is $Z_g = 120\pi\lambda_g/\lambda_0$ (Ω). The superposition of left and right propagating waves gives rise to standing waves as illustrated in Fig. 3.2. You should be able to show that the reflection coefficient ζ , and hence the termination impedance, can be determined by measuring the Voltage Standing Wave Ratio (VSWR)

$$VSWR = \frac{V_{max}}{V_{min}} \quad (3.5)$$

and the phase of the voltage maxima and/or minima with respect to the end of the guide.

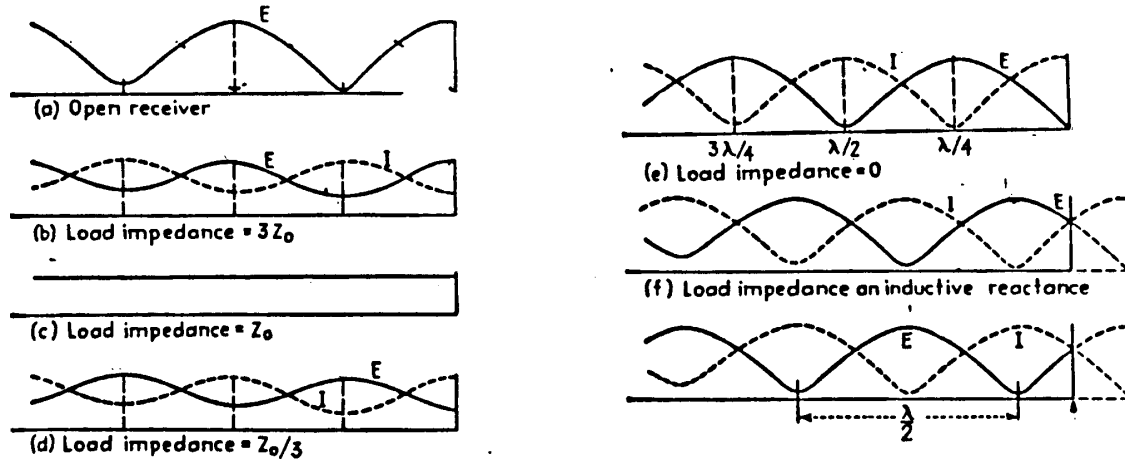


Figure 3.2: Solid lines show the absolute magnitude of the net electric field with zero baseline. Here Z_0 means the guide impedance Z_g .

The Smith chart is an instrument designed to simplify the conversion from VSWR and phase measurements to the reflection coefficient or load impedance. The theory of the Smith chart is in the Appendix and several books can be found explaining the use of the Smith chart. “Microwave Theory” and “Measurements and Handbook of Microwave Measurements” are both in the lab library.

3.3 Procedure

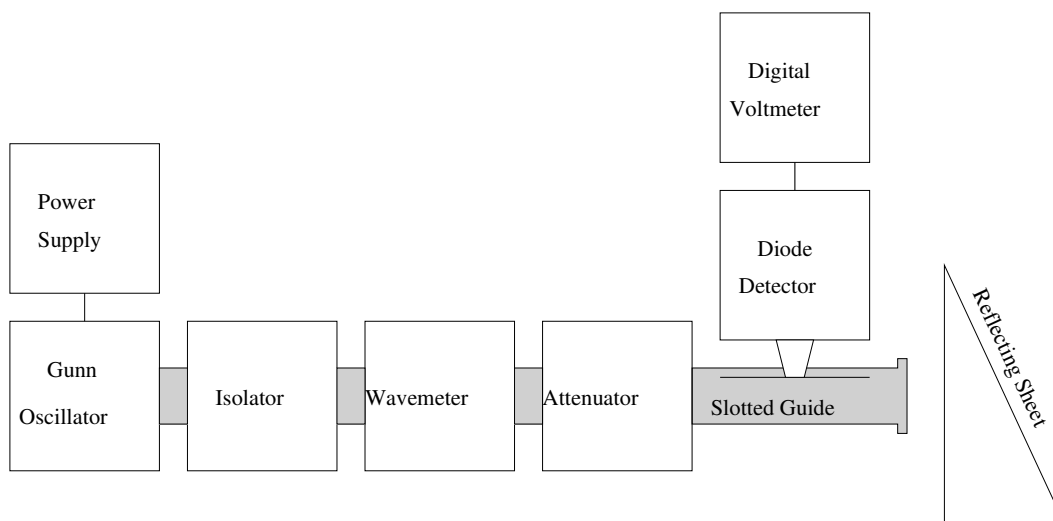


Figure 3.3: Schematic diagram of the apparatus. Operate in CW mode.

The Gunn oscillator produces microwave power at a given frequency when the applied voltage and the cavity micrometer are adjusted to the values specified on the manufacturer’s specification

chart. Check you have the correct one for your diode. The slotted guide allows you to sample the field in the waveguide with a small copper probe; the voltage induced in the probe is rectified by a microwave diode in the probe assembly and the resulting DC voltage is observed on the digital voltmeter. The rectified DC voltages observed at low power levels are proportional to the square root of the power level in the guide, and are therefore proportional to the voltage in the guide at the probe wire.

Since the probe is required to sample the field without also interfering with the propagating wave, you may have to adjust the depth of the probe into the waveguide so that you are not loading the line but can still pick up a good signal. To determine whether you must adjust the depth, follow these steps:

1. Turn on the power and attach the silvered plate as the waveguide termination.
2. Move the detector along the guide to obtain a maximal reading.
3. Adjust the tuning plunger on the detector mount to further optimize the output.
4. Move the detector along the guide recording the positions at which successive maxima and minima are observed.
5. The maxima and minima should occur at approximately equal distances from each other along the length of the line. If they are not, then you will have to adjust the depth.

The depth is adjusted by loosening the locking mechanism at the base of the detector mount and raising the entire mount. Once you have found a good depth you can re-tighten the locking mechanism. Adjust the tuning plunger on the detector mount to get the largest voltage output. You can also adjust the wave-meter micrometer and attenuator to get a reasonable signal from the probe. The manual for the detector mount will be located at the bench. You must use the same settings for all parts of both tasks.

3.4 TASK 1 — Determination of Cut-off Wavelength

1. With the reflecting sheet fixed in place, and no termination attached to the waveguide end, measure λ_g by moving the probe carriage along the guide.
2. Next keep the probe fixed and move the aluminum reflecting sheet to determine λ_0 .
3. Deduce a value for λ_c and compare it with the value you obtain by measuring the dimensions of the waveguide cross-section with a pair of calipers.

3.5 Task 2 — Impedance Measurement

1. Determine the VSWR and the fractional wavelength from the end of the waveguide to the nearest maximum with a short-circuiting termination, using the silver-coated plate. How do these values compare to their expected values?
2. Remove the short circuit, and replace the reflecting sheet used in Part 1 by a sheet of microwave absorbing material inclined at a slight angle to the axis of the waveguide to prevent reflections back to the waveguide system. With nothing attached to the end of the slotted guide, measure the VSWR and deduce the distance of the nearest voltage maximum to the end of the slotted guide. From these measurements, deduce the normalized impedance at the end of the guide using the Smith Chart.

3. Repeat step 2 using a rectangular horn attached to the end of the slotted guide. Measure the distance from the nearest voltage maximum to the input flange of the horn.
4. From the normalized impedances found in steps 2 and 3, deduce the termination impedance for each case by multiplying the normalized impedance by the impedance in the rectangular guide.
5. Which method of termination provides a better match to the guided waves? Why is this so?

3.6 Appendix — The Smith Transmission Line Chart

Many graphical aids for transmission line computation have been devised. Of these, the most generally useful has been one presented by P.H. Smith, which consists of loci of constant resistance and reactance plotted on a polar diagram in which radius corresponds to magnitude of reflection coefficient, and angle corresponds to phase of reflection coefficient referred to a general point along the line. The chart enables one to find simply how impedances are transformed along the line, or to relate impedance to reflection coefficient or standing wave ratio and positions of voltage minima. By combinations of operations, it enables one to understand the behaviour of complex impedance-matching techniques and to devise new ones.

The normalized impedance, $\frac{Z_i}{Z_0}$, that would be measured at a distance l from the end of the guide is given by

$$\frac{Z_i}{Z_0} = (r + jx) = \frac{1 + \rho(l)}{1 - \rho(l)} \quad (3.6)$$

where ρ is the complex voltage reflection coefficient ζ , multiplied by a phase factor corresponding to the accumulated phase from the observation point to the end of the guide and back again.

Now if we let $\rho = u + jv$ then

$$r + jx = \frac{1 + (u + jv)}{1 - (u + jv)} \quad (3.7)$$

which may be separated into real and imaginary parts as

$$r = \frac{1 - (u^2 + v^2)}{(1 - u)^2 + v^2} \quad (3.8)$$

$$x = \frac{2v}{(1 - u)^2 + v^2} \quad (3.9)$$

or

$$\left(u - \frac{r}{1 + r}\right)^2 + v^2 = \frac{1}{(1 + r)^2} \quad (3.10)$$

$$(u - 1)^2 + \left(v - \frac{1}{x}\right)^2 = \frac{1}{x^2} \quad (3.11)$$

If we then wish to plot the loci of constant resistance r on the ρ plane (u and v serving as rectangular coordinates), Eq. 3.10 shows that they're circles centred on the u axis at $(r/[1 + r], 0)$ and with radii $1/(1 + r)$. The circles for $r = 0, 1/2, 1$, and 2 are sketched on Fig. 3.4. From Eq. 3.11, the curves of constant x plotted on the ρ plane are also circles, centred at $(1, 1/x)$ and with radii $1/|x|$. Curves for $x = 0, \pm 1/2, \pm 1$, and ± 2 are sketched on Fig. 3.4. These circles appear as arcs as they are only drawn until they meet the $r = 0$ boundary. Any point on a given transmission line will have some impedance with a positive resistive part, and will then correspond to some particular point on the inside of the unit circle of the ρ plane.

The Complete Smith Chart

Black Magic Design

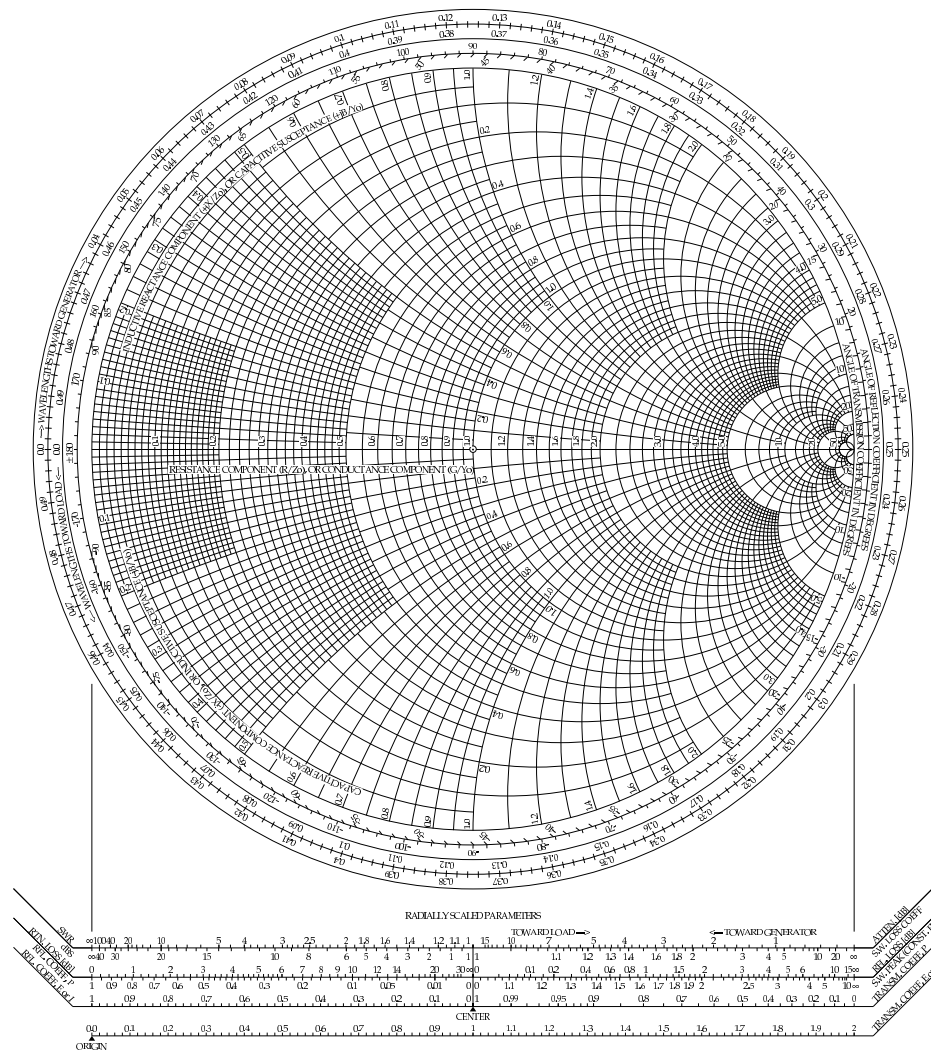


Figure 3.4: The Smith chart, as stolen from Spread Spectrum Scene,
<http://www.sss-mag.com/smith.html> .

Experiment 4

Gamma Ray Spectroscopy

4.1 Purpose

1. To gain experience with single particle detection apparatus and spectroscopic analysis techniques.
2. To become acquainted with particle-matter interaction phenomena.

4.2 Theory

The ability to measure the energy of particles is fundamental to experimental investigations in many branches of physics. Applications range from high-energy studies of elementary particles (quarks, muons, pions, gamma rays etc. at the MeV to GeV level), to low energy studies of solids (luminescence, Raman scattering etc. at the 1 eV level). Gamma emitters are used in analytical chemistry and as tracers in medicine. One typically deals with a well-defined source that emits a flux of the relevant particles either spontaneously (radioactive decay) or as a result of external excitation (collisions or laser excitation etc.). The energy of the particles and the absolute flux depends strongly on the type of source and on the excitation conditions. The design of appropriate detectors thus depends strongly on the nature of the source. However, it is generally true that the detection and energy-analysis of the particles is based on monitoring their interaction with a medium, or collection of matter (e.g. scintillator, photocathode, ionization chamber etc.) **wherein the interaction of the particles with the medium is well-characterized.**

In the present experiment we deal with the detection of gamma radiation (photons) using a scintillator, a photomultiplier tube, and a pulse-height analysis system (see figure 4.1). The scintillator acts as a transducer that converts the energy of the original gamma ray into many lower-energy photons which can be detected by the phototube. The phototube is really another transducer that converts these low energy photons into electrical current that can be easily analyzed using conventional electronic circuitry. The following describes the basic processes involved in this detection system. For a more detailed discussion see the references listed at the end of the lab.

Primary Interactions

The incident particles initially interact with the doped NaI crystal that makes up the scintillator. There are three primary interaction routes, i) photoemission, ii) Compton scattering, and iii) electron-positron pair production, the relative strengths of which depend on the energy of the incident particles.

Photoelectric Effect

This effect represents the process in which the photon is completely absorbed and all its energy is transferred to a single atomic electron.

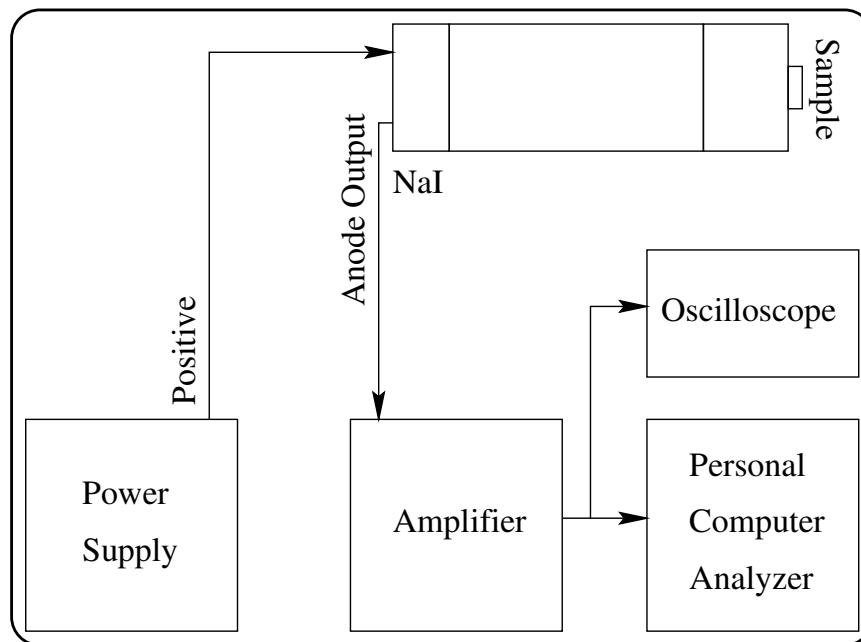


Figure 4.1: Schematic diagram of the apparatus.

Compton Effect

This effect represents the process in which the photon scatters off an atomic electron and transfers only a fraction of its energy to that electron.

Electron-Positron Pair Production

In the pair production process a photon of energy greater than twice the electron rest mass is annihilated and an electron-positron pair is created. In order to conserve both energy and momentum this process can only occur in the coulomb field of a nucleus.

For a more detailed account of the three processes, see the Appendix (section 4.5). Figure 4.2 shows the energy dependence of the relative contributions of the the three processes.

For processes i) and ii), the effect on the scintillator of the primary interaction is the liberation of a high-energy electron, leaving an empty core orbital in the associated host atom. In case iii), one or both of the secondary gamma rays from the ensuing electron-positron annihilation process will act essentially as the primary gamma ray, again resulting in a high-energy electron and an associated core hole. These high-energy electrons will then initiate a cascade of further ionization processes (electron-atom collisions) that produce more and more free electrons, each with less and less energy as the process continues. At the same time, electrons from higher-energy orbitals will fall into the vacant core states, emitting X-rays. Some of these X-rays may escape the scintillator, and others will be absorbed just as the gamma rays were, producing more energetic electrons. Eventually the original energy of the gamma ray is converted into many low energy electrons and holes that drift through the NaI crystal until encountering one of the impurities, which act as recombination centres. The visible photons given off in this “scintillation” process at the impurities are then detected by the photomultiplier tube. Higher energy gamma rays produce more low energy electrons and holes, which in turn produce more visible photons, each of which

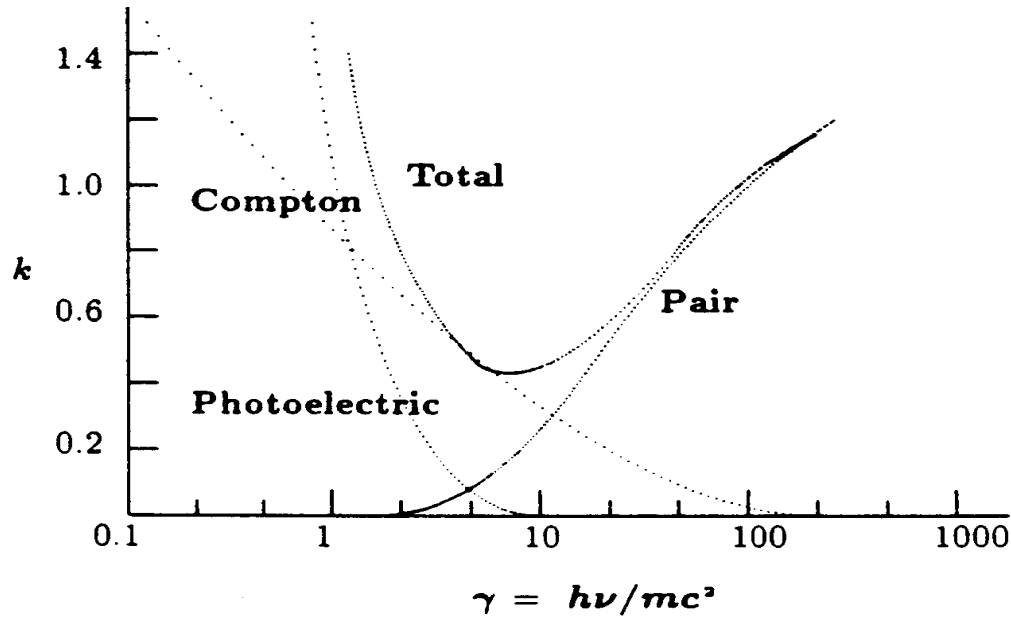


Figure 4.2: The energy dependence of the relative contributions of the three primary interactions of gamma rays with matter. The absorption coefficient in lead is plotted against the photon energy in units of 0.511 MeV.

contributes to the strength of the amplified electron pulse from the photomultiplier tube; hence the use of the phototube's pulse height as a measure of the incident gamma ray energy.

For gamma rays that initially decay via the photoelectric effect, virtually all of their initial energy will be converted to low energy electron-hole pairs, and a reasonable fraction of these, $\sim 1.5\%$, will produce visible photons. Including the collection and conversion efficiency of the phototube, the overall efficiency for converting the gamma ray energy into electric current is on the order of 0.15%. Each such gamma ray will thus produce an electrical pulse of a characteristic height, with some distribution about that height due to statistical effects involved in the overall transduction process. The corresponding electrical pulses are referred to as the photopeaks.

A gamma ray that initially Compton scatters within the scintillator may or may not escape the crystal. If it does not, it may eventually give up all its energy to the crystal, in which case it will also produce an electrical pulse of the same height as the photopeak. If the scattered gamma ray does escape the crystal, the energy detected by the phototube will be less than that associated with the photopeak, and will represent the amount of energy given to the electron in the Compton scattering process. The corresponding spectrum is continuous, and is characterized by a high-energy edge. Why?

When a gamma ray undergoes annihilation into an electron-positron pair, some of its energy goes into the excitation of high-energy electrons, while the rest is converted to two gamma rays, each of energy 0.511 MeV. If these two gamma rays are both absorbed in the detector, the result will be an electrical signal of height equal to the photopeak. If one or both of these secondary gamma rays escapes, there will be corresponding replicas of the photopeak at energies of 0.511 MeV and 1.02 MeV below the photopeak. These are called single and double escape peaks respectively.

Another possible process involves gamma rays that go right through the crystal, but then Compton scatter in the walls of the housing or in the phototube material itself. If the gamma ray

is **backscattered**, it will re-enter the crystal, where it might be detected. What sort of spectrum would you expect from such events?

Finally, some radioactive isotopes directly emit positrons when they beta decay. These positrons, of energy 0.511 MeV, can annihilate with an electron either in the crystal or within the original source, giving rise to two gamma rays of energy 0.511 MeV. What features would you expect these events to produce in the final spectra?

4.3 Procedure

BEFORE STARTING: Ensure that you are familiar with the techniques for safe handling of radioactive materials. Before you leave, make sure you *wash your hands*, as you may be handling both lead and radioactive sources!

1. The power supply voltage should be at 1300 V. Adjust the amplifier gain such that the ^{60}Co source gives a maximum signal that is not off-scale (if the spectrum goes off the right side of the screen you need to turn down the gain). Check your signals with an oscilloscope and familiarize yourself with the Personal Computer Analyzer software.
2. Record spectra from the ^{137}Cs , ^{109}Cd , and ^{60}Co sources. Using the known energies for the gamma rays emitted from these sources (chart on the west wall of the laboratory or a reference), generate a calibration curve for the gamma ray energy in terms of the channel number.
3. With this calibration, determine the energies of peaks observed in the ^{54}Mn , ^{22}Na and ^{133}Ba spectra, and compare with their expected values.
4. For all of the spectra, identify as many of the features as possible. You will need to determine and use the relationship between the energies of the Compton edge, photopeak and backscatter peak. Report the width of each photopeak.
5. For the ^{137}Cs source, determine the efficiency of this detection system. You will need to record the date and initial activity of the source.

4.4 References

<http://nucleardata.nuclear.lu.se/toi/nucSearch.asp>

<http://atom.kaeri.re.kr>

UBC radiation safety and methodology manual:

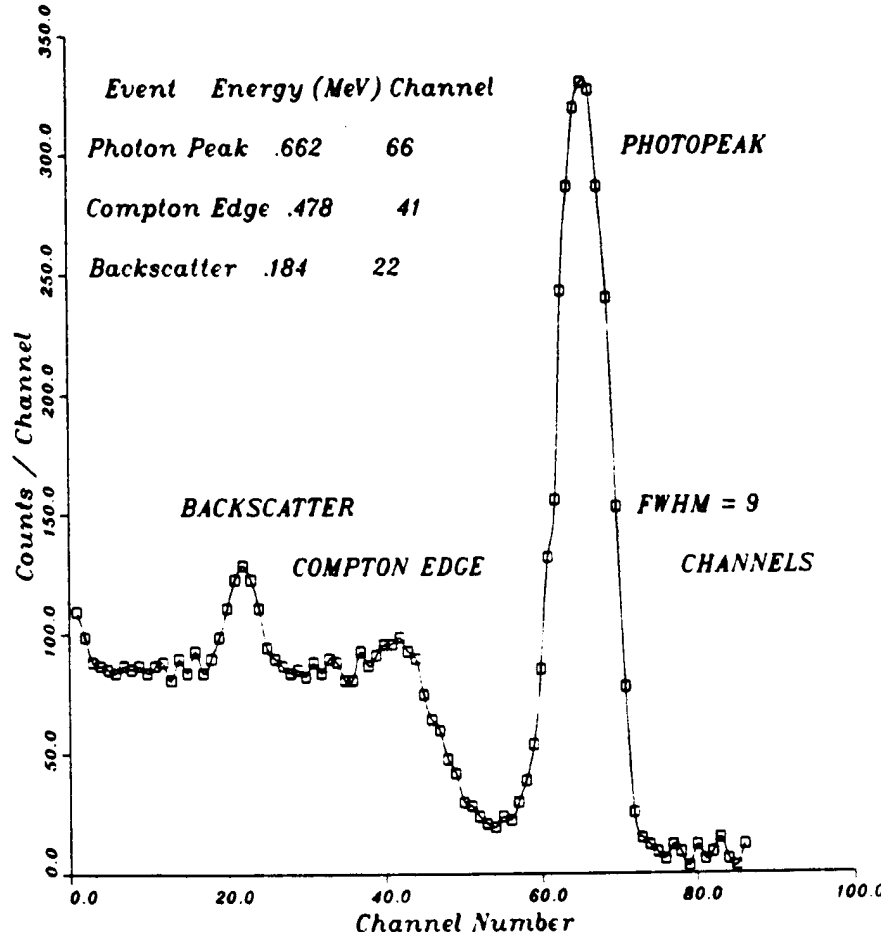
<http://riskmanagement.sites.olt.ubc.ca/files/2015/09/Radiation-Reference-Manual-2011.pdf>

4.5 Appendix

Photoelectric Effect

The photoelectric effect represents the process in which the photon is completely absorbed and all its energy is transferred to a single atomic electron. The cross-section for the photoelectric effect has been derived by Heitler and in the non-relativistic limit is

$$\sigma_p = \frac{\sigma_T Z^5}{137^5} 2\sqrt{2} \left(\frac{h\nu}{mc^2} \right)^{-\frac{7}{2}} \text{ cm}^2 \quad (4.1)$$

Figure 4.3: Example: Spectrum of a ^{137}Cs source.

where

Z = atomic number of the struck nucleus

$h\nu$ = energy of the incident photon

mc^2 = electron rest mass

$$\sigma_T = \frac{8\pi}{3} \left(\frac{e^2}{mc^2} \right)^2 = \frac{8\pi}{3} r_o^2$$

$$r_o = \frac{e^2}{mc^2} = \text{classical radius of the electron} = 2.8 \times 10^{-13} \text{ cm}$$

Compton Effect

This effect represents the process in which the photon scatters off an atomic electron and transfers only a fraction of its energy to that electron. (The dynamics of this process are discussed in greater detail below.) At low energies the Compton scattering cross-section is

$$\sigma_c = \sigma_T \left(1 - 2\gamma + \frac{26}{5}\gamma^2 \right) \quad \text{for } \gamma \ll 1 \quad (4.2)$$

and for high energies

$$\sigma_c = \frac{3}{8} \sigma_T \frac{1}{\gamma} \left(\ln 2\gamma - \frac{1}{2} \right) \quad \text{for } \gamma \gg 1 \quad (4.3)$$

where $\gamma = \frac{h\nu}{mc^2}$

Electron-Positron Pair Production

In the pair production process a photon of energy greater than the equivalent electron rest mass is annihilated and an electron-positron pair is created. In order to conserve both energy and momentum this process can only occur in the coulomb field of a nucleus. The cross-section for pair production rises rapidly above threshold and reaches a limiting value for $\frac{h\nu}{mc^2} \approx 1000$ of

$$\sigma_{pair} = \frac{Z^2}{137} r_o^2 \left(\frac{28}{9} \ln \frac{183}{Z^{\frac{1}{3}}} - \frac{2}{27} \right) cm^2 \quad (4.4)$$

Compton Scattering

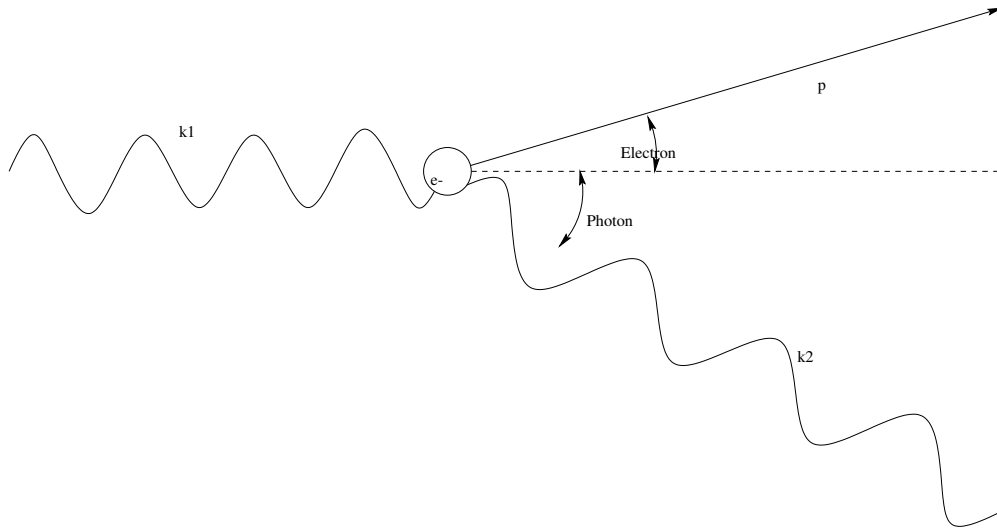


Figure 4.4: Compton Scattering of a photon from a free electron.

The Compton scattering process is shown schematically in Figure 4.4. An incident photon of momentum $\frac{h\nu}{c}$ scatters from an electron at rest. The photon scatters at an angle θ with momentum $\frac{h\nu'}{c}$ and the electron recoils at angle ϕ with momentum p . Using relativistic kinematics the energy of the recoiling electron is

$$E_{el}^2 = p^2 c^2 + m^2 c^4 \quad (4.5)$$

The three vectors $\frac{h\nu}{c}$, $\frac{h\nu'}{c}$ and p must lie in a plane. Energy conservation therefore requires that

$$h\nu + mc^2 = h\nu' + \sqrt{p^2 c^2 + m^2 c^4} \quad (4.6)$$

From momentum conservation, we obtain

$$h\nu = h\nu' \cos \theta + cp \cos \phi \quad (4.7)$$

$$0 = h\nu' \sin \theta + cp \sin \phi \quad (4.8)$$

Eliminating ϕ , the (unobserved) electron recoil angle, we obtain from equations 4.7 and 4.8

$$h^2 \nu^2 - 2h^2 \nu \nu' \cos \theta + h^2 \nu'^2 = c^2 p^2 \quad (4.9)$$

Squaring equation 4.6 and subtracting, we get

$$\frac{\nu - \nu'}{\nu\nu'} = \frac{h}{mc^2} (1 - \cos \theta) \quad (4.10)$$

Using $E = h\nu$ for photons, this can be written as

$$\frac{1}{E'} - \frac{1}{E} = \frac{1}{mc^2} (1 - \cos \theta) \quad (4.11)$$

The factor $\frac{h}{mc} = 2.42 \times 10^{-10}$ cm is called the electron Compton wavelength.

Experiment 5

Air Suspension Gyroscope

5.1 Purpose

To measure the absolute rotation rate of the Earth, and to verify equation 5.1.

5.2 Theory

The gyroscope precession equation is

$$\vec{\tau} = \vec{\Omega} \times \vec{J} \quad (5.1)$$

where $\vec{\tau}$ is the torque applied to an object spinning with angular momentum \vec{J} , and $\vec{\Omega}$ is its resulting precessional angular velocity.

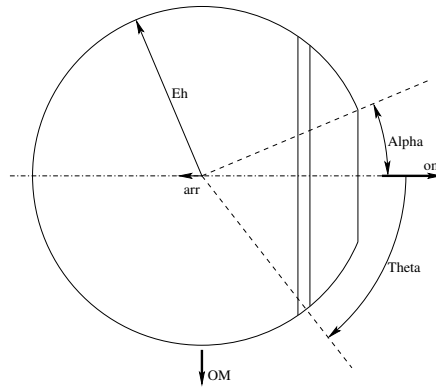


Figure 5.1: The gyroscope rotor.

Our gyroscope, consisting of a steel ball with one flat surface, is depicted in Figure 5.1. It spins about a horizontal axis with angular velocity ω , suspended by an air jet about its geometrical axis. The flat surface displaces the centre of gravity from the geometrical centre by a distance r , leading to a torque. In this configuration $\vec{\Omega}$ and \vec{J} are perpendicular, hence

$$\tau = mgr \quad (5.2)$$

$$\vec{J} = I\vec{\omega} \quad (5.3)$$

where the moment of inertia $I = mk^2$ and k is the moment of gyration. Thus equation 5.1 becomes

$$mgr = \Omega mk^2 \omega \sin \frac{\pi}{2} \quad \text{or} \quad (5.4)$$

$$\Omega = \frac{gr}{k^2 \omega} \quad (5.5)$$

The object of the experiment is therefore to measure Ω , $\frac{k^2}{r}$ and ω in order to verify equation 5.5. In the Appendix (section 5.5) it is shown that

$$\frac{k^2}{ra} = \frac{30(1 + \cos \alpha) - 20(1 + \cos^3 \alpha) + 6(1 + \cos^5 \alpha)}{15 \sin^4 \alpha} \quad (5.6)$$

where a and α are as shown in figure 5.1.

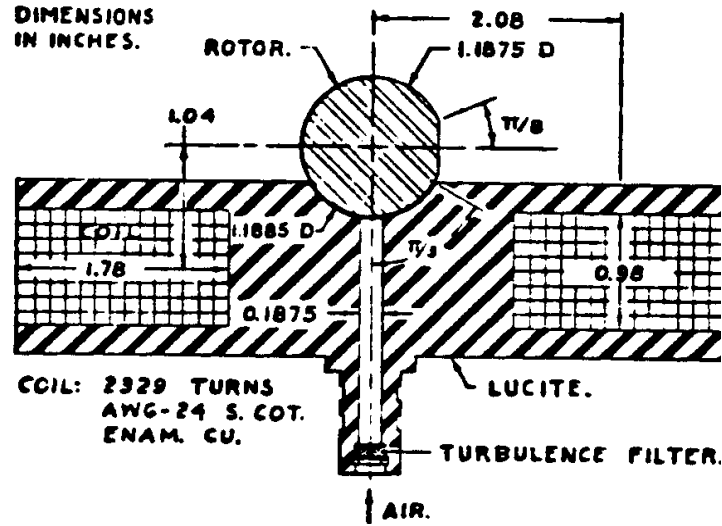


Figure 5.2: The air suspension gyroscope.

The essential parts of the apparatus are shown in Figure 5.2. The gyro rotor consists of a steel ball bearing freely suspended on a jet of air. A wire gauze filter in the air inlet fitting removes turbulence from the incoming air jet, to minimize spurious torques.

A flat spot ground on one side of the ball provides both an accurately measurable gravitational torque and a mirror from which to reflect a laser beam for precision timing of the precession period. The ball is permanently magnetized and the field coil, carrying a 60Hz oscillating current, drives the magnetized ball as a synchronous motor. The spin axis is perpendicular to the flat face of the ball.

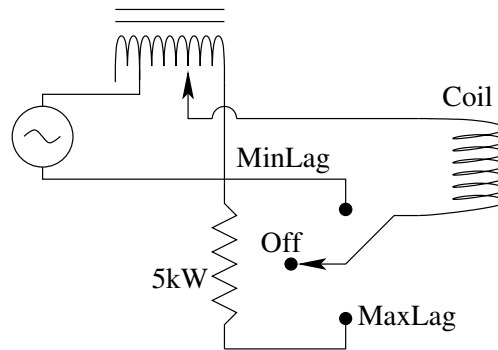


Figure 5.3: The field control circuit.

The driving magnetic field is controlled by the circuit shown in Figure 5.3. Power comes from

the Variac variable voltage source. “Minimum phase lag” provides maximum dynamic stability, for easy starting, for rapid correction of rotor orientation, and for rapid damping of nutation and hunting. With the field control switch in the “Maximum Phase Lag” (up) position a $5\text{ k}\Omega$ series resistor drops the coil current. Maximum phase lag minimizes spurious electromagnetic torques, for best experimental accuracy.

5.3 Procedure

1. Clean the rotor with methanol and mark the edge of the flat face with a felt pen to give an easily observable dot.
2. With the flat face of the rotor upward, slowly increase the suspension airflow until the rotor is freely suspended. To minimize spurious air torques, adjust the airflow to slightly above the minimum needed to provide a free stable suspension. Too much airflow will cause turbulence and too little airflow causes friction — both effects increase the precession period. You can investigate these effects once you have the rotor precessing. Orient the rotor with the normal to its flat face horizontal, and set it spinning about this normal by directing the accelerating air jet along its top surface. Where should the jet be directed to have maximum effect? Steady the centre of the flat face lightly with the point of the plastic rod. You will need to keep the rod there through the initial acceleration. Once the rotor is spinning, remove the rod and allow the ball to precess as you accelerate it. The stroboscope should be set to “Line” for 60 flashes per second (think about why “Line” is necessary and simply setting the flash rate to 60 flashes per second manually won’t work?). Watching the dot on the flat face, what sequence of stationary patterns do you see as the gyro accelerates? A small amount of wobble usually damps out if the angular momentum is built up smoothly. Never let the wobble become large enough to carry the flat face of the rotor below the rim of the jet. Any periodic uncovering of the jet orifice produces an unstable rotor bounce, which can damage the jet. If the wobble becomes enough to blur the flat face, stop the rotor and start over.

CAUTION: The rotor reaches 3600 rpm in a minute or two. You should be aware that if you were successful in spinning it above 7000 rpm or so, there exists a possibility of explosion from centripetal stress.

3. When the rotor reaches 3600 rpm, apply 120V minimum phase lag power to the coil. Damp out any hunting about the dynamic equilibrium by antisynchronous application of the air jet. Describe in your report the orientation of the magnetization of the rotor, the direction of the magnetic field produced by the drive coil, and how these together keep the rotor at 3600 rpm.
4. Direct the laser beam at the rotor so that it hits the flat face and reflects from it. The height of the reflected beam on the black wall surrounding the apparatus, together with the height of the laser aperture, will allow you to check the vertical alignment of the flat face. Use a level to determine how flat and horizontal the bench is. If necessary, adjust the rotor’s vertical alignment by applying *small* torques with the air jet at the appropriate point on the rotor, remembering equation 5.1. Any residual nutation or hunting should be removed automatically by the minimum phase lag magnetic field during the first few precessions. As the initial oscillations subside, reduce the applied voltage. The dot on the face may rotate a little as you do this. The hunting period with maximum phase lag should be $\sim 5\text{--}6$ seconds.
5. Once you are familiar with getting the rotor up to speed and locked into synchronization, you can measure the rotor dimensions with the dial micrometer and the calibrated blocks.

★ The remaining steps must all be completed on the same day. Before taking data, make sure you are using the same rotor and that it is clean.

6. Get the rotor up to speed and turn on the minimum phase lag. Allow it to precess long enough that the nutation subsides, then reduce the voltage to take data. Measure the precession period several times, adjusting the suspension air flow rate to determine which air flow gives the minimum period. **Do not reduce the suspension air flow too much with the rotor at speed. The spherical surface of the suspension jet will be damaged if it is shut off with the rotor spinning.** Make a note of the directions of $\vec{\omega}$ and $\vec{\Omega}$ — verifying the vector equation 5.1 requires doing a quick check of the direction, not just the magnitude.
7. When you have found the best suspension airflow rate and the transient disturbances have damped out, record the next few (3-5) precession periods. Then shut off the magnetic field, slow the rotor with the air jet, and continue to accelerate it with opposite $\vec{\omega}$. Measure the precession period a few times in this direction. Make sure you do not change the suspension airflow rate between the two directions. The data should be taken in the second direction immediately after the first direction.
8. While you are waiting to take time data, calculate the difference in period you expect for the two directions. Do you use the sidereal or solar period of the Earth?
9. From the results of the two different directions, determine the absolute rotation rate of the Earth, Ω_{\oplus} . Combine the results from the two directions to find the absolute rotation rate of the gyroscope. Should you combine the periods or frequencies from the two directions?
10. In order to calculate $\frac{gr}{k^2\omega}$, you must first determine an accurate value of g for the lab. Hebb is located at 49.2661°N and 123.2516°W , and the elevation in the lab is about 110m.
11. Calculate the experimental values of $\frac{gr}{k^2\omega}$, Ω , and their uncertainties. You should find that there is one experimental quantity that contributes the most to the final uncertainty. State which quantity this is and compare your results with the expected result. Is equation 5.1 verified?

5.4 Error Analysis

It is fairly easy to validate equation 5.5 with relatively good accuracy, and furthermore to know what factors limit the accuracy. You are required to calculate these and to check that your result comes within the predicted uncertainty. The analysis is performed in the Appendix. Proceeding

in the usual way, one differentiates equation 5.5 to obtain:

$$\left[\frac{d \left(\frac{gr}{k^2 \omega} \right)}{\frac{gr}{k^2 \omega}} \right]^2 = \left[\frac{d\omega}{\omega} \right]^2 + \left[\frac{da}{a} \right]^2 + \left[\left\{ \frac{-30 \sin \alpha + 20 (3 \cos^2 \alpha \sin \alpha) - 6 (5 \cos^4 \alpha \sin \alpha)}{30 (1 + \cos \alpha) - 20 (1 + \cos^3 \alpha) + 6 (1 + \cos^5 \alpha)} - \frac{15 \sin^3 \alpha (4 \cos \alpha)}{15 \sin^4 \alpha} \right\} d\alpha \right]^2 \quad (5.7)$$

$$= \left[\frac{d\omega}{\omega} \right]^2 + \left[\frac{da}{a} \right]^2 + \left[\left\{ \frac{-30 \sin^5 \alpha}{30 (1 + \cos \alpha) - 20 (1 + \cos^3 \alpha) + 6 (1 + \cos^5 \alpha)} - \frac{4 \cos \alpha}{\sin \alpha} \right\} d\alpha \right]^2 \quad (5.8)$$

Convince yourself that these equations are correct.

5.5 Appendix

The radius of gyration k^2 with respect to the horizontal axis of symmetry and the distance r to the centre of gravity as shown in Figure 5.1 can be evaluated using the two integrals

$$Mk^2 = \iiint \rho (r \sin \theta)^2 dV \quad (5.9)$$

$$Mr = \iiint \rho (r \cos \theta) dV \quad (5.10)$$

where M is the mass, ρ is the density and dV is the volume element. The most convenient volume element is a thin disk, as shown in figure 5.1, for which the radius of gyration $k^2 = \frac{1}{2}$ and

$$dV = -\pi (a \sin \theta)^2 d(a \cos \theta) \quad (5.11)$$

With these values, and throwing in a $(-)$ sign because r is negative in this co-ordinate system,

$$\begin{aligned}
 \frac{k^2}{r} &= - \frac{\int_{\alpha}^{\pi} \frac{1}{2} (a \sin \theta)^2 \pi a^2 \sin^2 \theta d(a \cos \theta)}{\int_{\alpha}^{\pi} (a \cos \theta) \pi a^2 \sin^2 \theta d(a \cos \theta)} \\
 \frac{k^2}{ra} &= - \frac{- \int_{\alpha}^{\pi} \frac{1}{2} \sin^5 \theta d\theta}{- \int_{\alpha}^{\pi} \sin^3 \theta \cos \theta d\theta} \\
 &= \frac{- \frac{1}{2} \int_{\alpha}^{\pi} \sin \theta (1 - \cos^2 \theta)^2}{\frac{\sin^4 \theta}{4} \Big|_{\alpha}^{\pi}} \\
 &= \frac{\left[-\cos \theta - 2 \left(-\frac{\cos^3 \theta}{3} \right) - \frac{\cos^5 \theta}{5} \right]_{\alpha}^{\pi}}{-\frac{1}{2} (-\sin^4 \alpha)} \\
 &= \frac{(1 + \cos \alpha) + \frac{2}{3} (-1 - \cos^3 \alpha) + \frac{1}{5} (1 + \cos^5 \alpha)}{\frac{1}{2} \sin^4 \alpha} \tag{5.12}
 \end{aligned}$$

$$= \frac{30(1 + \cos \alpha) - 20(1 + \cos^3 \alpha) + 6(1 + \cos^5 \alpha)}{15 \sin^4 \alpha} \tag{5.13}$$

Experiment 6

Alpha Particle Range in Air

6.1 Purpose

1. To study the energy loss of charged particles in matter.

6.2 Theory

As charged particles traverse matter, they lose energy by ionizing atoms along their path. As the amount of energy lost per collision is approximately constant, each particle will have a path length or range in a given stopping material dependent on its incident energy. Thus for any particular type of particle the range is a definite function of the energy as shown in Figure 6.1. The mean range of particles is defined as shown in Figure 6.2, where n_o is the number of particles reaching a detector with no stopping material present and n is the number reaching the detector with stopping material of x cm between the source and the detector.

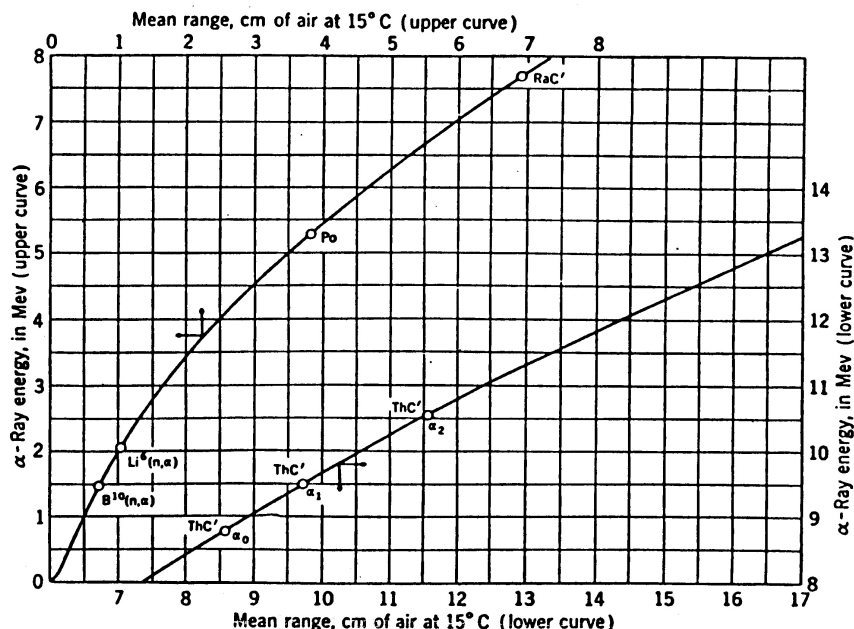


Figure 6.1: Range-energy relationship for α particles.

The mean range of alpha particles can also be found by plotting the differential range or the difference in the number of alpha particles detected for each increment of absorber as shown in Figure 6.3. The distribution of ranges about the mean range is Gaussian i.e.

$$\frac{\Delta n_i}{n_0} = \frac{\Delta x_i}{\alpha\sqrt{\pi}} e^{-\frac{(x_i - R)^2}{\alpha^2}} \quad (6.1)$$

where $\Delta n_i/n_o$ is the fraction of particles having range between x_i and $x_i + \Delta x_i$. The range straggling parameter, α , is the half width of the range distribution at $1/e$ of maximum as shown in Figure 6.3. The best measurements have shown that $\alpha = 0.15R$

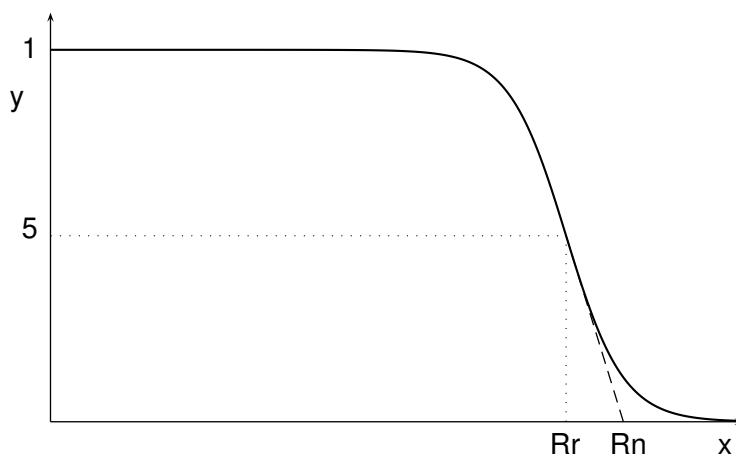


Figure 6.2: The extrapolated number-distance range R_n exceeds the mean range R by 0.886α , where α is the range-straggling parameter.

The distribution is broadened by alpha particles scattering off the inside of the chamber, the finite energy resolution of the detector, and the thickness of the source itself. If the width of the differential range curve is broad or asymmetric, the energy might be best determined using the extrapolated range.

The rate of energy loss of alpha particles is given as

$$-\frac{dE}{dx} = \frac{4\pi Z^2}{m_e v^2} \left(\frac{e^2}{4\pi\epsilon_0} \right)^2 n_e \ln \frac{2m_e v^2}{I} \quad (6.2)$$

where I is some average ionization potential of the material, Z is the atomic number of the incoming particle, v is its (non-relativistic) velocity, and n_e is the electron density of the scattering material.

While the concepts explored in this experiment have plenty of applications in nuclear physics and nuclear medicine, there are less obvious applications. In particular, semiconductors are often doped in a similar way, although the dopants are normally neutral atoms and are slowed by collisions with the lattice.

Chamber Air Pressure Measurement

A solid state pressure transducer is used to convert pressure into voltage readings. The transducer uses strain gauges in a bridge configuration to measure the displacement produced in a solid plate by having an absolute vacuum (static) applied to one side and the working pressure applied to the other.

The transducer is calibrated at $P = 1$ atm and vacuum. Measure the atmospheric pressure when you do the lab using the Fortin barometer on the end of the bookshelves near the lab door. The other calibration point is obtained by pumping the chamber to $P \approx 0$ mmHg using the vacuum pump. A linear interpolation is used to determine the chamber pressure from the transducer response.

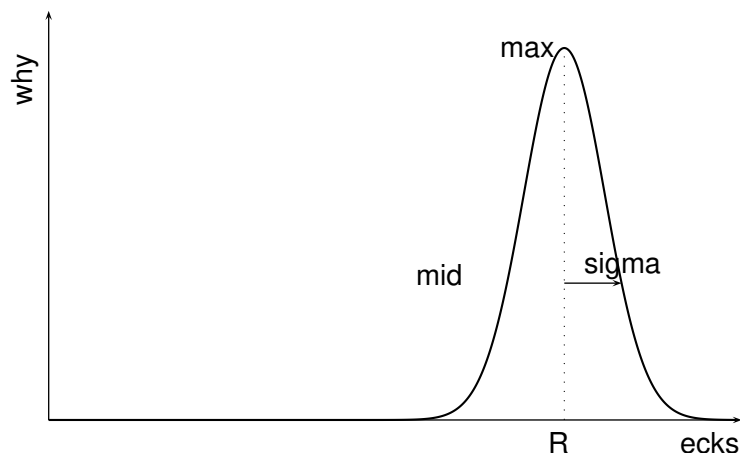


Figure 6.3: Schematic “number-range curve,” illustrating a symmetric distribution of ranges about the mean range R . The “range straggling parameter” α is $\sqrt{2}$ times the standard deviation of the range distribution.

In this experiment, the range will be varied by increasing the air pressure in the vacuum chamber. Adjust the source-detector distance to $d_0 \approx 4.5$ cm, so that the effective distance, d , between the source and detector will be approximately given by

$$d = \frac{P}{P_{atm}} d_0 \quad (6.3)$$

6.3 Procedure

BEFORE STARTING: Read the precautions on using the surface barrier detector located at the lab bench. Do not touch either the detector or the radioactive sample ($\sim 1\mu\text{Ci } ^{241}\text{AmO}_2$).

1. Connect the apparatus as shown in Figure 6.4, and turn on the equipment. Open the UC530 application. Ensure that the bias voltage (“high voltage”) for the detector is set to zero. Check that when you turn it on it will be negative (hardware switch in one setup, software in the other).
2. Calibrate the pressure transducer as outlined above, and verify the separation between source and detector is ≈ 4.5 cm, recording the actual value. Evacuate the chamber when finished.
3. **START THE NEGATIVE BIAS VOLTAGE AT 10-20 VOLTS AND TURN UP SLOWLY, MAKING SURE NOT TO EXCEED THE MAXIMUM ALLOWED FOR THE DETECTOR, THE BIAS POWER SUPPLY GOES UP TO 1000V!**

Detector serial number	Max voltage
16-625J	-100 volts
16-721J	-75 volts
16-469A	-100 volts

4. Adjust the bias voltage for best signal to noise and adjust the amplifier gain. On one set-up with the older data acquisition system, adjust the gain so that the pulses are approximately

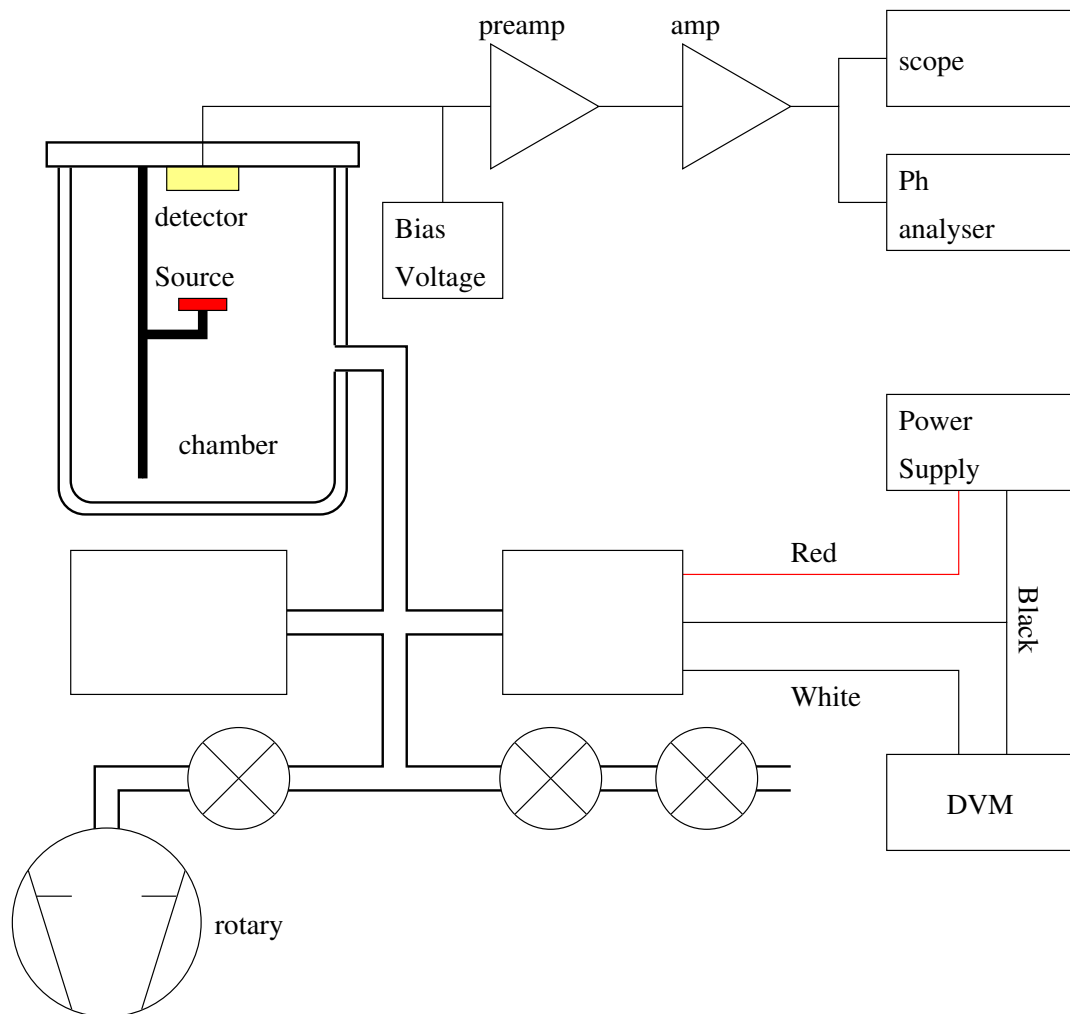


Figure 6.4: Schematic diagram of the apparatus.

8 volts on the oscilloscope. With the newer data acquisition system you should set the gain so that the highest energy pulses are on scale.

5. Observe the pulse height spectrum using the pulse height analyzer, perhaps re-adjusting the amplifier gain so that the energy spectrum is at the right of the display. Note: to clear the spectrum in the older setup, use control-F2.
6. Close the valve to the pump and observe the change in pulse height as air is admitted to the chamber.
7. Now re-evacuate the chamber and record the count rate and the centroid on the pulse height analyzer. You will want to set your Region-Of-Interest (ROI) to be just above the noise in the first several channels. Observe the rate and centroid channel at several different pressures. The points near the end of the range (near atmospheric pressure) are the most important, so get plenty of data in this range. How would you calculate the error on the number of counts?
8. Convert the transducer voltage readings into pressure values using your calibration.

9. Convert the channel of the centroid into energy assuming a linear calibration. Take the centroid channel at vacuum to equal the full source energy and assume channel 0 is at 0 MeV.
10. Plot the centroid of the energy as a function of effective distance in air and fit a curve to the data (the curve you fit should be based on Eq. 6.2).
11. Plot the derivative of the curve, again as a function of effective distance, and display together with the curve from above on the same axis. This gives you the energy loss per unit length and is called the Bragg Curve. Is it what you expected?
12. Plot the count rate as a function of effective distance. Also plot the derivative of the curve as a function of effective distance and again display the curves together.
13. Determine the range and range straggling parameter.

When you are finished with the equipment, please turn the bias power supply back down to 0 V, and vent the pump when you turn it off: fully open the two air admittance valves and then open the pump valve and then shut off the pump.

6.4 References

- Evans, **The Atomic Nucleus**, Pages 650 - 667.
- Melissinos, **Experiments in Modern Physics**, sections 5.2.2, 5.2.3, and 5.5.3 (first edition).

Experiment 7

Electromagnetic Skin Depth of Metals

7.1 Purpose

1. To understand and familiarize yourself with the occurrence and principles of electromagnetic shielding.
2. To quantitatively examine the skin depth problem by determining the skin depths of some metallic pipes.

7.2 Theory

It is common knowledge that electromagnetic radiation does not pass easily through a metal. The time-varying electric and magnetic fields generate relatively large screening currents in the metal; the characteristic length scale of the fields' resulting attenuation is the skin depth. This shielding "efficiency" is strongly dependent on the frequency of the radiation, as determined by the Maxwell equations.

Let a long metal pipe be immersed in a uniform magnetic field which is varying with time as $e^{-i\omega t}$. The magnetic field is parallel to the cylinder axis, and this direction is taken to be the \hat{z} direction of a cylindrical co-ordinate system. The pipe has an outer diameter $2R_2$ and inner diameter $2R_1$.

The amplitude and phase of the magnetic field inside the pipe can be calculated using Maxwell's equations. Our situation has cylindrical symmetry, so \vec{E} and \vec{H} depend only upon the radius. Moreover, \vec{H} has only one component, H_z , and this component does not depend on z – how good is this approximation? Applying boundary conditions at the inner and outer surfaces of the pipe and taking the conductivity σ to be non-zero, an exact solution may be found to compute the attenuation and phase difference for the fields inside and outside the pipe. Due to the cylindrical nature of the problem, the solution involves Bessel's functions.

The solution can be simplified at high frequencies because Bessel's functions have rather simple limiting forms for large arguments. This solution is:

$$\frac{H_i}{H_o} = \rho e^{i\phi} \quad (7.1)$$

$$\rho = 2\sqrt{\frac{R_2}{R_1}} \left\{ \frac{e^{-k_o(R_2-R_1)}}{\sqrt{1 + R_1 k_o + \frac{R_1^2 k_o^2}{2}}} \right\} \quad (7.2)$$

$$\phi = k_o(R_2 - R_1) + \arctan\left(\frac{R_1 k_o}{2 + R_1 k_o}\right) \quad (7.3)$$

$$k_o = \sqrt{\frac{\omega\sigma\mu}{2}} \quad (7.4)$$

where

H_o = magnetic field outside the pipe

H_i = magnetic field inside the pipe

R_1 = inner radius of the pipe

R_2 = outer radius of the pipe

σ = conductivity of the metal ($\approx 3 \times 10^5 \frac{1}{\Omega \cdot \text{cm}}$ for Al)

μ = permeability of the metal

ω = angular frequency

★NOTE: This high frequency approximation breaks down for $k_o(R_2 - R_1) \lesssim 1$. You should check what frequency this is. It is recommended that you still take data below this point, to see how seriously the equations' breakdown is, and to check where it occurs.

7.3 Procedure

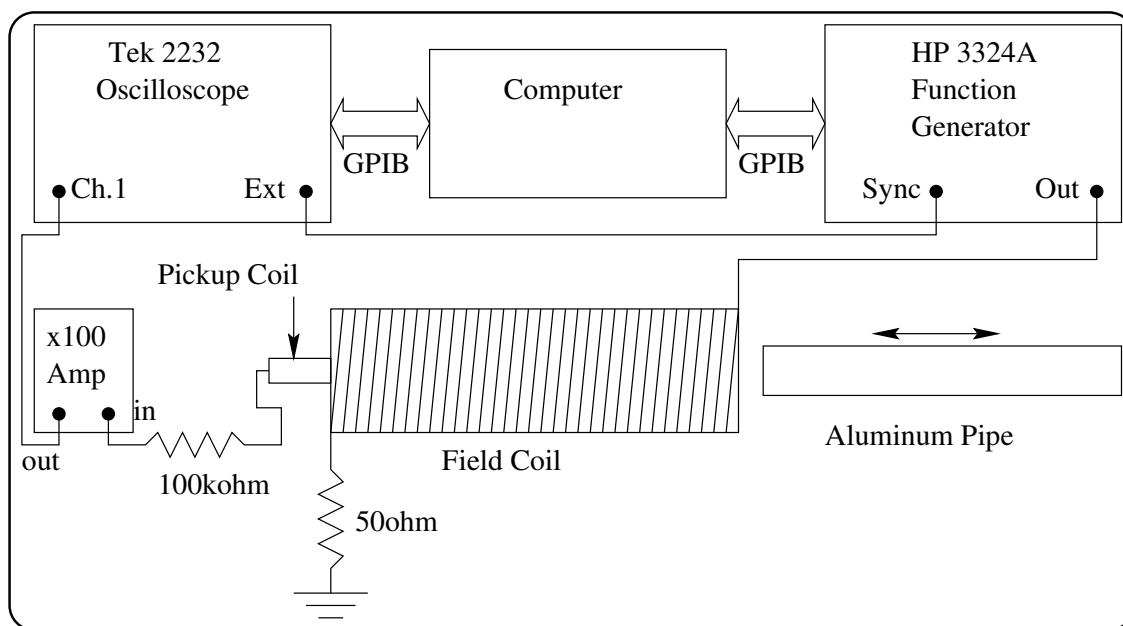


Figure 7.1: A schematic diagram of the skin depth apparatus.

In this experiment you will measure the phase and amplitude of an alternating magnetic field inside a metal pipe relative to the field without the pipe. The schematic diagram of the apparatus is shown in figure 7.1. A Physics 409 lab at the same station uses steel pipes as well as aluminum and copper, so make sure that your aluminum pipe is really aluminum – there are some very significant differences between aluminum and steel!

A coil approximately 6" long, 2" in diameter, and wound with approximately 10 turns per cm, is connected to an HP3324A synthesized function generator through a 50Ω resistor to avoid short circuiting the output from the oscillator. This system is used to generate an AC magnetic field

over the frequency range 100 Hz to 80 kHz. A pick-up coil consisting of 200 turns of #38 Formex insulated copper wire wound on a $\frac{3}{8}$ " diameter form is used to probe the magnetic field generated in the primary coil. The small e.m.f. generated in the pick-up coil is first amplified by a pre-amp with a $100\text{k}\Omega$ termination, then displayed on a Tek 2232 digital storage scope.

A LabView-based program on the computer's desktop is used to input the data from the scope to the PC. It will guide you through the data collection process and will control the function generator; you must control the oscilloscope. The program obtains a digitized version of the oscilloscope trace (1024 points), then fits it to a sinusoid of the form $A + B \cos(\omega t - \phi)$. For the most accurate fit, the voltage settings on the oscilloscope should keep the waveform as large as possible and there should be between 2 and 5 waveform periods visible. The program will prompt you to change the time scale on the oscilloscope between data points. The program outputs a tab-separated text file (*.SKD) with the frequency and fitting parameters (A , B and ϕ). It can also output waveform files (the digitized scope traces) if you want to check the fit.

The phase is measured from the nearest peak to the leftmost edge of the waveform image, so there is some ambiguity about what "phase" precisely means. While the data acquisition program is working, plot out the equation for ϕ as a function of ω with MATLAB and compare the result with what you see emerging from the experiment.

1. Open the Skin Depth program and follow the equipment setup instructions.
2. Using calipers, accurately measure the inner and outer radii of the two pipes. Using an accepted value for each conductivity, determine at what point the high-frequency approximation should break down.
3. Take data at frequencies between 100 Hz and 80 kHz, ensuring that the signal is not clipped or distorted by the pre-amp. Measure the amplitude and phase at each frequency for aluminum, copper, and air. You may need to re-take some of the high-frequency pipe data with a higher-amplitude signal from the function generator if the signal devolves into noise. This is easily corrected for later, especially if there's overlap in the data. Note that the program only attempts to save your data once, so save it to the hard disk first, where there will certainly be space for it. You can transfer it elsewhere later, by floppy, SSH/SFTP or web.
4. Calculate the expected values of the amplitude ratio and phase difference at each frequency, and compare them to their measured values.
5. Do a non-linear least squares fit to your data to find the conductivities. How different are your values from the accepted values?
6. For each metal, compare the results obtained by solving each data point for a skin depth value versus the expected results using your average σ found above and the expected σ .

Experiment 8

NMR: Spin-Spin Coupling

8.1 Introduction

Nuclear Magnetic Resonance (NMR) is a quantum mechanical effect which has been well-studied in physics and has been put to extensive use in chemistry, and more recently in medicine as Magnetic Resonance Imaging or MRI (people are often scared of the word “nuclear”). Many nuclei, most notably the proton, have non-zero spin angular momentum (which is quantized), and these magnetic moments tend to align with an applied DC field. The timescales for growth toward equilibrium and decay of any transverse magnetization are in general quite different, and can provide information about the nuclei’s environments.

Despite the fact that NMR is a quantum phenomenon, we recognize that most students in Physics 352 do not have the quantum background necessary to fully understand the derivation of NMR. A classical picture can be used to convince you of many of the effects you will observe, but keep in mind that they offer a misleading view of NMR. As long as you don’t think too hard about what’s going on or attempt to predict behaviour that isn’t mentioned, classical mechanics should be perfectly adequate. As an example of what can go wrong, the first sentence of the Theory section seems perfectly reasonable until you look up the radius of a proton or electron and compare the required speed with the speed of light.

8.2 Theory

Classically, nuclei with spin act like spinning charged spheres — you can convince yourself that these have both angular momentum and a magnetic moment. In this experiment, we will work with the hydrogen nucleus (a proton) and ^{19}F — since ^{19}F behaves very much like a proton, we will only concern ourselves with the proton in this section. The proton will have a magnetic moment $\vec{\mu}$ and angular momentum \vec{J} , related by

$$\vec{\mu} = \gamma \vec{J} \quad (8.1)$$

where γ is called the gyromagnetic ratio (use caution when reading the references — the meaning of this term is highly source-dependent), and varies by isotope. Angular momentum is quantized in units of \hbar , so $\vec{J} = \hbar \vec{I}$, where \vec{I} is the nuclear spin.

The energy U of the nucleus due to an applied \vec{B} field is

$$U = -\vec{\mu} \cdot \vec{B} \quad (8.2)$$

The direction of the applied field \vec{B}_0 is taken to be the \hat{z} direction, so

$$U = -\mu_z B_0 = -\gamma \hbar I_z B_0 \quad (8.3)$$

As for all angular momenta, the allowed values of I_z , m_I , are quantized as $m_I = I, I-1, \dots, -I$. Since both ^1H and ^{19}F have $I = \frac{1}{2}$, the allowed values of I_z are $m_I = \pm \frac{1}{2}$, shown in figure 8.1. A key tenet of quantum mechanics is that energy and frequency are proportional, with the constant of

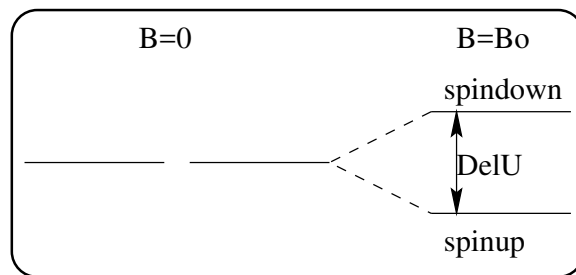


Figure 8.1: A proton's spin states with and without an applied magnetic field.

proportionality being Planck's constant, so the energy difference (splitting) between the two states may be written as an angular frequency:

$$\Delta U = 2 \left(\gamma \hbar \frac{1}{2} B_o \right) = \hbar \omega_o \quad (8.4)$$

where the resonant frequency is $\omega_o = \gamma B_o$.

Since we're working at non-zero temperature, the lower and higher energy states' populations (N_1 and N_2 respectively) will be governed by Boltzmann statistics:

$$\frac{N_2}{N_1} = e^{-\frac{\Delta U}{k_B T}} = e^{-\frac{\hbar \omega_o}{k_B T}} \quad (8.5)$$

giving the net magnetization

$$M_z = (N_1 - N_2) \mu_z = N \mu \tanh \left(\frac{\mu B}{k_B T} \right) \approx N \frac{\mu^2 B}{k_B T} \quad (8.6)$$

8.3 Spin-Lattice Relaxation Time

Equilibrium magnetization doesn't appear spontaneously; M_z grows exponentially toward equilibrium when the sample is placed in a magnetic field or displaced from equilibrium (see figure 8.2). The time constant governing this growth is called T_1 , the spin-lattice relaxation time.

$$\frac{dM_z(t)}{dt} = \frac{M_o - M_z(t)}{T_1} \quad (8.7)$$

If an unmagnetized sample is placed in a magnetic field ($M_z(0) = 0$), then direct integration of equation 8.7 gives

$$M_z(t) = M_o \left(1 - e^{-\frac{t}{T_1}} \right) \quad (8.8)$$

T_1 values can vary from microseconds to seconds for solid and liquid samples, and can be several weeks for some gas samples (^3He for example). If a nucleus finds itself in the higher-energy state when the field is turned on, it will be inclined to decay to the lower-energy state. In doing so, it must change not only its energy but also its angular momentum, and both the energy and angular momentum must be transferred out of the system, either through collisions or radiation. In order for it to decay in the first place, it requires an interaction of some sort (usually a collision), since the initial and final states are both eigenstates, and their orthogonality prohibits transitions under

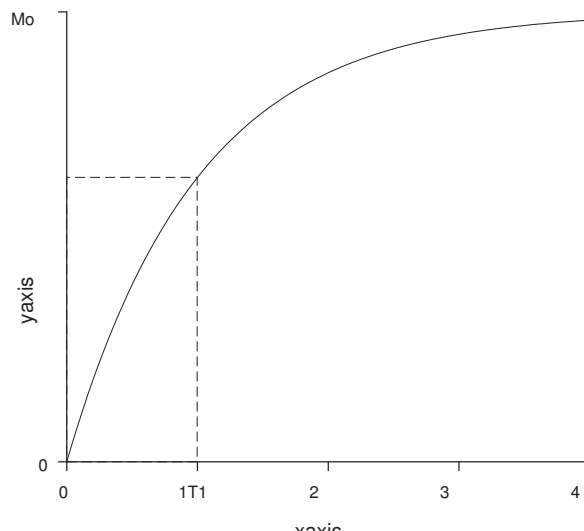


Figure 8.2: Exponential growth of the magnetization toward its equilibrium value.

normal circumstances. Variations in T_1 between different materials are due to the frequency and effectiveness of interactions between particles and their surroundings (the “lattice”, whether or not it actually is a lattice) at producing a transition and removing energy and angular momentum. The study of these processes is a major topic in NMR research.

8.4 Spin-Spin Relaxation Time

In thermal equilibrium, there is no magnetization in the xy plane, since angular momentum can only be known about one axis at a time. This can also be justified classically: The torque $\vec{\tau}$ on each is $\vec{\mu} \times \vec{B}$, but $\vec{\tau} = \frac{d\vec{J}}{dt}$ and $\vec{J} = \frac{\vec{\mu}}{\gamma}$ from equation 8.1, so

$$\vec{\mu} \times \vec{B} = \frac{1}{\gamma} \frac{d\vec{\mu}}{dt} \quad (8.9)$$

or, for the whole sample,

$$\frac{d\vec{M}}{dt} = \gamma \vec{M} \times \vec{B} \quad (8.10)$$

It can be shown from equation 8.10 that the magnetic moment will precess, with the precessional frequency $\omega_o = \gamma B_o$ first seen in equation 8.4. Since the particles in the sample started out with random phases, they will continue summing to zero.

What would happen, though, if we started out with the magnetic moments rotating in phase in the xy plane? This situation is a combination of spin-up and spin-down (in z) states, and will decay exponentially with a time constant T_2 , the spin-spin relaxation time:

$$\frac{dM_{xy}}{dt} = -\frac{M_{xy}(t)}{T_2} \quad (8.11)$$

As the name suggests, this decay is due not only to the T_1 processes, but also to the spins' magnetic moments interacting with each other. Each spin sees not only the DC field \vec{B}_o , but the

fields from its neighbours. This means that different protons see different fields depending on their environment, and there is actually a range of precessional frequencies. If the spins start out in phase, they soon dephase, and the rotating coherent xy magnetization goes to zero. T_2 , then, provides information on the distribution of local fields at the nuclear sites.

8.5 Spin-Spin Coupling

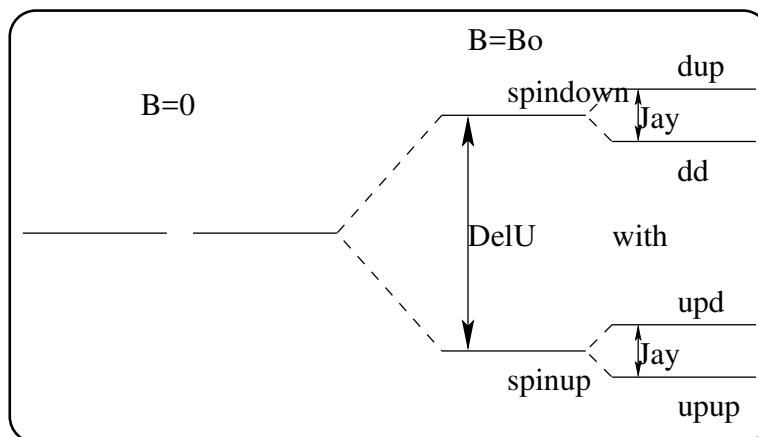


Figure 8.3: A proton's spin states in the presence of a second nuclear spin, where having the two spins aligned is energetically favourable.

When two NMR-active nuclei are coupled to each other, whether they interact directly or via electrons in the molecule, their energies split. The energy for the first spin to be up will depend on whether the other spin is up or down, and vice versa. When one spin is flipped, it changes the sign of its interaction with both the applied field and the second spin. Figure 8.3 shows the states present when having the two spins aligned is energetically favourable. Note that flipping the first spin does not change the energy by $\hbar\omega_o$, but by $\hbar\omega_o \pm \frac{J}{2}$ depending on the state of the second spin.

The splitting, J , between the observed transition energies (for flipping the first spin) is an indication of how strongly it interacts with the other spin. The second spin will have the same splitting J appear in its spectrum.

If we can flip one spin independent of the other (e.g. if they have different gyromagnetic ratios and thus resonant frequencies), we should find absorptions at energies of $\hbar\omega_o \pm \frac{J}{2}$, and the up and down first spins will precess at frequencies $\omega_o \pm \frac{J}{2\hbar}$ about an applied field. If the second spin's populations were equal (infinite temperature), we would have a signal proportional to

$$N_1 e^{i(\omega_o + \frac{J}{2\hbar})t} + N_2 e^{i(\omega_o - \frac{J}{2\hbar})t} = \frac{N}{2} e^{i\omega_o t} \left(e^{i\frac{J}{2\hbar}t} + e^{-i\frac{J}{2\hbar}t} \right) \quad (8.12)$$

$$= N e^{i\omega_o t} \cos \frac{Jt}{2\hbar} \quad (8.13)$$

where $N e^{i\omega_o t}$ describes the precession in the absence of interloping neighbours. This result amounts to putting the unperturbed precession signal inside a sinusoidal envelope.

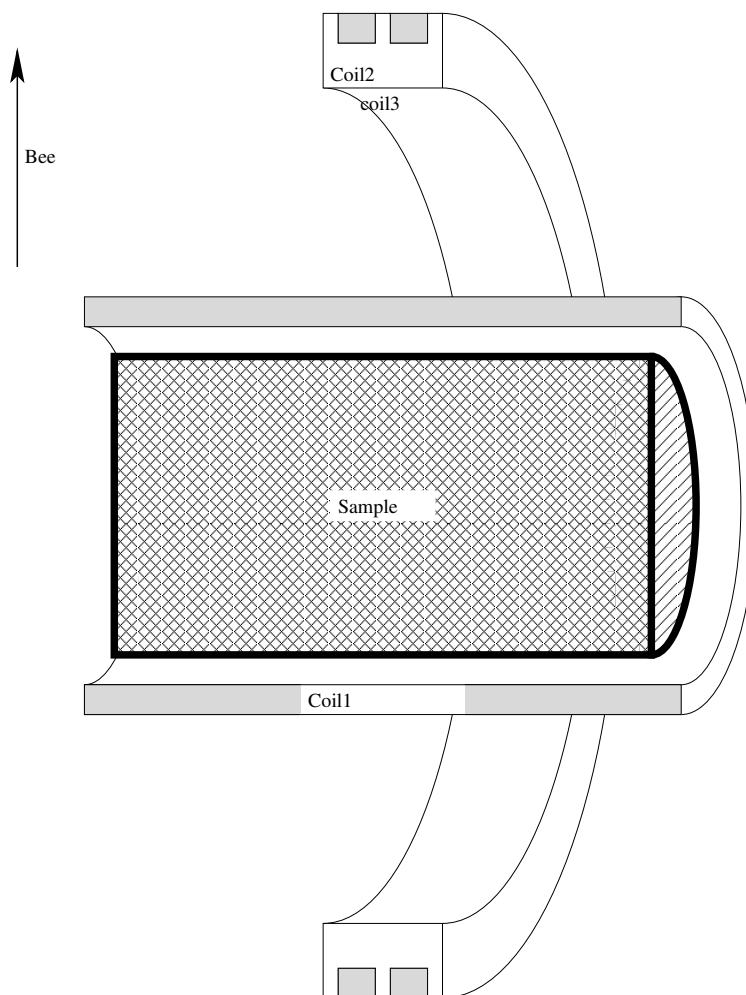


Figure 8.4: Schematic diagram of the EF-NMR apparatus and sample. The more distant gradient coils are not shown.

8.6 Apparatus

The sample is held in a Nalgene bottle, which is placed inside a set of three coils (which should be perpendicular to the earth's field) — see figure 8.4. The central coil is used to apply a DC field to polarize the sample and is later reused to measure its precession. A set of two bucking coils surround this, farther from the sample. The bucking coils combined have the same product of turns times area as the inner coil. Any stray fields will induce the same voltage in the bucking coils as the inner coil, so the coils are connected in series such that this noise cancels out. Rotating magnetization in the sample induces much stronger currents in the inner coil than the outer, so this signal survives essentially intact. The coil assembly is mounted as far as possible from noise sources and ferromagnetic materials.

If you have rotating magnetization inside a coil, and the axis of rotation is not parallel to the coil's axis, an AC signal is induced in the coil — this is how AC wall power is generated, and it allows you to measure M_{xy} .

8.7 Procedure

1. Turn on the main EF-NMR controller and its power supply, place a 125 mL Nalgene bottle full of water inside the centre coil, and connect an oscilloscope to the outputs.
2. Ensure you have an optimal signal (see procedure in the manual on the bench). Note you may need to change the field gradient adjustment.
3. Depressing the start button runs a current through the central coil for a set period of time (controlled via a dial below the digital readout), polarizing the sample along an axis that's (hopefully) perpendicular to the earth's field. When this polarizing field shuts off, the newly formed magnetization slowly decays while precessing about the earth's field. The timescale for the former process is T_1 , while the timescale for the latter is T_2 . Measure T_2 and, by varying the polarization time, determine T_1 .
4. In place of the water, insert a bottle of a fluorinated oil. Repeat the above experiment to determine T_1 and T_2 for ^{19}F in the oil.
5. From the precession frequencies of ^{19}F and ^1H , determine ^{19}F 's gyromagnetic ratio. Determine the magnitude of the earth's magnetic field.
6. Look carefully at the free induction decay signals from the water and the fluorinated oil. Aside from the amplitude and frequency, do you see any difference? Take a Fourier transform of the two free induction decays and plot the spectra. Can you explain the differences between them?
7. It's also possible to study the effect of changing concentrations of dirt in water. Dirt probably meaning CuSO_4 , as it's actually magnetic.
8. There are field gradient coils around the sample, allowing x , y and z gradient fields. If you have time and the inclination, you can explore the use of the gradients (please record the current settings on the gradients before you adjust them, and return them to their optimal settings when you are done). Is it possible to use the gradients to create an image of your sample?
9. Tip: To write to the computer the baud rate has to be 38400 - if this gets set to something else, you can't get the data out.

8.8 References

1. The Basics of NMR, by Joseph P. Hornak: <http://www.cis.rit.edu/htbooks/nmr>
2. WebElements: <http://www.webelements.com>

Experiment 9

Pulsed NMR

9.1 Purpose

To become familiar with NMR principles and techniques.

9.2 Introduction

Nuclear Magnetic Resonance is a quantum mechanical effect which has been well-studied in physics and has been put to extensive use in chemistry, and more recently in medicine as MRI (many people are scared of the word “nuclear”). Many nuclei, notably the proton, have spin angular momentum, and these magnetic moments will tend to align with an applied DC field. With a pulse of radio frequency (RF) magnetic field, the net magnetization can be rotated to an arbitrary angle, from where it will decay back to equilibrium. The timescales for growth toward equilibrium (parallel to the field) and decay of the transverse component of the magnetization are in general quite different, and can provide information about the nuclei’s environments.

Despite the fact that NMR is a quantum phenomenon, we recognize that most students in Physics 352 do not have the quantum background necessary to fully understand the derivation of NMR. A classical picture can be used to convince you of many of the effects you will observe, but keep in mind that they are the wrong way of looking at NMR. As long as you don’t think too hard about what’s going on or attempt to predict behaviour that isn’t mentioned, classical mechanics should be perfectly adequate. As an example of what can go wrong, the first sentence of the Theory section seems perfectly reasonable until you look up the radius of a proton or electron and compare the required speed with the speed of light. A short Appendix (section 9.11) is provided with a simplified quantum mechanical derivation of some of the main results.

9.3 Theory

Classically, nuclei with spin act like spinning charged spheres – you can convince yourself that these have both angular momentum and a magnetic moment. In this experiment, we will only concern ourselves with the hydrogen nucleus (a proton). The proton will have a magnetic moment $\vec{\mu}$ and angular momentum \vec{J} , related by

$$\vec{\mu} = \gamma \vec{J} \quad (9.1)$$

where γ is called the gyromagnetic ratio (use caution when reading the references – the meaning of this term is highly source-dependent). \vec{J} is quantized in units of \hbar , $\vec{J} = \hbar \vec{I}$, where \vec{I} is the nuclear spin.

The magnetic energy U of the nucleus in an applied \vec{B} field is

$$U = -\vec{\mu} \cdot \vec{B} \quad (9.2)$$

The direction of the applied field \vec{B}_o is taken to be the \hat{z} direction, so

$$U = -\mu_z B_o = -\gamma \hbar I_z B_o \quad (9.3)$$

The allowed values of I_z , m_I , are quantized as $m_I = I, I - 1, \dots, -I$. Since the proton has spin one-half ($I = \frac{1}{2}$), the allowed values of I_z are $m_I = \pm\frac{1}{2}$, so there are only two magnetic states. These are shown in figure 9.1. A key tenet of quantum mechanics is that energy and frequency are

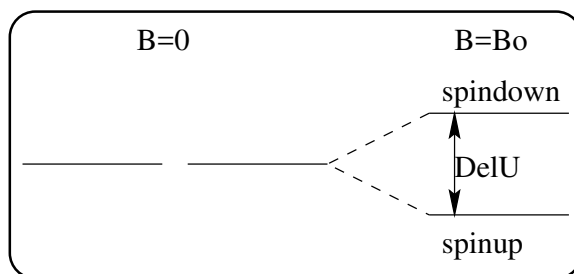


Figure 9.1: A proton's spin states.

proportional, with the constant of proportionality being Planck's constant, so the energy difference (splitting) between the two states may be written as an angular frequency:

$$\Delta U = 2 \left(\gamma \hbar \frac{1}{2} B_o \right) = \hbar \omega_o \quad (9.4)$$

So the resonant frequency $\omega_o = \gamma B_o$. For the proton, $\gamma = 2.675 \times 10^8 \frac{rad}{s \cdot T}$, or

$$f_o = 42.58 \frac{MHz}{T} B_o \quad (9.5)$$

Since we're working at non-zero temperature, the lower and higher energy states' populations (N_1 and N_2 respectively) will be governed by Boltzmann statistics:

$$\frac{N_2}{N_1} = e^{-\frac{\Delta U}{k_B T}} = e^{-\frac{\hbar \omega_o}{k_B T}} \quad (9.6)$$

giving the net magnetization

$$M_z = (N_1 - N_2) \mu_z = N \mu \tanh \left(\frac{\mu B}{k_B T} \right) \approx N \frac{\mu^2 B}{k_B T} \quad (9.7)$$

9.4 Spin-Lattice Relaxation Time

This equilibrium magnetization doesn't just appear; M_z grows exponentially toward equilibrium when placed in a magnetic field or displaced from equilibrium (see figure 9.2). The time constant governing this growth is called T_1 , the spin-lattice relaxation time.

$$\frac{dM_z(t)}{dt} = \frac{M_o - M_z(t)}{T_1} \quad (9.8)$$

If an *unmagnetized* sample is placed in a magnetic field ($M_z(0) = 0$), then direct integration of equation 9.8, with *these* initial conditions, gives

$$M_z(t) = M_o \left(1 - e^{-\frac{t}{T_1}} \right) \quad (9.9)$$

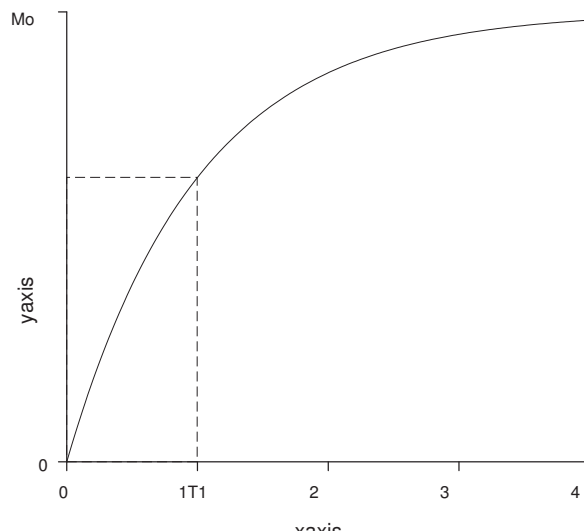


Figure 9.2: Exponential growth of the magnetization toward its equilibrium value.

This is absolutely **NOT** what you will be dealing with in this experiment – you will have different initial conditions!

T_1 values can vary from microseconds to seconds for solid and liquid samples, and can be several weeks for some gas samples (^3He for example). If a particle finds itself in the higher-energy state when the field is turned on, it will be inclined to decay to the lower-energy state. In doing so, it must change not only its energy but also its angular momentum, and both the energy and angular momentum must be transferred out of the system, either through collisions or radiation. In order for it to decay in the first place, it requires an interaction of some sort (usually a collision), since the initial and final states are both eigenstates, and their orthogonality prohibits transitions under normal circumstances. The great variation in T_1 is therefore due to the frequency and effectiveness of interactions between particles and their surroundings (the “lattice”, whether or not it actually is a lattice) at producing a transition and removing energy and angular momentum. The study of these processes is one of the major topics in NMR research.

In practice, T_1 is measured using a sequence of two pulses of radio frequency radiation (RF). A π pulse is used to invert the magnetization, then after a delay of τ , a $\frac{\pi}{2}$ pulse rotates whatever magnetization there may be into the xy plane where it can be measured (see figure 9.3). How and why the magnetization can be rotated is described in section 9.6, and why it’s measured in the xy plane is described in section 9.7.

9.5 Spin-Spin Relaxation Time

In thermal equilibrium, there is no magnetization in the xy plane, since angular momentum can only be known about one axis at a time. This can also be justified classically: The torque $\vec{\tau}$ on each is $\vec{\mu} \times \vec{B}$, but $\vec{\tau} = \frac{d\vec{J}}{dt}$ and $\vec{J} = \frac{\vec{\mu}}{\gamma}$ from equation 9.1, so

$$\vec{\mu} \times \vec{B} = \frac{1}{\gamma} \frac{d\vec{\mu}}{dt} \quad (9.10)$$

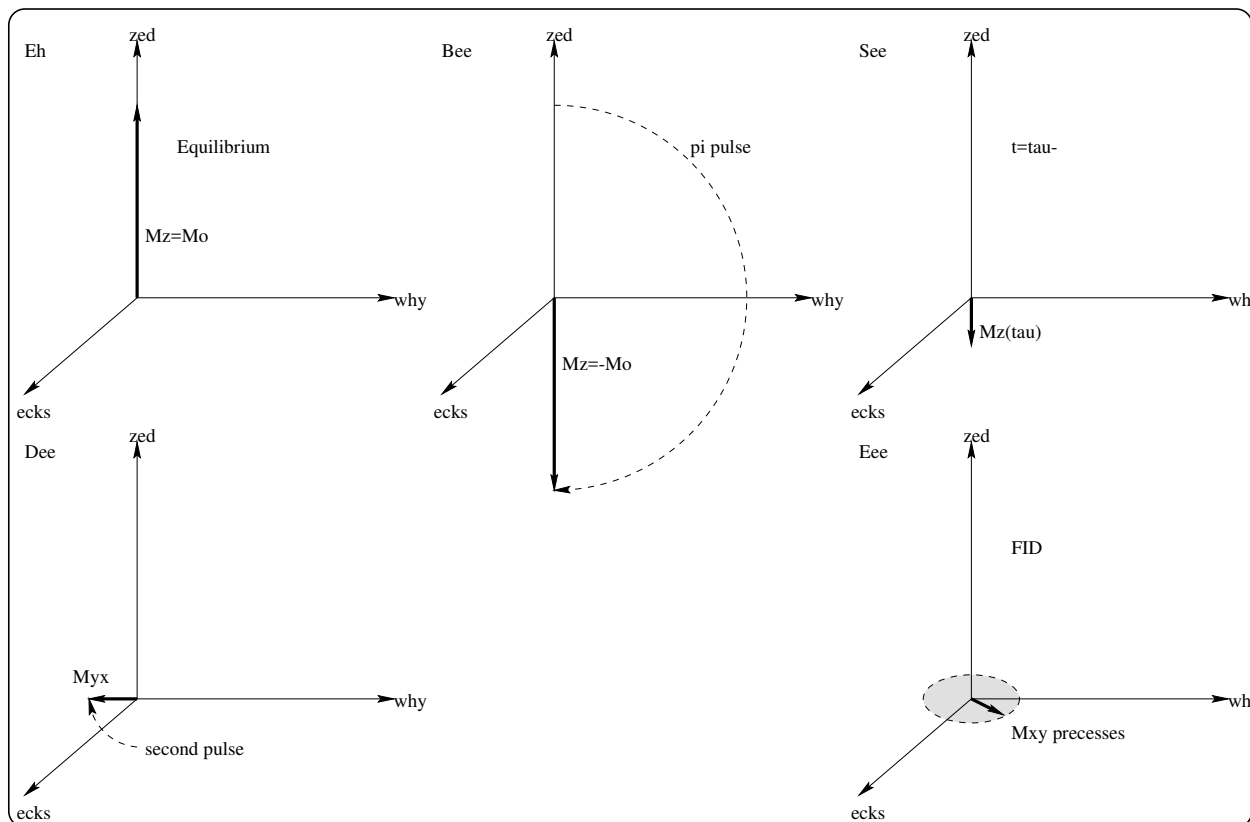


Figure 9.3: Measuring T_1 : **a)** The initial magnetization is $M_o\hat{z}$. **b)** A π pulse is used to invert the magnetization to $-M_o\hat{z}$. **c)** M_z decays back toward equilibrium until $t = \tau$... **d)** when a $\frac{\pi}{2}$ pulse is used to rotate the magnetization into the xy plane... **e)** where it precesses briefly, and can be measured, before it vanishes again. In these figures, $\vec{B} = B_o\hat{z}$.

or, for the whole sample,

$$\frac{d\vec{M}}{dt} = \gamma\vec{M} \times \vec{B} \quad (9.11)$$

It can be shown from equation 9.11 that the magnetic moment will precess, with the precessional frequency $\omega_o = \gamma B_o$ first seen in equation 9.4. Since the particles in the sample started out with random phases, they will continue summing to zero.

What would happen, though, if we started out with the magnetic moments rotating in phase in the xy plane? This situation is a combination of spin-up and spin-down states, and will decay exponentially with time constant T_2 , the spin-spin relaxation time:

$$\frac{dM_{xy}}{dt} = -\frac{M_{xy}(t)}{T_2} \quad (9.12)$$

As the name suggests, this decay is due not only to the T_1 processes, but also to the spins' magnetic moments interacting with each other. Each spin sees not only the large applied field \vec{B}_o , but the small fields from its neighbours. This means that different protons see different fields depending on their neighbours, and there is actually a range of precessional frequencies. Even if the spins started out in phase, they soon have random phases, and the rotating xy magnetization goes to zero. T_2 , then, provides information on the distribution of local fields at the nuclear sites.

The sensible way to find T_2 would seem to be flipping the equilibrium M_z into the xy plane and watching it decay. This is called the Free Induction Decay (FID). Unfortunately, the magnet in the lab has its own field inhomogeneities, such that the “sweet spot” in the middle allows a maximum 0.3ms decay time. If $T_2 \lesssim 0.3\text{ms}$, this isn’t a problem, but most samples require an additional trick.

The spin-echo technique allows the measurement of any T_2 , without the necessity of buying a better and more expensive magnet. If we first rotate the magnetization from \hat{z} into the xy plane, then rotate by a further π a time τ later, the dephasing due to the magnet’s inhomogeneity is reversed, and the spins rephase a further time τ after that, for another FID. This works like the following egalitarian kindergarten footrace: Each kid runs in a straight line as fast as he or she can until the teacher blows a whistle, at which point the kids run back. The faster kids go farther, and must return a greater distance, so all return at the same time. The whistle in this case is the π rotation. The spins in larger fields precess faster by $\Delta\theta(t)$ until $t = \tau$, at which point the magnetization is flipped π , and their headstart becomes an impediment. At $t = 2\tau$, the $\Delta\theta$ from $t = \tau$ to 2τ has completely cancelled the opposite $\Delta\theta$ from $t=0$ to τ , and all spins are back in phase. The spin-spin interactions can’t be reversed in this manner, so the echo’s height will be lower than the original FID, due to these T_2 processes. A plot of echo height vs. delay time is a graph of the T_2 decay with the magnet’s inhomogeneity cancelled out.

9.6 Rotating \vec{M} by π or $\frac{\pi}{2}$

An RF magnetic field at ω_o will rotate the magnetization, with the length of the pulse determining the angle. The quantum mechanical explanation is contained within the appendix (section 9.11). What follows is the classical explanation, using rotating co-ordinate frames.

If we add to our DC field a rotating (circularly polarized) field \vec{B}_1 , our total field is

$$\vec{B}(t) = B_1 \cos \omega t \hat{x} + B_1 \sin \omega t \hat{y} + B_o \hat{z} \quad (9.13)$$

The convenient rotating co-ordinate frame for this problem has its axis along the static field and rotates at ω . In this frame, B_o and B_1 are joined by an effective field along the \hat{z}^* direction, of magnitude $-\frac{\omega}{\gamma}$ (this keeps the magnetization stationary in our rotating frame, which is why we chose it). The effective field in the rotating co-ordinate frame is

$$\vec{B}_{eff}^* = B_1 \hat{x}^* + \left(B_o - \frac{\omega}{\gamma} \right) \hat{z}^* \quad (9.14)$$

The equation of motion from equation 9.11 is

$$\frac{d\vec{M}}{dt} = \gamma \vec{M} \times \vec{B}_{eff}^* \quad (9.15)$$

which shows that \vec{M} will precess about \vec{B}_{eff}^* .

If the rotating field is at ω_o , $\frac{\omega}{\gamma} = \frac{\omega_o}{\gamma} = B_o$, and $\vec{B}_{eff}^* = B_1 \hat{x}^*$. The magnetization precess about this effective field at a rate $\omega_1 = \gamma B_1$. If we turn off B_1 at the instant that \vec{M} reaches the xy plane, we have created a coherent magnetization in the xy plane. This is a $\frac{\pi}{2}$ pulse, rotating M_z into M_y . If we leave B_1 on for twice as long, we have a π pulse, which inverts the original magnetization to $-M_z$. Keep in mind that the magnetizations thus created will decay back to equilibrium, and that any xy magnetization will rotate in the lab frame.

Now a graphical explanation of the spin echo is possible – see figure 9.4.

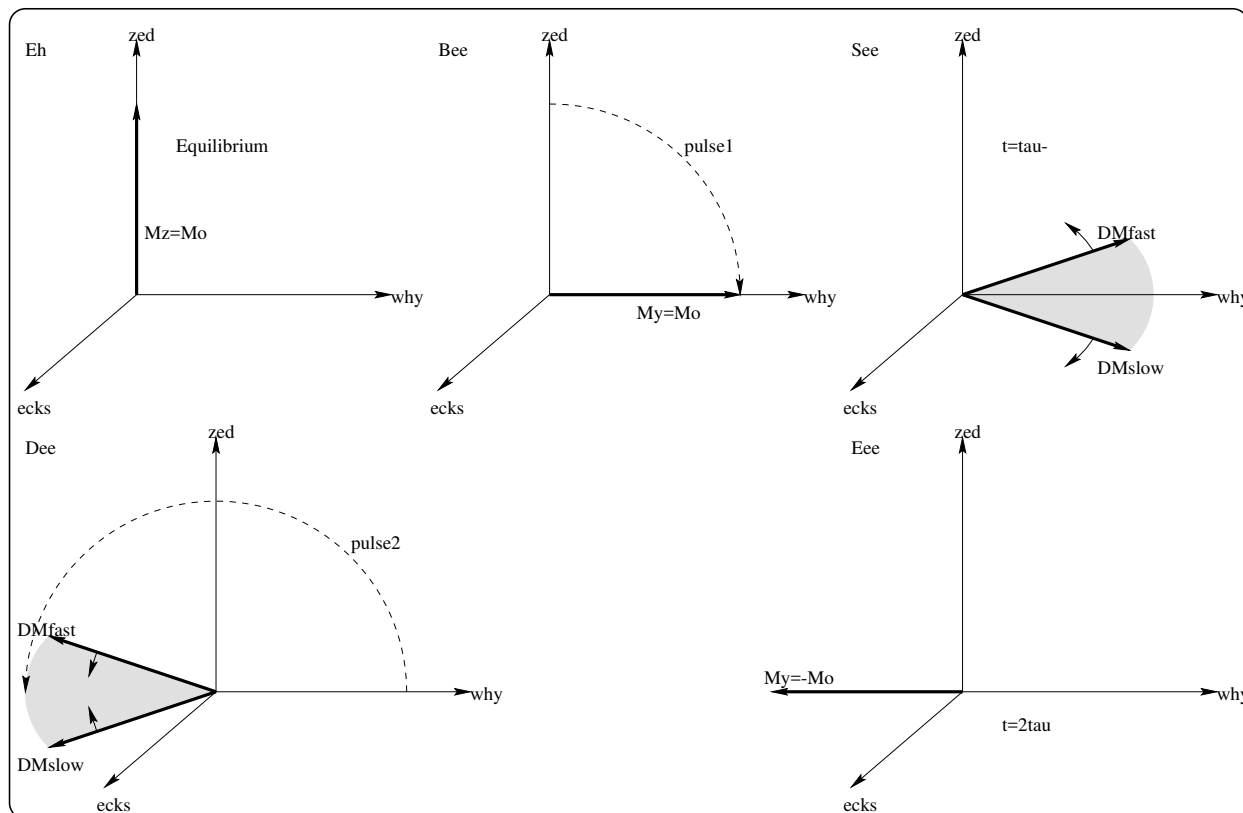


Figure 9.4: The spin echo: **a)** The initial magnetization is $M_o\hat{z}$. **b)** A $\frac{\pi}{2}$ pulse is used to rotate the magnetization into the xy plane. **c)** The xy magnetization dephases (within the xy plane) due to inhomogeneous field distributions, with the extremes being ΔM_{fast} (high field) and ΔM_{slow} (low field), until $t = \tau$. **d)** when a π pulse is used to flip the magnetization (flip the xy plane like a pancake). The spins continue to precess as before, until... **e)** $t = 2\tau$, when they are again in phase, and an echo may be observed. After $t = \tau$, the spins again dephase, and the signal disappears. In these figures, the decay of the xy magnetization and the growth of M_z have been omitted for clarity.

9.7 Apparatus

The glass sample vial is inside three mutually orthogonal coils (see figure 9.5). The large DC field required is provided by an 8.8kG ($=0.88\text{T}$, at 10A) water-cooled electromagnet. A smaller coil of similar shape (Helmholtz) is located toward and away from you as you look at the magnet, and a third, smaller, coil is wrapped around the space where you insert the sample vial. The innermost coil is the receiver, the other is the transmitter. Since you want the entire sample to be at the centre of all three coils, it's important that you only load $\sim 4\text{-}5\text{mm}$ of sample into your vial.

As first mentioned in section 9.4, magnetization may only be measured in the xy plane. Left unmolested, M_z would grow to its equilibrium value and be completely boring, but any M_{xy} will precess with angular frequency ω_o (see section 9.5). If you have rotating magnetization inside a coil, and the axis of rotation is not the coil's axis, an AC signal is induced in the coil – this is how AC wall power is generated, and it allows you to detect M_{xy} .

The NMR spectrometer unit consists of several parts (see figure 9.6): An RF source (the master

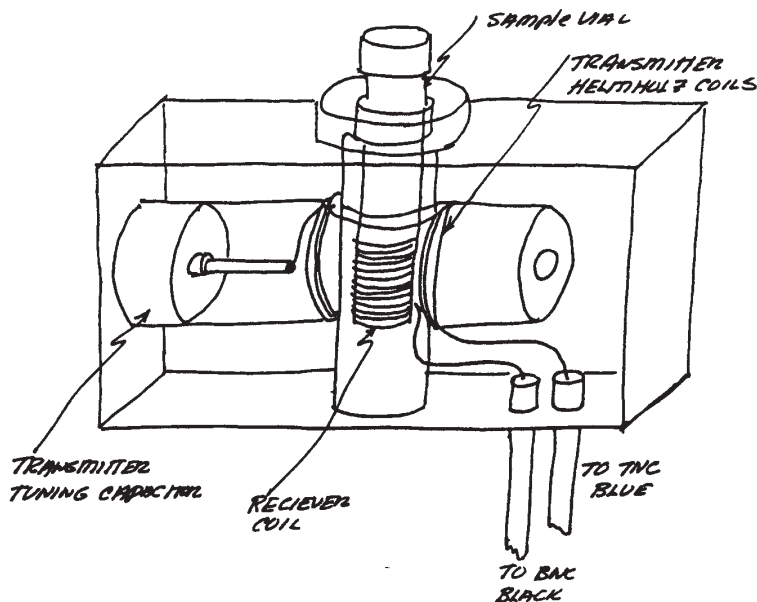


Figure 9.5: A sketch of the NMR probe.

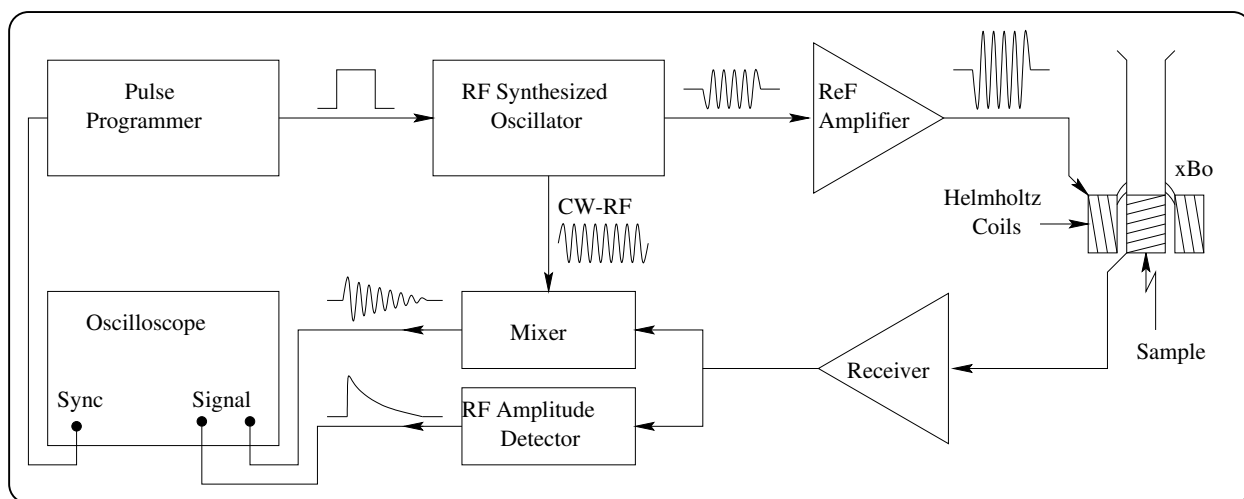


Figure 9.6: A block diagram of the NMR spectrometer.

oscillator), a pulse programmer to turn the RF on and off in short pulses, and the mixer. The mixer effectively multiplies the detector signal with the original RF, to generate an envelope waveform, which will have beats if the oscillator is not tuned to ω_o . You have a dual-channel oscilloscope to let you view the detector and mixer signals simultaneously.

To allow the equilibrium magnetization \vec{M}_o to be established between repetitions of the experiment, one must wait at least $3T_1$, and preferably 6-10 T_1 's, between pulse sequences. Water ($T_1 \approx 3\text{s}$) would be annoying to work with, and you can imagine your frustration if you tried using ^3He gas, with a T_1 of about a week. Since several adjustments must be made before data can be taken, these samples would make for an infuriating experiment. Mineral oil has a T_1 on the order of a few

tens of milliseconds at 25°C, so a repetition time of 100-200 ms should be adequate.

9.8 Getting Started

At the beginning of the lab period, turn on the magnet and its water cooling. The magnet's field may never completely stabilize, but the greater its headstart, the easier your measurements will be.

Open LabView file “NMR”; this will set up the 'scope and allow you to save data.

Single Pulse

Typical NMR pulse widths range from 1-35 μs . To start with, let's observe a single A pulse. The pulse programmer settings are:

A-width	halfway
Mode	Int
Repetition time	~ 500 ms
Sync	A
A, B pulses	On, Off
Sync Out	To scope's external trigger input
A+B Out	To scope Channel 1

Set the oscilloscope to trigger on the rise of the sync pulse, use a sweep rate of 2-10 $\mu\text{s}/\text{cm}$, and 1V/cm vertical scale. Change the A-width and observe the effect on the pulse. Switch the mode to Man, and observe the pulse when you press the “man” start button. Set the scope's sweep rate to 1ms/cm and repetition time to 10ms, then change the variable repetition time from 10% to 100% – what do you observe?

The Pulse Sequence

To measure T_1 or observe a spin echo, at least two pulses are required.

Delay Time	0.10×10^0 (100 μs)
Mode	Int
Repetition Time	~ 500 ms
Sync	A
A, B pulses	On, On

The pulse train should now appear like figure 9.7. Change the A and B widths, change the delay time, change sync to B, turn off A, then B, change the number of repetitions, and observe what happens (i.e. fiddle with the equipment). Look at a two-pulse sequence with delay times from 1 to 100ms (1.00×10^0 to 1.00×10^2). Be careful reading this number – note the decimal point.

9.9 Procedure

Before you can do anything else, the spectrometer must be tuned to resonance, and this must be done for each measurement. When on resonance, the free induction signal will produce a zero-beat signal with the master oscillator as observed on the Mixer's output (see figure 9.8). Once the spectrometer is tuned to resonance, the shortest A pulse that produces a maximum FID amplitude is a $\frac{\pi}{2}$ pulse. The setup is:

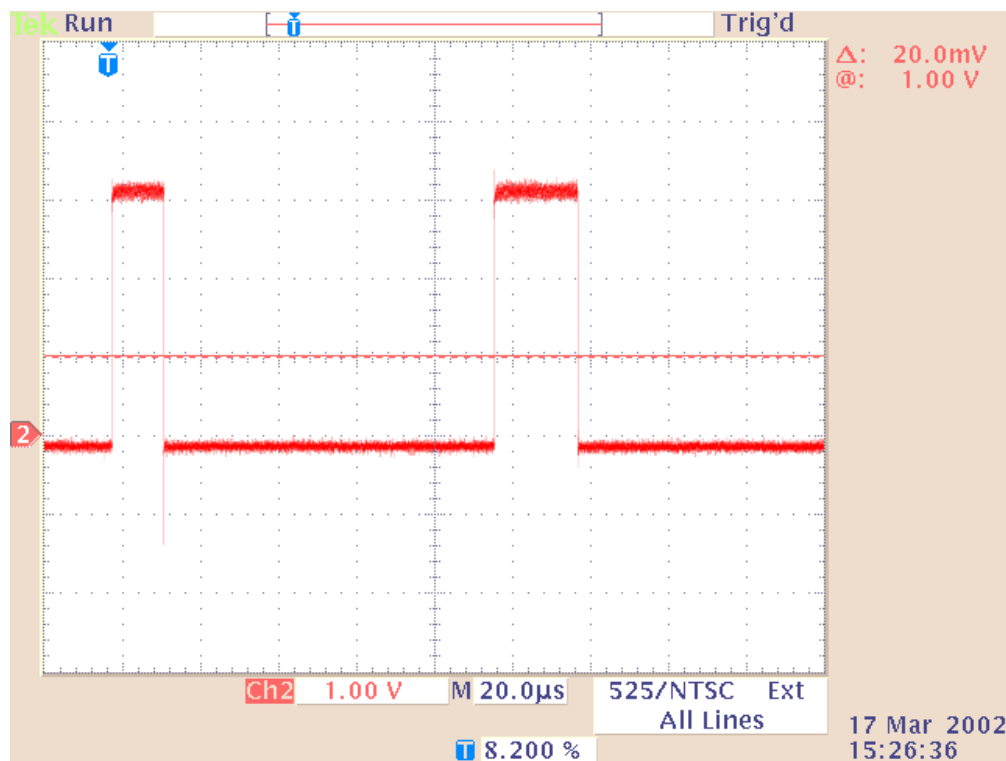


Figure 9.7: A two-pulse sequence

A-width	~20%
Mode	Int
Repetition Time	~ 500 ms
Sync	A
A, B pulses	On, Off
Time constant	0.01 ms
Gain	30%

Load a small sample of mineral oil (3-5 mm deep only) into one of the small sample vials, and adjust its height in the apparatus, using the rubber O-ring, to get a maximum signal. Tune the receiver input for maximum signal, then tune the frequency for a zero-beat signal. Find the pulse widths corresponding to $\frac{\pi}{2}$ and π (a π pulse ideally leaves no magnetization in the xy plane, so it should have no signal following it). How are you going to do this?

Spin-Lattice Relaxation Time T_1

As the time constant for exchange of energy and angular momentum with the surroundings, T_1 is one of the most important parameters to know and understand in NMR. Let's start with a quick, order-of-magnitude estimate:

1. Re-tune the spectrometer to resonance for a single pulse FID signal.
2. Change the repetition time, reducing the FID to roughly $\frac{1}{2}$ of its largest value. This gives an idea of the order of magnitude of T_1 .

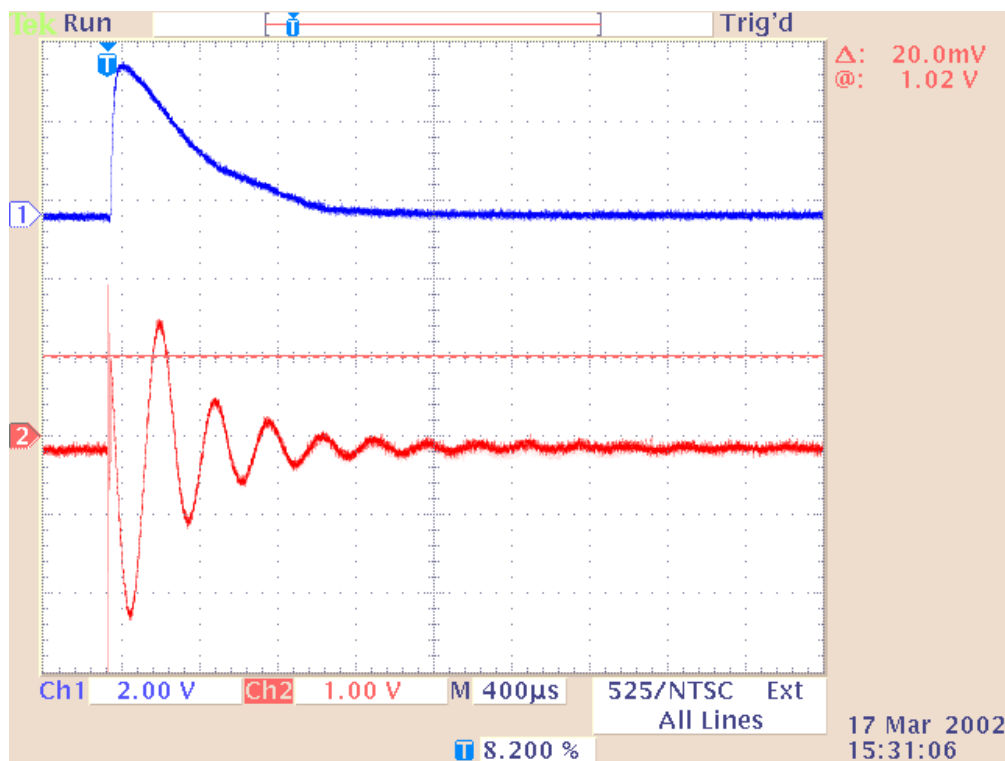


Figure 9.8: A free induction decay envelope and the detector signal mixed with the original RF, with the spectrometer not quite tuned to resonance. The beats are clearly visible.

At this repetition, the magnetization can't fully return to equilibrium, but does make it partway back. This measurement is useful as it gives you an idea of the time constant you want to measure, and helps you choose the delay settings.

The pulse sequence we'll use to find T_1 is

$$\pi \xrightarrow{\tau} \frac{\pi}{2}, \text{ FID}$$

The π pulse inverts the magnetization ($M_z \rightarrow -M_z$). A time τ later, whatever magnetization exists gets rotated $\frac{\pi}{2}$ into the xy plane for observation, where it decays in an FID. After the first pulse, the magnetization grows exponentially back from $-M_z$ to M_z (it does **not** rotate!), but the spectrometer can only measure precessing xy magnetization, so the magnetization must be knocked over into the xy plane to be seen. The $\frac{\pi}{2}$ pulse acts to sample M_z at the time selected.

You should be able to easily work out from equation 9.8 the equation governing the growth back to equilibrium. A two-digit value of T_1 may be found by finding the zero-crossing point (which is not itself T_1), but a better value is obtained by graphing the decay back to equilibrium and fitting to the correct function. Find T_1 by both methods.

Spin-Spin Relaxation Time T_2

To find T_2 , a simple $\frac{\pi}{2}$ pulse will not suffice, due to inhomogeneities in the DC field. You'll need to use the spin-echo technique. The pulse sequence is

$$\frac{\pi}{2} \xrightarrow{\tau} \pi \xrightarrow{\tau} \text{echo}$$

The $\frac{\pi}{2}$ pulse creates transverse (xy plane) magnetization, which dephases because of inhomogeneities in the applied field. The π pulse reverses these dephasing effects, and the magnetization eventually rephases, forming an echo signal. The reduction in height from the original FID to the echo is due to T_2 processes, so plotting the echo height versus the total delay time (2τ) will give T_2 .

Determine T_2 .

9.10 References

1. The Basics of NMR, by Joseph P. Hornak: <http://www.cis.rit.edu/htbooks/nmr>

9.11 Appendix: Quantum Mechanics of NMR

In NMR, the large DC magnetic field $\vec{B}_o = B_o \hat{z}$ defines the system's \hat{z} -direction. Any particles which have spin angular momentum (e.g. protons, neutrons, or electrons), and aren't already paired in full orbitals/states, will align parallel or anti-parallel to the field, so as to reduce the system's energy. In proton NMR, we're interested, not surprisingly, in protons. These particles are spin $\frac{1}{2}$, meaning that their allowed spin states are $m_I = \pm\frac{1}{2}$.

The portion of the Hamiltonian due to the magnetic field is

$$H = \frac{e}{2m} g \vec{B}_o \cdot \vec{I} = \frac{eg}{2m} B_o \left(\pm \frac{1}{2} \hbar \right). \quad (9.16)$$

For free protons, $g = 5.586$, and is usually called the Landé g -factor. \vec{I} is the nuclear spin.

For anything interesting to happen, we must add a small, time-varying magnetic field $\vec{B}_1 = B_1 \hat{x} \cos \omega t + B_1 \hat{y} \sin \omega t$. In order to deal with this field in a comparatively straightforward manner, I must now introduce some notation:

I will be using spinors, because life becomes much simpler when the problem can be turned into 2×2 matrices. The first time you see spinors, they usually look like a bizarre way to represent spin, but once you wrap your mind around them, they can be *extremely* handy. Spin up (\hat{z} -direction) $\equiv \begin{pmatrix} 1 \\ 0 \end{pmatrix}$, spin down $\equiv \begin{pmatrix} 0 \\ 1 \end{pmatrix}$. These are identical to the \uparrow and \downarrow you know and love from first year chem. All possible spin states can be constructed from these two spinors. For example, it can be shown that the state where spin is up in the \hat{x} direction corresponds to $\frac{1}{\sqrt{2}} \begin{pmatrix} 1 \\ 1 \end{pmatrix} = \frac{1}{\sqrt{2}} (\uparrow + \downarrow)$. In quantum mechanics, you can know the angular momentum around only one axis at a time. If you know the spin about the x -axis, the particle is in some superposition of spin-up and spin-down states in the \hat{z} direction.

Using spinors, the Hamiltonian with both magnetic fields is

$$H = \frac{eg\hbar}{4m} \begin{pmatrix} B_o & B_1 e^{j\omega t} \\ B_1 e^{j\omega t} & -B_o \end{pmatrix} \quad (9.17)$$

The wavefunction $\psi = \begin{pmatrix} a \\ b \end{pmatrix}$, where a and b are time-varying and $a^2 + b^2 = 1$. When B_1 is first turned on, it finds the spin in its equilibrium state $\begin{pmatrix} 1 \\ 0 \end{pmatrix}$, so $a(0) = 1$ and $b(0) = 0$. In order to minimize mess, I must now introduce a couple more ω 's. As above, ω is the angular frequency of the applied field, but we now have ω_o , the resonant (Larmor) frequency from field B_o , and ω_1 , which is the B_1 equivalent. I.e.

$$\frac{\omega_o}{2} \equiv \frac{eg}{4m} B_o \quad \text{and} \quad \frac{\omega_1}{2} \equiv \frac{eg}{4m} B_1 \quad (9.18)$$

If we apply the Schrödinger equation ($j\hbar\partial_t\psi = H\psi$) to $\begin{pmatrix} a \\ b \end{pmatrix}$, we get

$$j\hbar\partial_t \begin{pmatrix} a \\ b \end{pmatrix} = H \begin{pmatrix} a \\ b \end{pmatrix} = \frac{\hbar}{2} \begin{pmatrix} \omega_o & \omega_1 e^{j\omega t} \\ \omega_1 e^{j\omega t} & -\omega_o \end{pmatrix} \begin{pmatrix} a \\ b \end{pmatrix} \quad (9.19)$$

This gives

$$j\partial_t a = \frac{\omega_o}{2}a + \frac{\omega_1}{2}be^{j\omega t} \quad \text{and} \quad j\partial_t b = -\frac{\omega_o}{2}b + \frac{\omega_1}{2}ae^{j\omega t} \quad (9.20)$$

It is now convenient to define two new “constants”, $A \equiv ae^{j\frac{\omega_o}{2}t}$ and $B \equiv be^{-j\frac{\omega_o}{2}t}$. Now,

$$j\partial_t A = \frac{\omega_1}{2}Be^{j(\omega_o-\omega)t} \quad \text{and} \quad j\partial_t B = \frac{\omega_1}{2}Ae^{-j(\omega_o-\omega)t} \quad (9.21)$$

This can be solved by $A = A(0)e^{j\lambda t}$ and $B = B(0)e^{j\lambda t}e^{-j(\omega_o-\omega)t}$, where the roots of λ are

$$\lambda_{\pm} = \frac{\omega_o - \omega \pm \sqrt{(\omega_o - \omega)^2 + \omega_1^2}}{2} \quad (9.22)$$

The general solution for A is then

$$A = A_+e^{j\lambda_+t} + A_-e^{j\lambda_-t} \quad (9.23)$$

Substituting this into the first part of equation 9.21 gives

$$B = -\frac{2}{\omega_1}e^{-j(\omega_o-\omega)t} \left[\lambda_+A_+e^{j\lambda_+t} + \lambda_-A_-e^{j\lambda_-t} \right] \quad (9.24)$$

The initial conditions $A(0) = a(0) = 1$ and $B(0) = b(0) = 0$ imply that $A_+ + A_- = 1$ and $\lambda_+A_+ + \lambda_-A_- = 0$, or

$$A_+ = \frac{\lambda_-}{\lambda_- - \lambda_+} \quad \text{and} \quad A_- = -\frac{\lambda_+}{\lambda_- - \lambda_+} \quad (9.25)$$

We can now obtain a result for the probability that the spin has flipped to down (or how much “down” there is in the superposition of states):

$$P_{a \rightarrow b}(t) = |b|^2 = |B|^2 = \frac{4}{\omega_1^2} \left| \frac{\lambda_+\lambda_-}{\lambda_- - \lambda_+}e^{j\lambda_+t} - \frac{\lambda_+\lambda_-}{\lambda_- - \lambda_+}e^{j\lambda_-t} \right|^2 \quad (9.26)$$

$$\begin{aligned} &= \frac{4}{\omega_1^2} \left[\frac{(\omega_o-\omega)^2}{4} - \frac{(\omega_o-\omega)^2 + \omega_1^2}{4} \right]^2 \left| e^{j\frac{\omega_o-\omega}{2}t} \left(e^{j\frac{\sqrt{(\omega_o-\omega)^2 + \omega_1^2}}{2}t} - e^{-j\frac{\sqrt{(\omega_o-\omega)^2 + \omega_1^2}}{2}t} \right) \right|^2 \\ &= \frac{\frac{\omega_1^2}{4}}{(\omega_o - \omega)^2 + \omega_1^2} \left| e^{j\frac{\omega_o-\omega}{2}t} 2j \right|^2 \sin^2 \frac{\sqrt{(\omega_o - \omega)^2 + \omega_1^2}}{2}t \\ &= \frac{\omega_1^2}{(\omega_o - \omega)^2 + \omega_1^2} \sin^2 \frac{\sqrt{(\omega_o - \omega)^2 + \omega_1^2}}{2}t \end{aligned} \quad (9.27)$$

At this point, it should suddenly become clear why the spectrometer needs to be tuned to resonance ($\omega = \omega_o$). The simplification is dramatic:

$$P_{a \rightarrow b}(t) = \sin^2 \frac{\omega_1}{2}t \quad (9.28)$$

It should also be clear now what $\frac{\pi}{2}$ and π pulses correspond to. It should be noted that, while this was derived for a single particle, the same result works for the system as a whole, with the energies multiplied by $(N_1 - N_2)$, where N_1 and N_2 are the numbers of particles in the lower and upper energy states respectively.

Experiment 10

Lock-in Detection: High- T_c Superconductivity

10.1 Purpose

To introduce you to lock-in amplifiers and some topics of current interest to researchers in the department.

10.2 Introduction

Superconductivity was first observed in 1911, by Dutch physicist Heike Kammerlingh-Onnes. When he cooled mercury in liquid helium, its DC resistivity abruptly vanished around 4K. It wasn't until the 1950's that a satisfactory explanation was found — two electrons couple to a phonon (quantized lattice vibration), lowering their energy and changing even their most basic properties. By the 1970's, superconductors were fully understood, metallic compounds had been found with superconducting transition temperatures (T_c) as high as 23K, and theorists had proven that it would be impossible for anything to have a T_c much higher than 25K.

In late 1986, Swiss physicists J. Georg Bednorz and K. Alex Müller discovered superconductivity at nearly 40K in $\text{La}_{2-x}\text{Ba}_x\text{CuO}_4$, an otherwise poorly-conducting ceramic. This startling discovery sparked an intense effort to find and study more such compounds. In January 1987, the first compound was found with a T_c above the temperature of liquid nitrogen (77K) — $\text{YBa}_2\text{Cu}_3\text{O}_{7-x}$ (YBCO, $T_c = 93.7\text{K}$ for $x = 0.08$). Today, many such compounds are known, the highest recorded ambient-pressure T_c is 138K, and there is no accepted explanation for why they superconduct. While these temperatures are still quite cold by most people's standards, they're extremely high for low-temperature physics, and are readily attainable.

Low-temperature (conventional) superconductors are in common use for high-field magnets (as used in MRI machines), but the liquid helium required to keep them cold makes the cost prohibitive for most other uses. Liquid nitrogen is far cheaper than helium, so high- T_c superconductors should eventually see far more common use. An application of particular current interest is in cellphone base stations and satellites, where the absence of electrical resistance can make bandwidth constraints less of a problem. A variety of superconductor-based quantum computing schemes have also been suggested, and are being investigated.

10.3 Theory

Aside from having zero DC resistance, superconductors are also perfect diamagnets. This well-understood property, known as the Meissner Effect, is commonly used for spectacular demonstrations — a magnet placed atop a piece of YBCO will spontaneously levitate when the YBCO goes superconducting. The ground state for this system is to have currents on the surface of the superconductor, cancelling out the magnetic field. The currents, and thus the fields, in fact decay exponentially into the sample (Figure 10.1), with a characteristic length λ_L , the magnetic (or London) penetration depth. In the high- T_c superconductors, λ_L depends on the temperature and what

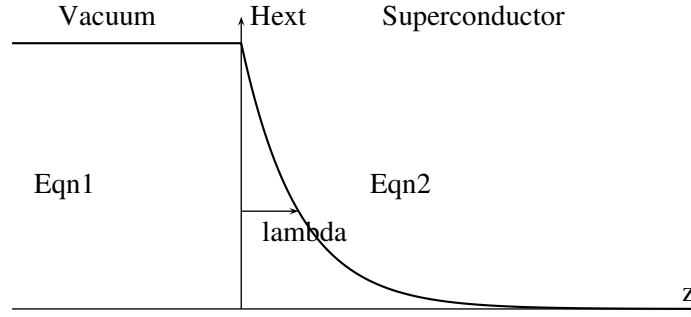


Figure 10.1: Magnetic field decaying into a superconductor.

direction the currents are travelling, and ranges from ~ 0.1 to $10\mu\text{m}$. Figures 10.2a and b show our superconducting crystal in an applied magnetic field above and below T_c .

From Faraday's Law, the voltage induced in a wire loop in a time-varying magnetic field is

$$V_{loop} = -\frac{d\Phi}{dt}$$

where the magnetic flux $\Phi = \iint \vec{B} \cdot d\vec{a}$. In our setup, an external AC magnetic field

$$\vec{B}_{ext} = B_{ext} \sin(\omega t) \hat{x} = \mu_o H_{ext} \sin(\omega t) \hat{x} \quad (10.1)$$

is applied, and the voltage in a pickup coil (of length L , cross-sectional area A , and N turns per unit length) would be

$$V_{coil} = -NLA\mu_o H_{ext} \omega \cos(\omega t), \quad (10.2)$$

or

$$|V_{coil}| \propto LAH_{ext}. \quad (10.3)$$

It is customary to use \vec{H} , the field in matter, instead of \vec{B} , because \vec{H} is the field we can directly control. Ampère's Law in matter reads

$$\vec{\nabla} \times \left(\frac{1}{\mu_o} \vec{B} - \vec{M} \right) = \vec{J}_f$$

or

$$\vec{\nabla} \times \vec{H} = \vec{J}_f \quad (10.4)$$

where \vec{J}_f is the free current and \vec{M} , the “magnetization”, is the magnetic dipole moment per unit volume.

However, we're not interested in measuring the applied field; we're looking for small changes to it due to the presence of a superconducting sample. The apparatus used has two identical coils a short distance apart, wound in opposite directions and connected in series. In a uniform AC field,

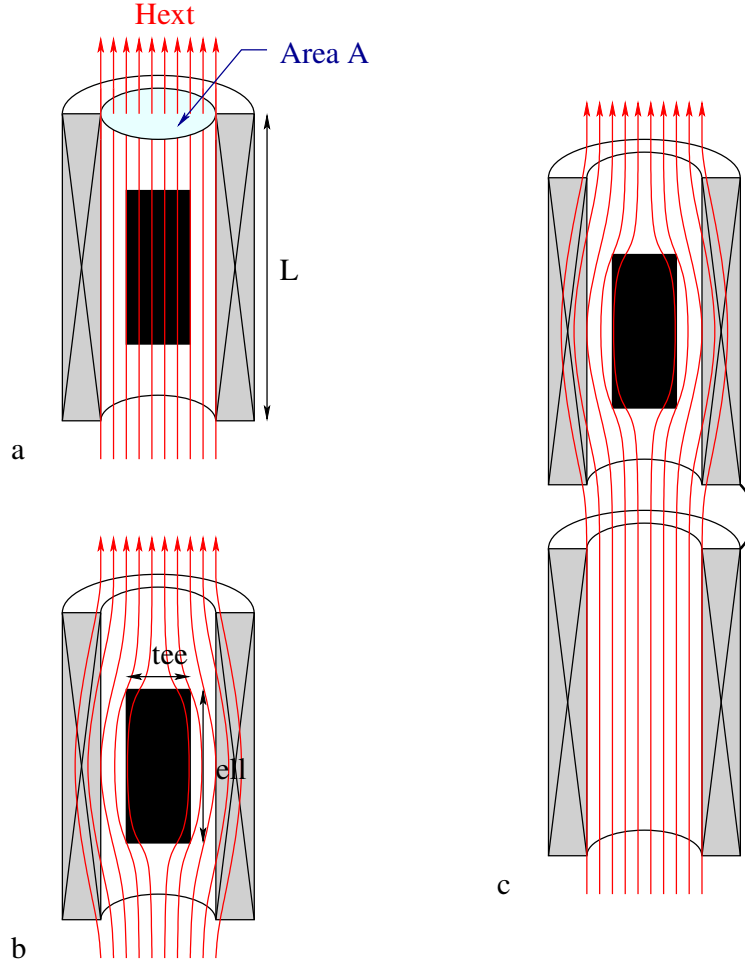


Figure 10.2: Perfect diamagnetism in a superconductor. **a)** For $T > T_c$, YBCO is slightly metallic, and does not significantly alter the magnetic field. **b)** For $T < T_c$, the superconductor expels the applied field, and the pickup coil sees a reduced field. **c)** In our apparatus, the sample is in the upper of two counterwound coils connected in series. In a uniform field (above T_c), there is no net field, but below T_c the two coils see different fields, so there is a net field detected in the circuit.

they will contribute equal voltages, and these will cancel, leaving no signal. However, if one half contains a piece of YBCO (Figure 10.2c), that half will give a different voltage

$$|V'_{coil}| \propto \left[LA - \ell_x \ell_y t \left(1 - \frac{2\lambda_L}{t} \right) \right] \quad (10.5)$$

$$= C (LAH_{ext} - |\vec{m}|) \quad (10.6)$$

where C is a calibration constant and \vec{m} is the sample's total magnetization. The voltage detected will be

$$|V_{coil} - V'_{coil}| = C|\vec{m}| = C' \left(1 - \frac{2\lambda_L}{t} \right). \quad (10.7)$$

A measurement of the sample's magnetization, then, can be used to determine the London penetration depth.

10.4 The Apparatus

Figure 10.3 shows the key components of the apparatus.

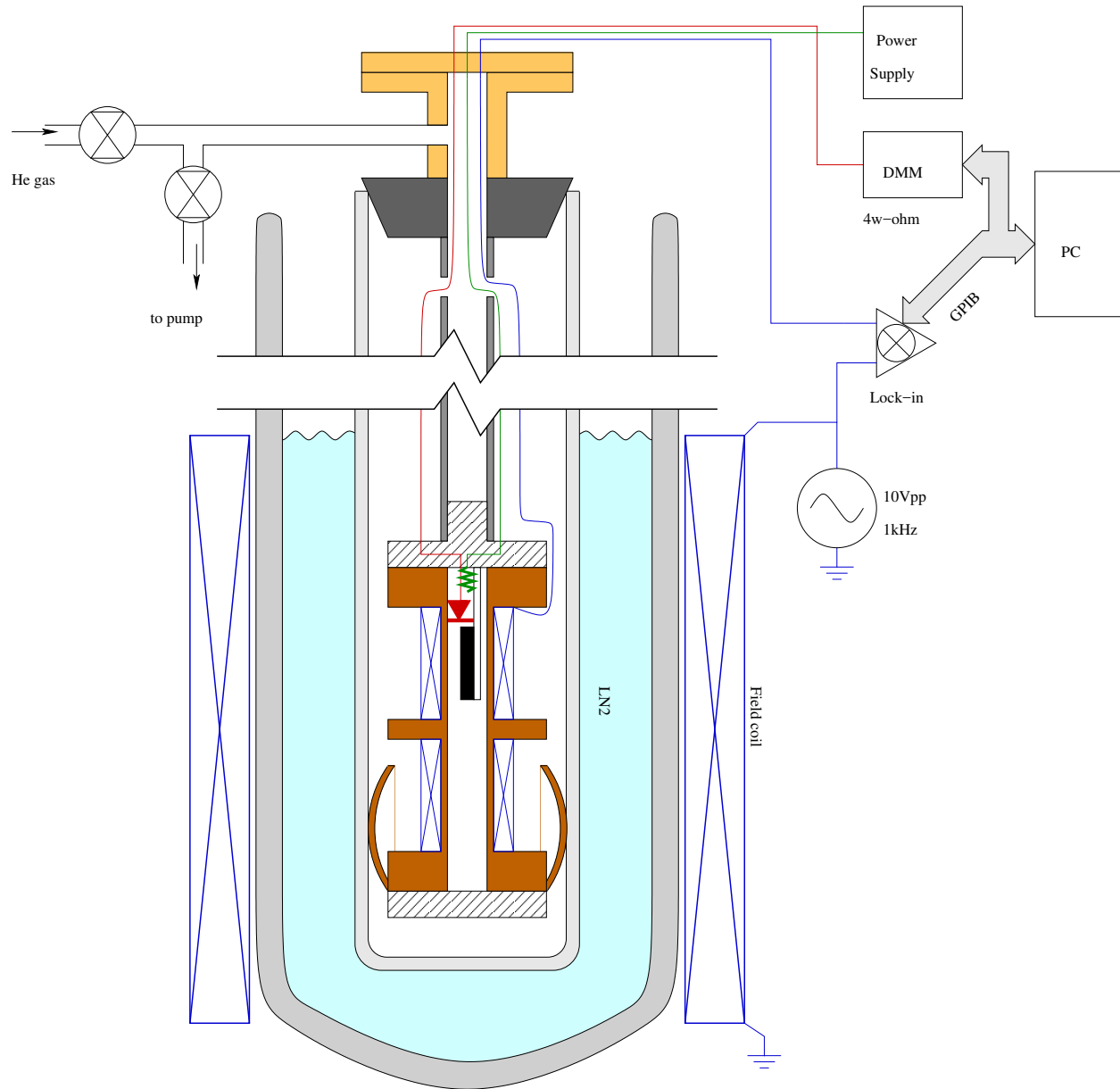


Figure 10.3: Schematic diagram of the apparatus. There are four subsystems — the vacuum/cryogenics plumbing and the magnetic detection, thermometry and heating circuitry. The computer monitors the temperature and detected signal, and runs current through the 50Ω resistor to heat the probe.

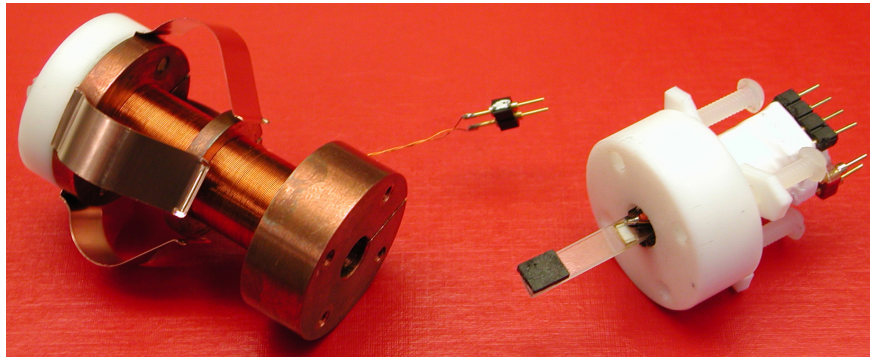


Figure 10.4: Photograph of the susceptometer.

Plumbing and Temperature Control

The probe is cooled to 77.4K in liquid nitrogen, which is held in a dewar flask. A quartz test tube separates the liquid nitrogen from the probe, which allows the probe to reach temperatures other than 77K and prevents damage from thermal shock. Beryllium-copper springs make thermal contact between the copper coil assembly and the test tube, to keep the coils cold. The sample and the thermometer and heater chips are mounted on a sapphire (Al_2O_3) plate, which is a very good thermal conductor. This is thermally insulated from the rest of the probe with teflon/quartz. Figure 10.4 shows a photo of this part of the probe.

To cool the probe, the quartz tube is filled with helium gas, which is then pumped out for thermal isolation. How does this helium business work, and why do we use helium for this purpose? To warm the sapphire plate, a current is applied to the chip resistor; the temperature reached will depend on the current applied.

Thermometry

The sapphire plate also holds a silicon diode which acts as a thermometer. Diodes thermometers are usually used by passing a constant current through them and measuring the voltage. We will use the four-wire resistance function of the multimeter to do this. (see Figure 10.5).

In a four-wire resistance measurement, a constant current is supplied to the load through two leads, and the voltage across it is measured using the remaining two leads. The resistance is then obtained through Ohm's law. Four-wire measurements are far superior to two-wire for small resistances, because the latter measures the resistance of the load *and* the wires. In a four-wire measurement, there is negligible current in the voltage leads, so only the load is measured. In the case of the diode thermometer shown in figure 10.5, the thermal gradient we apply would make it virtually impossible to account for the resistance of the leads, making 4-wire measurements crucial. The diode is also extremely non-Ohmic, so a constant bias current is required.

The current through a diode varies as

$$I = I_o \left(e^{eV/nk_B T} - 1 \right) \quad (10.8)$$

where $I_o(T)$ is the reverse-biased saturation current, V is the diode voltage, and T is the temperature, and n is diode-dependent factor known as the 'nonideality factor'. Usually $1 < n < \sim 2.5$. I_o is also a function of temperature, and is often expressed as:

$$I_o = K T^{5/2} e^{-V_g/2k_B T}, \quad (10.9)$$

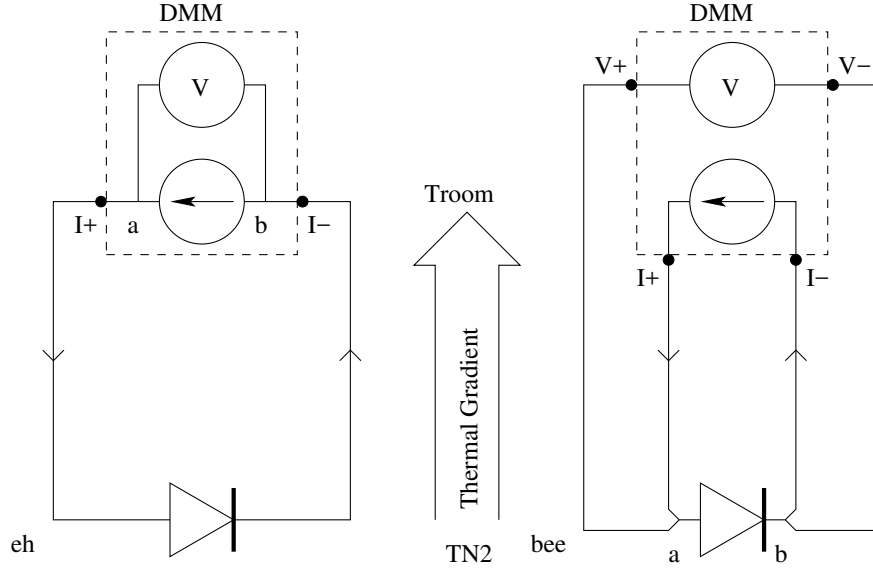


Figure 10.5: a) Two-wire and b) four-wire measurements on a diode thermometer. The DMM's current and voltage connections are marked.

in which K depends on the details of the diode and E_g is the band gap of the semiconductor. Taking the logarithm of I , we find:

$$V = \frac{n/2e}{V_g} - \frac{nk_B}{2} \left(\frac{5}{2} \ln T - \frac{\ln I_f}{K} \right). \quad (10.10)$$

The weak logarithmic dependence on T can usually be ignored, and so we find

$$V = V_0 - m(I)T. \quad (10.11)$$

The voltage measured across the diode, for fixed forward bias current is thus expected to vary linearly with temperature, and can be calibrated using measurements at 77.4 K and room temperature. It is important to note that the measurements **must** be performed on the same (manually set) range on the DMM, to ensure a constant bias current.

Magnetometry and Lock-in Detection

Outside the dewar, a large coil is used to apply an AC field (\vec{H}_{ext}) to the probe. To ensure field uniformity, it is quite useful to have the probe centred inside this coil. The probe itself has two counterwound coils, as described in the Theory section, to detect magnetization in the sample rather than just the applied field.

While the signal due to the sample is already quite small, we're looking at an even smaller signal — we want to determine how λ_L changes with temperature. Recall from Equation 10.7 that the detected signal \propto (sample size — shell of thickness λ_L). The λ_L term is the interesting one, but it's the smaller term by a factor $\frac{2\lambda_L}{t} \sim 10^3 - 10^5$. Any minute changes in λ_L will be completely drowned out by noise proportional to the sample size.

The advantage we have in this experiment is that we know exactly what frequency our signal should have. To separate it from broadband noise, all we need is a filter. Because the noise

is much stronger than the signal, we need a very narrow filter — our signal has a vanishingly small frequency width, so the probability of having broadband noise at exactly the same frequency also vanishes. Unfortunately, the feasibility of constructing such a narrow filter for an arbitrary frequency vanishes at least as quickly.

A common solution would be to do a Fourier transform of your detected signal, so you can look at the frequency spectrum and pick off the frequency you want. The problem is getting a frequency spectrum in the first place. Fourier transforms require significant amounts of data and data analysis. The solution implemented in this experiment instead uses a special type of phase-sensitive filter and voltmeter known as a lock-in amplifier.

The lock-in is given reference and sample signals, with phases ϕ_r and ϕ_s , and the reference signal is converted to a sine wave of unit amplitude:

$$\begin{aligned} V_r &= \sin(\omega_r t + \phi_r) \\ V_s &= \mathcal{A} \sin(\omega_s t + \phi_s) \end{aligned}$$

The reference and sample signals are then mixed to yield an output at their sum and difference frequencies.

$$V_r \times V_s = \frac{\mathcal{A}}{2} [\cos((\omega_s - \omega_r)t + \phi_s - \phi_r) - \cos((\omega_s + \omega_r)t + \phi_s + \phi_r)] \quad (10.12)$$

In this experiment, the output frequency will be the same as the input frequency, so the first term will be at DC and the second at a frequency of 2ω .

Next, the mixed signal passes through a low-pass filter to yield only the DC component:

$$V_r \times V_s \xrightarrow{\text{low-pass filter}} \frac{\mathcal{A}}{2} \cos(\phi_r - \phi_s)$$

Frequencies other than the reference frequency do not give DC components, and can be removed by the low-pass filter. However, while it's far easier to make a low-pass filter than a band-pass filter at arbitrary frequency, the filter still has a width — the inverse of its time constant. You may have noticed, though, that signals are maximized for $\phi_r = \phi_s$, and a phase difference of $\pi/2$ will not contribute to the output. So we're getting phase information for free (or we can take advantage of a known phase relationship to further improve our data).

This is the basis of phase- and frequency-specific detection. Lock-in amplifiers provide an immense advantage when measuring small signals if the system can be driven by an AC voltage with a very stable amplitude and phase.

Why is phase-sensitive detection important in this experiment? Because of the derivative in Equation 10.2, we're interested in the inductive response of the detector coils, which will be $-\pi/2$ out of phase with the driving field. Since the driving coil is out of phase with the function generator by $+\pi/2$, the voltage from the sample's magnetic moment will be *in phase* with the function generator. On the other hand, there will be resistive signals $\pi/2$ out of phase with the function generator — resistance both in the wires and in the superconductor (it has zero DC resistivity, but a small AC resistivity). Phase-sensitive detection allows us to distinguish between the inductive and resistive components.

In this experiment, the counterwound detector coils provide V_{sample} and we're primarily interested in the inductive response, at zero phase shift. If time permits and you feel like investigating the resistive response, then you can set the reference phase to $\pi/2$.

10.5 Procedure

Study I — Lock-in Signal Detection

This part of the experiment will introduce you to lock-in detection of small signals.

1. What are the highest and lowest available time constants on the lock-in? What is the best frequency resolution you would expect from each? (This unit has a second filter stage, labelled as “Post,” for steeper roll-off. You should disable it, by setting it to “None.”)
2. As a test, we’ll use the lock-in amplifier to measure the resistance of a very small resistor. You should find a small slab of aluminum at your bench, with four female banana connectors. Use the digital multimeter’s four-wire resistance function (method mentioned earlier) to find its resistance, and thus its resistivity. The voltage-sensing leads are labelled as “ $\Omega 4W$ Sense” and the current source (I_+) is marked with a lightning bolt (⚡). Remember, you want to measure the voltage due to a current, and you’re trying to eliminate any effects from resistance in the leads or contacts. Perform a two-wire measurement for comparison.
3. Now, connect the function generator to a $\sim 50\Omega$ resistor (use the resistance box) in **series** with the aluminum bar. This acts as a current source. You can measure the current through the bar by measuring the (AC) voltage across the known resistance with the multimeter. Now connect the lock-in amplifier to the aluminum bar. Using the lock-in voltage measurement and the previous current measurement, determine the resistance, and resistivity, of the bar.

Study II — Magnetization of $\text{YBa}_2\text{Cu}_3\text{O}_{6.95}$

You will now determine the magnetic properties of a crystal of YBCO by AC susceptometry. Refer to Figure 10.3 for a diagram of the apparatus.

1. Open LabView program.
2. Take a measurement of the diode voltage under bias current, using the four-wire resistance measurement function of the multimeter, with the range manually set to $10\text{k}\Omega$. The multimeter must remain on this resistance range for the duration of the experiment. As long as the bias current stays fixed, it is ok for you to record the diode voltage in units of ohms (these are the units that the multimeter will supply the voltage in - because it thinks its making a resistance measurement). A resistance value for 77K should already be present in the LabVIEW program, completing the temperature calibration — you don’t need to adjust this point.
3. Connect the function generator (10kHz , $10V_{pp}$) to the lock-in’s Reference input and the outer coil, and the detector coil (susceptometer output) to the lock-in’s A input. Raise the drive coil to envelope the susceptometer, watching the signal on the lock-in. It should reach a maximum, then decrease toward the centre of the drive coil. Why? Find the position that minimizes the magnitude of the signal (i.e. get it close to zero), and use this position for the remainder of the experiment.
4. The test tube containing the probe needs to have 1 atm He gas in it. To this end, pump out whatever gases may be in it using the vacuum pump, then gently fill it with helium gas and close the valve. Fill the dewar with liquid nitrogen. The diode’s resistance should rise rapidly, then level off as the probe approaches 77K.

5. With the probe at liquid nitrogen temperature, remove the helium. Start the pump, and, leaving the He-line valve closed, pump down to $\lesssim 200$ torr. Set the phase on the lock-in to zero, and ensure that the signal is not off the scale. **Leave the pump pumping on the dewar for the duration of the experiment, and then leave it pumping when you leave the room.** With the helium removed, you may *slowly* warm the sample, using the DC power supply as necessary. Take data as you do so. You want the probe to warm at about 0.5 K/min. Continue recording the lock-in output and resistance to at least 105K.
6. You might expect your plot of lock-in voltage vs. temperature to be zero above T_c , where the field fully penetrates the superconductor, but your graph will probably show an offset and a slope in this regime. What causes can you think of for the slope and offset? To remove this background signal, fit the linear portion above T_c , and subtract this line from the *entire* data set.
7. Rescale your data so the voltage values vary from zero to one. Since $V \propto |\vec{m}(T)|$, this plot shows $\frac{|\vec{m}(T)|}{|\vec{m}(T_o)|}$ vs. T .
8. Finally, use Equation 10.16 or 10.17 to extract $\lambda_L(T)$. To do this, take $\lambda_L(77\text{K}) = 3000\text{\AA}$, and the sample's dimensions as $5.50 \times 4.35 \times 1.30 \text{ mm}^3$, ± 0.05 in each. Generate a log-log plot of $\lambda_L(T)$ over the range $T_c - 10\text{K} \rightarrow T_c$. The x-axis should use $\frac{T_c - T}{T_c}$ instead of T . Is there any evidence of a power law $\lambda_L(T) \propto \left(\frac{T_c - T}{T_c}\right)^n$? (Note that the assumption $\lambda_L \ll t$ is not true very close to T_c , because λ_L diverges at T_c .)
9. Leave pump on (Tongkai will turn off). Lower coil, and put a piece of paper over the top to catch dripping condensation from the susceptometer.

10.6 References

For E&M, any undergraduate text will work (e.g. Griffiths' *Introduction to Electrodynamics*). A high school-level (and overly optimistic and partially wrong) introduction to superconductivity may be found at <http://www.superconductors.org>, but Tinkham's 4th year-level text *Introduction to Superconductivity* is **much** better. Additionally, some similar research has been done at UBC — Chris Bidinosti's Ph.D. thesis, available from on-campus at <http://www.physics.ubc.ca/~supercon/archive/bidinosti-phd.pdf> may be useful, particularly parts of its Introduction. The growth of the YBCO crystal is described in <http://arxiv.org/abs/cond-mat/0209418>.

For diode thermometry: T. Huen, Rev. Sci. Instrum. **41**, 1368 (1970).

10.7 Appendix — Magnetic Moment of a Superconducting Platelet

Consider a superconducting platelet of thickness t and broad dimensions $\ell_x \times \ell_y$ in a uniform external magnetic field $H_{ext}\hat{x}$, as shown in Figure 10.6. Furthermore, assume that $\ell_i \gg t$, so that we can consider the platelet to be an infinite slab (λ_b becomes λ_L and λ_c plays no role).

The magnetic flux density (\vec{B}) at any point inside the platelet will be the sum of the exponentially decaying fields from the two sides of the sample:

$$B_x(z) = D \left[e^{(z-t/2)/\lambda_L} + e^{-(z+t/2)/\lambda_L} \right] \quad (10.13)$$

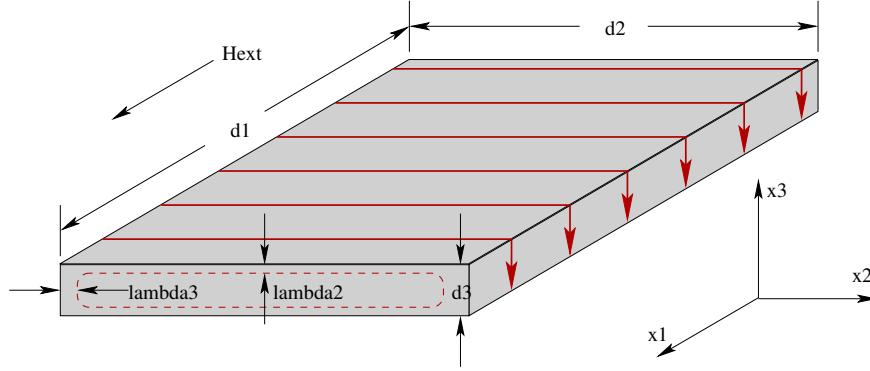


Figure 10.6: The crystal provided, with the currents and penetration depths shown. $\ell_x \approx 5.50$ mm, $\ell_y \approx 4.35$ mm, and $t \approx 1.30$ mm.

where D is a constant that must be chosen to satisfy the boundary conditions $B_x(\pm t/2) = \mu_o H_{ext}$. The result is

$$B_x(z) = \mu_o H_{ext} \frac{\cosh(z/\lambda_L)}{\cosh(t/2\lambda_L)}. \quad (10.14)$$

Finally, using the general expression $\vec{B} = \mu_o (\vec{H} + \vec{M})$, we can derive the magnetization of an infinite slab of thickness t :

$$\vec{M} = H_{ext} \left(\frac{\cosh(z/\lambda_L)}{\cosh(t/2\lambda_L)} - 1 \right) \quad (10.15)$$

The total magnetic moment \vec{m} is a good measure of how effectively the sample screens the field, and can be obtained experimentally. For our case,

$$\begin{aligned} \vec{m} &= \iiint \vec{M} dV \\ &= \ell_x \ell_y t \left(1 - \frac{2\lambda_L}{t} \tanh(t/2\lambda_L) \right) H_{ext} \hat{x} \end{aligned} \quad (10.16)$$

or, $|\vec{m}| = \text{Volume of sample} \times \text{fraction of volume screened} \times H_{ext}$.

In the limit where $\lambda_L \ll t$, this becomes

$$|\vec{m}| \approx \ell_x \ell_y t \left(1 - \frac{2\lambda_L}{t} \right) H_{ext}. \quad (10.17)$$

In this limit, the field effectively penetrates the sample to a depth of λ_L on each broad side. Either Equation 10.16 or 10.17 can be used to relate the magnetic moment to the London penetration depth.

Experiment 11

Vacuum Systems

11.1 Purpose

1. To become familiar with the use and calibration of vacuum systems and mass flow controllers.
2. To study the flow properties of several gases in a vacuum system.

11.2 Introduction

Vacuum chambers are used in a variety of scientific and industrial applications to provide a controlled atmosphere at reduced pressures. In many cases it is desirable to remove as much of the ambient gas as possible. Examples where this is important include the preparation and study of high-purity materials that are sensitive to corrosion, impurities or oxidation, electron microscopes where gas molecules scatter the electron beam used to image the specimens, and industrial vacuum coating systems for a combination of the above reasons. In other applications, one wants to replace the ambient atmosphere with a controlled mixture of “process gases” whose chemical properties can result in thin-film growth or oxidation (e.g. oxygen for SiO₂ gate dielectrics on Si), or highly selective etching of substrates placed in the chamber. These are but a few of the many applications of vacuum and gas-flow-control technologies.

Regardless of whether one wishes to work in a reduced atmosphere or none at all, vacuum pumps are required to maintain the desired pressure and gauges are required to observe it. There are many different types of pumps, pressure transducers and flow controllers available, each with a unique set of attributes which make it useful for specific applications. For example, rotary pumps are inexpensive, robust, and relatively simple to use, but they only work at relatively low vacuum (high pressure). Diffusion pumps are relatively inexpensive, simple, and capable of achieving higher vacuums, but they require oil for their operation and therefore are potentially disastrous sources of contamination, particularly in the event of failure or incorrect usage – diffusion pump oil has a well-earned reputation for being nearly impossible to clean off.

The detailed mechanisms involved in the operations of vacuum system components are beyond the scope of this manual, but some generic issues associated with them will be covered. These include: accurate measurement of total and partial pressures of constituent gases, and the relationship between pumping speed, chamber volume, pressure and flow rate.

11.3 Theory

The analysis of pumping systems is similar to electrical circuit analysis with pressure playing the role of electrical potential (voltage). The role of current is played by the system’s *throughput*, Q , defined as the quantity of gas (the volume of gas at a known pressure) that passes through a plane per unit time,

$$Q = \frac{d(PV)}{dt}. \quad (11.1)$$

Notice that Q has units of work (Watts). This not the kinetic or potential energy contained in the gas molecules, but rather the work required to transport the molecules across the plane. Note that the number of molecules of gas per unit time that a given value of Q describes depends on temperature. The *conductance* C of an object, such as a piece of tubing or an orifice, is defined in terms of the throughput associated with a pressure drop across that object assuming it is connected to two large reservoirs on either side:

$$C = \frac{Q}{P_2 - P_1} \quad (11.2)$$

C has units of volume per unit time. The conductance of an object is in general a nonlinear function of the pressure, but it can frequently be approximated as being independent of pressure.

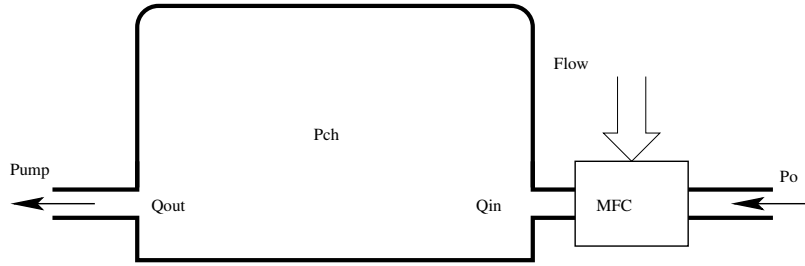


Figure 11.1: Schematic diagram of a simple vacuum system.

At a fixed temperature and for a single-component gas, the throughput Q across any plane in a connected system is simply proportional to the rate of particle flow; hence one can apply particle conservation principles to derive the dynamical equations of motion. Consider the simple system shown in Figure 11.1, consisting of a chamber connected to a pump and a mass flow controller (MFC). If the volume of the chamber is V_{Ch} , then it follows that

$$-V_{Ch} \frac{dP_{Ch}}{dt} = Q_{out} - Q_{in} \quad (11.3)$$

$$Q_{in} = S_{MFC} P_o \quad (11.4)$$

$$Q_{out} = S_{Pump} P_{Ch} \quad (11.5)$$

where S_{MFC} is the *volumetric flow* of the Mass Flow Controller (MFC) at temperature T_o and pressure P_o , and S_{Pump} is the *pumping speed* at T_o and P_{Ch} , assuming the temperature to be constant. Both S_{Pump} and S_{MFC} are volume flow rates; to determine the actual amount of gas (eg molecules per time) the density of the gas must also be known. In steady state operation the chamber pressure is a constant, so one obtains the relation

$$S_{Pump} = S_{MFC} \frac{P_o}{P_{Ch}}. \quad (11.6)$$

This provides one method of estimating the speed of the pump if one has a calibrated MFC and accurate pressure sensors. In practice, gas flow rates are more often measured in terms of sccm or slm (Standard Cubic Cm per Minute or Standard Litres per Minute). These measurements specify mass flow, and are the quantities that the mass flow controllers control. They describe the volume that would be occupied by the gas flow in one minute, if that gas had been at standard temperature

($T_s = 273.15\text{K}$) and pressure ($P_s = 760\text{ Torr}$). The volumetric flow can be found from standard flow using

$$S_{MFC} = S_{SMFC} \frac{P_s T_o}{T_s P_o} \quad (11.7)$$

Here, S_{SMFC} is the volumetric flow of the MFC under standard conditions.

Suppose the pumping speed is a constant and the flow rate S_{MFC} is changed instantaneously to S'_{MFC} from a steady state ($Q_{in} = Q_{out}$). P_{Ch} responds (in this idealized model) exponentially with time constant $\frac{V_{Ch}}{S_{Pump}}$. From the above relations, the following differential equation is obtained:

$$\frac{V_{Ch}}{S_{Pump}} \frac{dP_{Ch}}{dt} = \frac{S'_{MFC}}{S_{Pump}} P_o - P_{Ch} \quad (11.8)$$

For $t > t_o$, the solution is

$$P_{Ch}(t) = \frac{S'_{MFC}}{S_{Pump}} P_o + \left[\frac{S'_{MFC}}{S_{Pump}} P_o - P_{Ch}(t_o) \right] e^{-\frac{S_{Pump}}{V_{Ch}}(t-t_o)} \quad (11.9)$$

where t_o is the time when the flow rate changes from S_{MFC} to S'_{MFC} and the $P_{Ch}(t_o)$ is the pressure at t_o . This provides a method of estimating V_{Ch} if the pumping speed is known.

11.4 The Vacuum System

The vacuum system used in this lab is shown schematically in figure 11.2, with the components identified in figure 11.3. There are three vacuum chambers involved in this system: a Process Chamber, a 1.91 L Calibration Chamber and a Residual Gas Analyzer (RGA) Chamber.

The Process Chamber is on the top of the right-hand rack; it consists of an anodized aluminum housing (gold coloured) sealed to a base plate using an O-ring. The Calibration Chamber is connected to the Process Chamber through two valves which we'll refer to as the yellow and green valves, according to the colour of their knobs. To evacuate the Process Chamber and the Calibration Chamber, a rotary pump is connected to the Process Chamber via the Main Valve. The pressures of the Process and Calibration Chambers are measured by the capacitance heads. The sensitivities of the heads are 2 to 2000 mtorr for the Process Chamber and 1 to 1000 torr for the Calibration Chamber respectively. Two process gases (N_2 and He) can be fed into the system by appropriate controlling of the shut-off valves, bypass valves, MFC's, and green and yellow valves.

The RGA Chamber is in the left-hand rack and connects to the Process Chamber via a needle valve and an air-actuated valve. The RGA Chamber is quite small, just large enough to house the Residual Gas Analyzer. Since the filaments of the RGA must work at pressures lower than 1×10^{-5} torr, a cold cathode head is installed on the RGA Chamber to monitor the pressure. To evacuate the RGA Chamber, a turbo pump, backed with a diaphragm pump, is mounted directly to the chamber. The rotary pump alone cannot reach pressures in the 10^{-5} torr range, but a turbo pump would deform from heating and possibly explode if asked to operate in atmospheric pressure. The purpose of the micrometer-actuated needle valve is to set the pressure difference between the Process Chamber and the RGA Chamber if the gases in the Process Chamber must be analyzed while its pressure is greater than the maximum working pressure of the RGA.

In the panel on the left-hand rack, the RGA Controller (VACSCAN), the 4-channel controller and readout, and the cold cathode head indicator (PENNING 8) are mounted from top to bottom. The VACSCAN measures gases' partial pressures in the RGA Chamber by ionizing them with a hot filament and passing them through a mass spectrometer, which measures intensity versus charge-to-mass ratio. This instrument is controlled by computer via an RS-232 (standard serial)

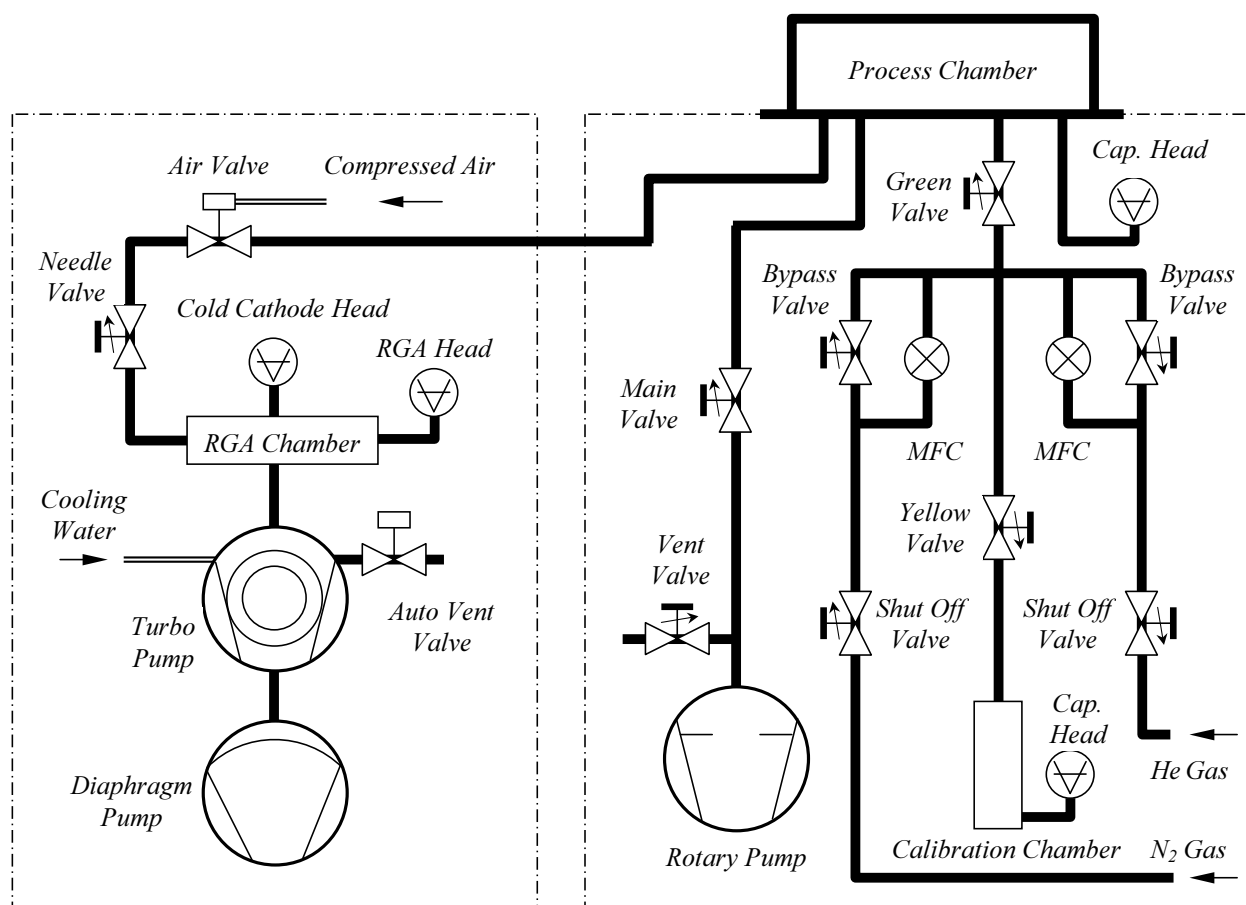


Figure 11.2: Schematic diagram of the vacuum system.

connection. The 4-channel controller and readout both controls and displays the flow rates of the MFCs (Channel 1 for N_2 and Channel 2 for He, both in sccm's). It also displays the pressures in the Calibration Chamber (Channel 3, in torr) and Process Chamber (Channel 4, in mtorr) - even though the display is labelled "Flow". The PENNING 8 indicates the pressure in the RGA Chamber; at the bottom, there are two LEDs for monitoring the RGA's protective circuit. The green one lights when the pressure in the RGA Chamber too high, and the RGA is locked. The red LED indicates that the pressure in the RGA Chamber is lower than 1×10^{-5} torr and the RGA is ready. The protective circuit is also interlocked to the pressure in the Process Chamber, which must be below 1000 mtorr for the protective circuit (and RGA) to function.

11.5 Method

IMPORTANT: The rotary pump must be run throughout the experiment!



Figure 11.3: The vacuum system. **A** is the turbo pump controller, **B** the PENNING 8 gauge, **C** the 4-channel controller and readout, as well as its outputs, **D** is the rotary pump (vent valve is hidden behind **B** and **C**), and **E** is the Calibration Chamber. The Process Chamber, Green and Yellow Valves, Main Valve, RGA, and mass flow controllers are also marked. The needle valve to the RGA Chamber is behind the RGA.

11.5.1 Task 1: Residual Gas Analysis

11.5.1.1 Gas Analysis for the RGA Chamber

Since only the gases already present in the RGA Chamber are to be analyzed here, the air valve should be turned off, using the switch on the panel on the left-hand rack.

1. Turn on the cooling water for the turbo pump, and turn on the Main Power switch, above the air valve switch, to start the diaphragm pump. Find the turbo pump controller (TCP 015), and press the lowest black button on. Set the Select Switch on the Penning 8 gauge to range "1" and turn the power on for the PENNING 8. Monitor the pressure in the RGA Chamber and record approximately how long it takes to fall below 6×10^{-6} torr. Note that the

unit of pressure on the PENNING 8 is **not** torr, but mbar ($760 \text{ torr} = 1 \text{ atm} = 101.325 \text{ kPa} = 1.01325 \text{ bar}$). Turn on the VACSCAN to warm it up, then open *Vacuum Scan and Bar Chart.vi* on the computer's desktop and read the brief description of the software provided there while waiting for the pressure to fall.

2. When the pressure in the RGA Chamber falls below 1×10^{-5} torr, you may analyze the gases in the RGA chamber, assuming the red LED is on. Open the appropriate part of the LabView code. Maintain the pressure below 8×10^{-6} torr before taking data, as the pressure in the chamber can sometimes fluctuate. Run the LabView VI and record the partial pressures of the five most abundant gas species as detected by the RGA. The filament is usually turned off automatically when data collection is completed. If you stop the VI while it is taking data, however, the filament will remain on – to avoid burning out the filament, please turn it off manually. We recommend you let the VI run its course.
3. Compare the composition of the gas in the chamber with that of air.

11.5.1.2 Gas Analysis for the Process Chamber

Now, the air-actuated valve must be opened, to allow the gases in the Process Chamber to reach the RGA.

1. Please check that all valves in the right-hand rack are closed. The Main Valve is operated by the black knob above the rotary pump. Find the toggle switch on the motor and switch on the rotary pump if you have not already done so. After a few minutes, slowly open the Main Valve to let the rotary pump pump on the Process Chamber.
2. Switch on the power to the 4-channel controller and readout and select to channel 4. Monitor and control the pressure of the chamber until it is about 500 mtorr. How can you control the pressure in the Process Chamber? If the pressure in the Process Chamber is much lower than 500 mtorr, you need to turn off the rotary pump and vent the Process Chamber – how do you do this?
3. The air-actuated valve is pneumatically controlled with a working pressure of 60 PSI – check that the regulator on the bottle of compressed air is set correctly. As explained above, a needle valve makes it possible to analyze gases at with Process Chamber pressures greater than 1×10^{-5} torr. Before turning the air valve's switch on, make sure the RGA filament is off. When you switch the air valve on, monitor the pressure of the RGA Chamber using the PENNING 8 gauge; if the pressure in the chamber increases, gas is flowing from the Process Chamber to the RGA Chamber. If the pressure is too high for your measurement, adjust the needle valve *slightly* to reduce the gas flow into the chamber.
4. Analyze the gases in the RGA Chamber as before, and compare the results with your previous measurements. After finishing this task, switch off the air-actuated valve.

It is important that you understand that the results you just obtained are the partial pressures of the various gas constituents in the RGA Chamber, which are proportional to, but much lower than, the partial pressures of the same species in the Process Chamber.

11.5.2 Task 2: Mass Flow Controllers

An MFC accurately measures and controls the mass flow rate of a gas. Here you will learn how to control the external gas flow (N_2 and He) from the bottles to the Process Chamber.

1. Check that all valves in the right-hand rack are closed except the main valve. Set the regulators on the bottles of N_2 and He to about 15 PSI. Slowly turn on the shut-off valve for N_2 . All the flow should pass through the MFC (the bypass valve is kept closed).
2. The MFC can be controlled either manually or automatically. For manual control, set the toggle switches for channel 1 to **FLOW** and **ON** and monitor channel 4 – the Process Chamber. The pressure will increase after you turn on the Green Valve. Channel 1 now indicates the flow rate of N_2 , which is about 20 sccm (the flow rate may not be displayed if the value is greater than 20 sccm). Make fine adjustments with the Main Valve until the system is balanced and the pressure in the chamber is about 500 mtorr.
3. Turn the toggle switch **ON**, repeat steps 3 and 4 of 11.5.1.2 to analyze the gases in the Process chamber, and compare the result with previous ones. Turn the toggle switch back **OFF**.
4. Pump the Process Chamber back down to its minimum pressure. Repeat the process for He, using channel 2.

11.5.3 Task 3: Measurement of Pumping Speed

11.5.3.1 Preparation

1. This task uses only the Process Chamber and Calibration Chamber, so you should turn the RGA filament and air valve off if you haven't already done so. Switch off the VACSCAN because it may impact the data.
2. Open *Gas Flow and Pumping Speed.vi* on the desktop computer, and read the instructions contained therein. In the description there, 'Alternative mode' indicates alternating - the mass flow is periodically turned alternated between two values.
3. In the "Setting and Testing" page of the VI, choose Testing Mode and vary all the setting parameters except the Measuring Chamber. Run the VI to see how the MFC drive voltage changes with different settings. If there are any problems, check that two cables have been connected from the DAC0 and DAC1 Analog Output to channels 1 and 2 of the Set Point Input on the 4-channel readout as well as the Analog Inputs ACH4 and ACH5. Check that four cables have been connected from ACH0, ACH1, ACH2 and ACH3 to the Transducer Scaled Outputs of channels 1 to 4 respectively. These cables are all connected on the rear side of the lower BNC breakout panel for the 4-channel readout.
4. To obtain the relation between the pressure in the Process Chamber and the flow rate, check that the shut-off valves, Green Valve and Main Valve in the right-hand rack are wide open – why must these valves be open? Set the toggle switches for channels 1 and 2 to EXT and ON; in the VI, set the Mode to Measuring and the Measuring Chamber to Process. Select proper settings, run the VI, and monitor the flow rate and total pressure with time. Vary the voltage applied to each channel (always keep it < 5 V) to get a rough idea of how the pressure changes with flow rate. You have the option of storing the data in a spreadsheet format on the hard disk when the VI terminates.

11.5.3.2 Calibration of the N₂ MFC

1. Ensure that there is no gas flow into the Process Chamber. Turn the Green and Yellow Valves wide open, and monitor the pressure in the Calibration Chamber from the Capacitance Head. Close the Green Valve when the pressure in the Calibration Chamber has stabilized. Make sure that channel 1's shut-off valve is open and that its toggle switch is set to EXT; set the Mode to Measuring and the Measuring Chamber to Calibration. Set the Flowing Gas to Nitrogen and the Driving Voltage (Max) for N₂ to be 5 V. Choose the period to be 30 seconds (Direct Flow Pattern) and the Number of Cycles to be 1. Turn channel 1's other toggle switch ON, and check that there is still no flow through the MFC – how can you check?
2. Run the VI; the N₂ gas flows through the MFC directly to the Calibration Chamber, whose pressure increases. Save your results to calibrate the maximum N₂ flow rate for the MFC (at 5 V). Compare your results with the standard flow rate using the equation in the Theory section (11.3), and obtain the MFC working temperature T_o. Do you need to calibrate the flow rate for the MFC with different driving voltages? Why or why not?

11.5.3.3 Measurement of the N₂ Pumping Speed

Close the Yellow Valve and open the Green Valve again. Vary the driving voltage to the N₂ MFC to obtain its flow rate (S_{MFC}) versus Process Chamber pressure (P_{Ch}), from which you can calculate the pumping speed of N₂ for different driving voltages. The flow rate of the MFC (S_{MFC}) is obtained from the value of S_{SMFC} , T_o, and P_o from step 1 in 11.5.3.2. Graph the pumping speed versus Process Chamber pressure – is the pumping speed a constant? Before starting the VI, ensure that you have pumped down to base pressure and that the period is long enough to establish a steady state before the MFC is turned off.

11.5.3.4 Volume of the Process Chamber

1. Using the maximum flow rates and the known calibration volume, carry out a procedure similar to 11.5.3.2 above to determine the effective volume of the Process Chamber. Measure the external dimensions of the Process Chamber and estimate its volume – how can you explain the difference between these two values?
2. Select Alternative Flow Pattern. Adjust the period to be a few time constants (about 30 seconds), and select a proper value for the Number of Cycles. Since the pumping speed varies with pressure, a small driving voltage change should be selected (e.g. 5 V for Max and 4.5 V for Min) where the pumping speed can be roughly considered to be constant. For N₂ flow, record the transient pressure data, and use it to obtain an independent value for the Process Chamber volume. Compare the results with those obtained above and give a detailed explanation.

11.6 Shutdown Procedures

The shutdown procedure is very important for this lab. If you aren't familiar with the procedure, you can usually follow this principle: the earlier you turned something on, the later you turn it off.

1. Turn the toggle switches OFF for all channels, and wait until the Process Chamber reaches its base pressure, then close all the valves in the right-hand rack.

2. Turn off the RGA filament and the air-actuated valve if you haven't already done so, then switch off the VACSCAN, the PENNING 8 and the turbo pump.
3. Turn off the rotary pump and the 4-channel controller and readout, then finally the Main Power.
4. Open the vent valve (a small toggle valve at the inlet to the rotary pump) and close it – this vents the rotary pump. Shut off the valves on the gas bottles, as well as the cooling water.
5. Check the system and confirm that you have performed all the above steps.

11.7 Reference

O'Hanlon, J.F., A Users Guide to Vacuum Technology, John Wiley & Sons, New York (1989).

Experiment 12

Fourier Transform Infrared Spectroscopy of Air and CO₂

12.1 Purpose

1. To understand and familiarize yourself with infrared spectroscopy as a measurement tool.
2. To measure and understand the absorption spectra of several gases.

12.2 Introduction

When radiation emitted from the earth's surface travels through the atmosphere, some of it is entirely absorbed by the gases present and some of it passes almost unaffected. The wavelength regions most useful for measuring surface emission are those away from atmospheric gases' absorption bands. These transparent "atmospheric window" regions are found in the infrared and microwave regions of the spectrum. For instance, the spectral regions 3.5 – 4 and 8 – 12 μm are "windows" in which very little thermal radiation is absorbed by the atmosphere. Carbon dioxide (CO₂) is a minor constituent of the atmosphere, but is the main gas responsible for the earth's greenhouse effect because it has an absorption band within these wavelengths, closing this window. Apart from keeping the planet warm, it is used in many applications, notably CO₂ lasers. Water vapor also has absorption bands within these wavelengths.

Fourier transform infrared (FTIR) spectroscopy is a common laboratory tool used for applications ranging from identification of species in chemical mixtures to quantized levels in semiconductor quantum well structures. It is a versatile tool that allows the resolution of extremely fine spectral lines in a reasonable time. Although the technique has been known for many years, practical implementations had to await the advent of both the Fast Fourier Transform (FFT) algorithm and computers. Today, FTIRs are ubiquitous tools in both research and applications laboratories.

12.3 Theory

Absorption Lines in Air and CO₂

Figure 12.1, reproduced from reference 1 shows the absorption spectra of common atmospheric molecules and air's aggregate absorption due to the sum of all the constituent gases. Some of these absorption lines are sharp, while others are broad. In the mid-infrared (MIR) region of the electromagnetic spectrum, molecules absorb (or emit) light through the interaction between the photons and the vibrating electric dipoles of the molecules. Hence, molecules such as CO, which have a polar bond (C has 4 valence electrons while O has 6), and thus a strong oscillating dipole moment when they vibrate, absorb strongly at specific energies. Non-polar molecules, such as O₂ and N₂, which together with monatomic gases constitute 99% of the atmosphere, do not have a resulting dipole moment and are therefore transparent in the MIR.

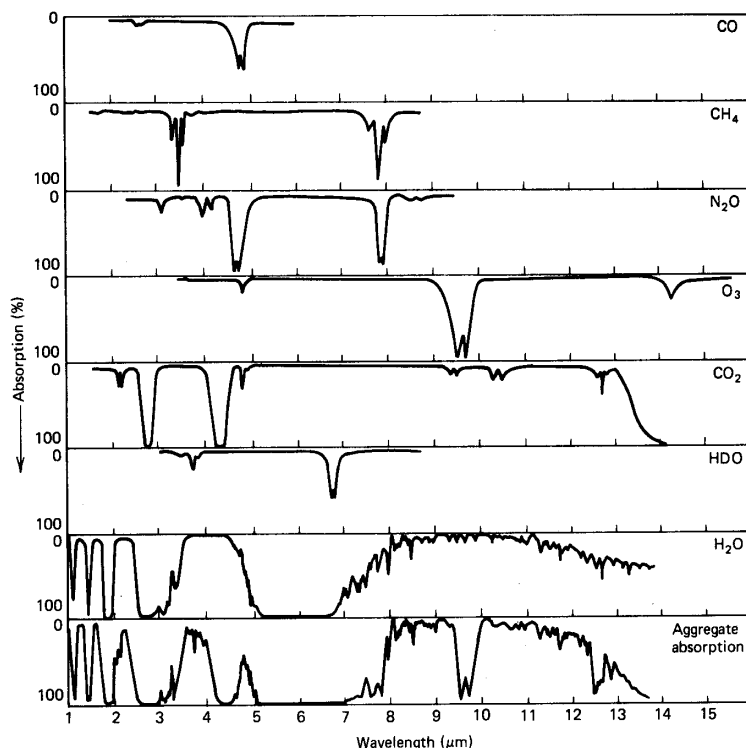


Figure 12.1: IR absorption spectra of common atmospheric gases, from *Handbook of Geophysics and Space Enviroments* by S.L. Valley, Ed. (1965), as reproduced in reference 1.

Vibrational Modes

Electromagnetic waves in the infrared (IR) region with wavelengths λ between 780 nm and 2000 μm , (wavenumbers ν between 12800 cm^{-1} and 5 cm^{-1}) can stimulate molecular vibration (and rotation) modes. Spectroscopists prefer using wavenumber because it scales linearly with energy. Often the symbol k is used for wavenumber, but since the instrument manual uses ν , we adopt nu for wavenumber as well. The light can only be absorbed if there is a net change of dipole moment due to the vibrational motion of the molecule, i.e. a transition dipole moment. If the molecule's atoms are modeled as balls and the bonds between them as perfect springs, any vibration can be described classically by Hooke's law for a spring. The frequency f for the resulting vibration is given in equation 12.1,

$$f = \frac{1}{2\pi} \sqrt{\frac{K}{\mu}} \quad (12.1)$$

where K is the spring constant and $\mu = \frac{m_1 m_2}{m_1 + m_2}$ is the reduced mass of the system.

The potential and kinetic energies of this harmonic oscillator may be obtained from quantum mechanics, where the eigenvalues (energy levels) are quantized as given in equation 12.2. The selection rules for IR absorption state that $\Delta n = \pm 1$.

$$E_n = hf \left(n + \frac{1}{2} \right) \quad (12.2)$$

where h is Planck's constant, f is the frequency from above and $n=0,1,2,\dots$ is an integer called

the vibration quantum number. At room temperature almost all molecules are in the vibrational ground state ($n=0$). The observed wavenumbers $\Delta\nu$ for the first harmonics can be calculated from the absorbed energy $\Delta E = E_1 - E_0 = hc\Delta\nu$, which combines with equation 12.1 to give

$$\Delta\nu = \frac{1}{2\pi c} \sqrt{\frac{K}{\mu}} \quad (12.3)$$

Therefore the observed wavenumbers (or frequencies) depend on the strength of the bonds between the atoms and on their masses.

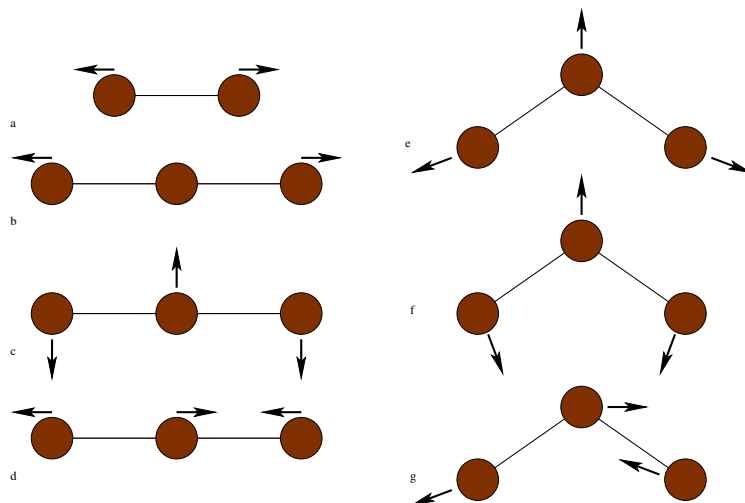


Figure 12.2: Vibrational modes of diatomic and triatomic species. **a)** Diatomic stretching mode ν_1 . **b)** and **e)** Triatomic symmetric stretching modes ν_1 . **c)** and **f)** Triatomic bending modes ν_2 . **d)** and **g)** Triatomic antisymmetric stretching modes ν_3 .

Diatomic molecules, such as CO, can only have one vibrational mode, consisting of a stretching (or compressing) along the axis of the molecule. This is illustrated in figure 12.2. Triatomic molecules, on the other hand, have additional degrees of freedom. This will create symmetric and anti-symmetric stretching modes in addition to bending modes. These vibrational modes are denoted by ν_1 , ν_3 and ν_2 respectively, and are also shown in figure 12.2. CO₂, a linear molecule, lacks a permanent dipole moment (it has a centre of inversion). Hence, it will have no absorption in the symmetric vibration mode. In the anti-symmetric and bending modes however, an oscillating dipole moment will be created and IR radiation can be absorbed. A more thorough discussion of these phenomena can be found in references 1 and 2. Table 12.1 shows the vibrational modes of some common atmospheric radiative molecules (adapted from reference 1).

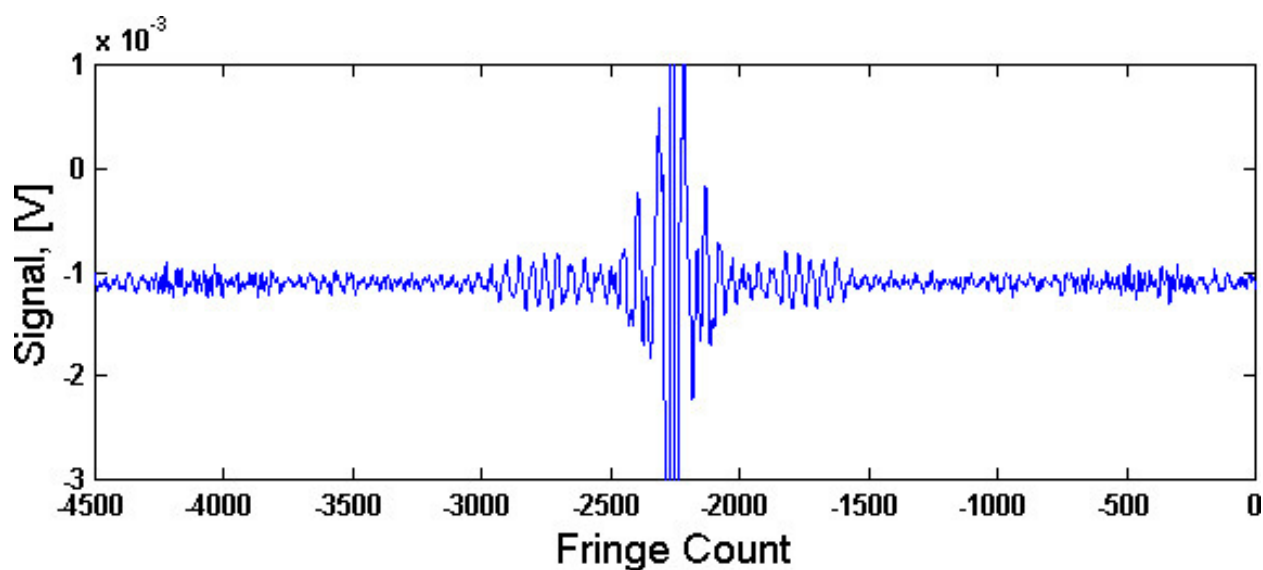
FTIR Spectrometers

Fourier transform infrared spectrometers have caught on against dispersive spectrometers since the 1980s. FTIR spectrometers are faster, more exact, and have a higher signal to noise ratio. The first advantage is often called Fellgett's advantage and comes from the fact that all wavelengths are measured simultaneously. Secondly, an FTIR spectrometer has a laser to measure the position of the moveable mirror, which allows simultaneous calibration of wavelengths. Finally, it does not require slits or monochromators, allowing for measurements at higher intensity. These advantages

Table 12.1: IR-active vibrational modes of various atmospheric gases in wavenumbers (cm⁻¹).

Species	ν_1	ν_2	ν_3	ν_4
CO	2143			
CO ₂		667	2349	
N ₂ O	1285	589	2224	
H ₂ O	3657	1595	3776	
O ₃	1110	705	1043	
NO	1904			
NO ₂	1306	755	1621	
CH ₄	2917	1534	3019	1904

can be utilized, since the Fourier transformation of the resulting interferograms to spectra can be calculated nowadays within seconds.

**Figure 12.3:** A sample interferogram.

The polychromatic IR source beam is split and sent through a Michelson interferometer before it probes the sample. A moveable mirror reflects the beam in such a way that it superimposes and interferes with the incoming one. As the system's path length is varied, each wavelength alternates between constructive and destructive interference, so the signal at the detector, the sum of all wavelengths present, is a complicated interferogram containing information about the intensity at each frequency (see figure 12.3). The absorption of the sample alters this interferogram. From the interferograms, usually single channel intensity spectra are calculated using the Fast Fourier algorithm (FFT). The principle of operation is depicted in Figure 12.4, with the actual device shown in figure 12.5.

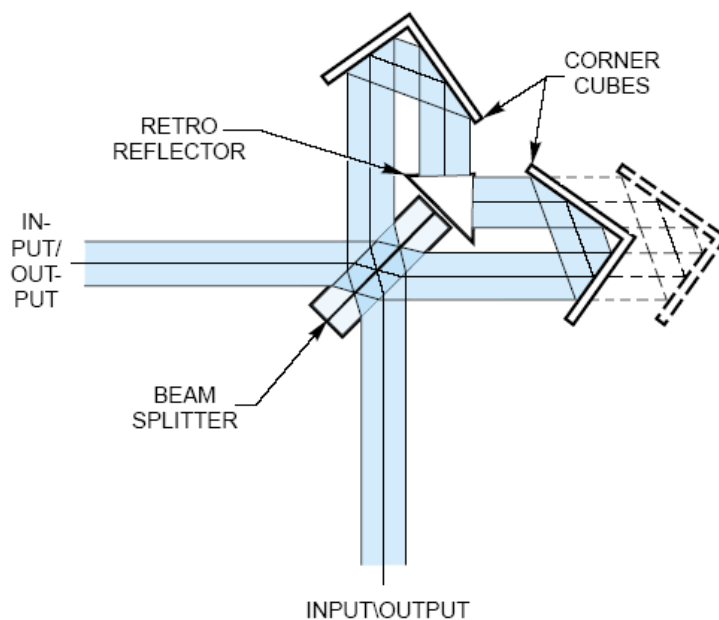


Figure 12.4: Schematic of the Michelson interferometer at the heart of the FTIR technique. Refer to reference 3 for a more detailed explanation.

Using equations 12.4 and 12.5:

$$\frac{I}{I_o} \equiv T = 10^{-\varepsilon cd} \quad (12.4)$$

$$A = -\log T = \varepsilon cd, \quad (12.5)$$

intensity spectra can be converted into transmission (T) or absorbance (A) spectra, with I_o representing the intensity of the background or reference spectra and I the intensity of the sample spectrum. Chemists usually prefer absorbance spectra because sample concentrations (c) can be estimated by the Beer-Lambert law 12.5 for a known molar absorption coefficient ε and sample thickness d . During the last decades FTIR spectroscopy has been increasingly used for investigations of biomolecules, like proteins and DNA. High signal-to-noise ratio and fast accumulation of scans made it possible to get highly-resolved difference spectra. Applications of FTIR spectroscopy include investigating kinetic pathways or interactions between proteins and their environment, like embedded membrane proteins and surrounding lipids.

More information on the FTIR technique can be obtained from the MIR 8000 spectrometer manual (Reference 3) as well as references 4 and 5.

Lineshape

Although the simplified theory presented here states that absorption lines are found at specific energies, each spectral line has a finite width. This width comes in part from the natural linewidth of the optical transition but is dominated by Doppler broadening, also called temperature broadening, and collision broadening which is also sometimes called pressure broadening. The natural linewidth arises in part from the Heisenberg uncertainty principle and is so small that it can be ignored in

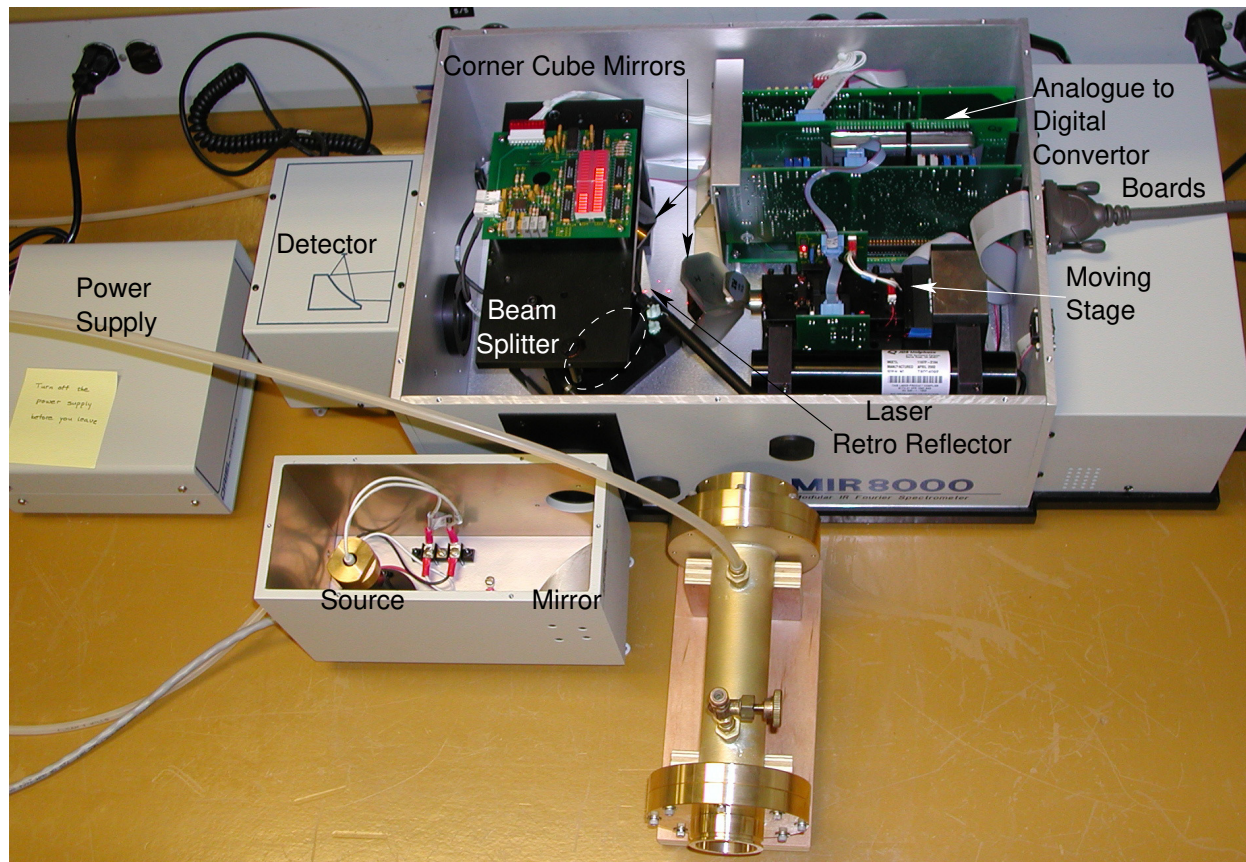


Figure 12.5: The interferometer's constituent parts. The gas cell (brass) must be inserted between the source and the interferometer unit for some parts of the lab.

our case. Doppler broadening is caused by the rapid translational motions of gas molecules. These motions are completely random and therefore have a Gaussian (Normal) distribution about an average value, ν_o , described by

$$P(\nu) = \frac{1}{\sqrt{2\pi}\sigma} e^{-\frac{(\nu-\nu_o)^2}{2\sigma^2}} \quad (12.6)$$

where σ , the standard deviation, describes the width of the line. What is relationship between σ and the full width at half maximum (FWHM) of the line?

Collision broadening is caused by disturbances to the absorption process during molecular collisions. Collision broadening varies directly with pressure and gives rise to a Lorentzian (Cauchy) lineshape:

$$P(\nu) = \frac{1}{2\pi} \frac{\Gamma}{(\nu - \nu_o)^2 + \left(\frac{\Gamma}{2}\right)^2} \quad (12.7)$$

where Γ is the FWHM of the line. The Gaussian shape is more compact while the Lorentzian lineshape is narrow but has “wings” that extend far beyond the centre energy.

12.4 The Apparatus

The apparatus consists of an FTIR spectrometer with a detector, an MIR source and a gas cell. The gas cell consists of a chamber with silicon windows at either ends. Ensure that you **turn on the FTIR and the MIR source as soon as you arrive** — they take at least 30 minutes to stabilize. The LEDs on top of the unit should be on and may be fluctuating at first but will eventually stabilize. You should also hear the mirror moving inside the unit.

The FTIR is controlled by an Arduino Due micro-controller which is connected to a computer. Communication between the Arduino micro-controller and the MIR8000 uses a proprietary protocol over a 25pin connector (<https://git.sarlab.ca/michal/due-ftir>). The interaction of the PC with the arduino is a low-level text communication over a serial port (native USB port of the Arduino). A python GUI (MIR8000) provides means to adjust the spectrometer settings (resolution , mirror speed etc) and retrieve data.

12.5 Procedure

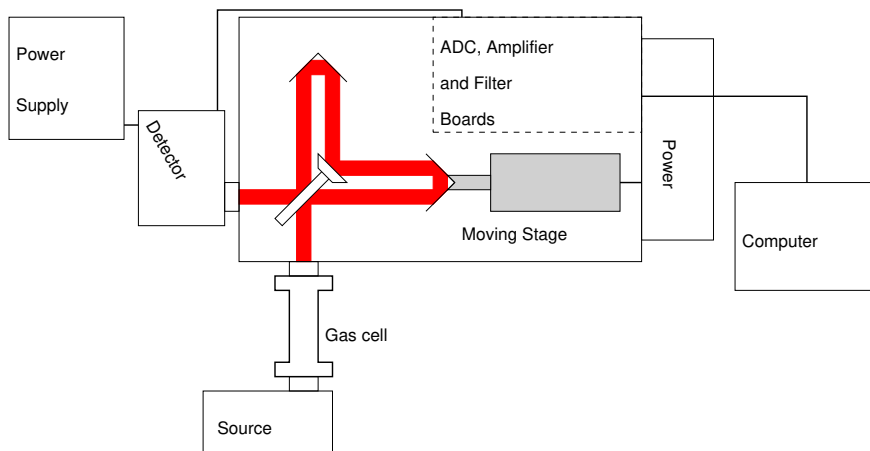


Figure 12.6: Block diagram of the FTIR Spectrometer apparatus.

1. A note on the computer DAQ system

This FTIR is a valuable piece of apparatus, costing around \$35K. Good hardware does not age if looked after, but in this case the hardware can only be run by a computer system that existed when the hardware was built, and computers do age, very rapidly. As a workaround the old DAQ computer plus ISA card has been replaced by an arduino, some glue hardware and general-purpose PC.

2. The interferogram and transmission throughput of the system:

Turn on the FTIR spectrometer and power supply. The MIR8000 software is accessible on the desktop. Ensure that the IR source is installed on the FTIR main unit as shown in figure 12.6, and that one of the connection flange setscrews is snug (**NOT TIGHT**). If the gas cell is in place, take it out (this is a simple press-fit connection; do not remove any screws or bolts). Open MIR8000 to write the default parameter to the scanner (indicated by asterisks: 64 cm⁻¹ resolution, 3.16 mm/s velocity, 3kHz LP filter, 100 Hz HP filter, gain 1 and no offset).

The sound from the MIR scanner might change to a clicking of different frequency (or become a lot less audible).

The interferometer should begin scanning and data can be transferred to the computer using 'Start ACQ'. Interferogram data will be written as one column to the GUI text window. Note that not all combinations of parameters will result in meaningful data. In our experience only the 3.16m/s mirror velocity is required. Resolution better of 64 cm⁻¹ up to 4 cm⁻¹ tend to give useful data. You might observe erratic sound from the mirror motor when better resolutions are used. Check your acquired data as you perform your acquisitions.

The software does not provide even the most basic of data post processing. This is left as an exercise to the student; consider the tutorial provided here:

www.essentialftir.com/fftTutorial.html and the references listed below. Investigate the optimal process of a bi-directional spectrum using forward and reverse mirror direction and the application of the appropriate phase correction (Mertz method).

To perform your analysis, the acquired data in the text window can be directly copied to the clipboard and simultaneously to a temporary file (MIR8000data.tmp). From there, a simple gnuplot script can immediately display the acquired data and be used to fine-tune the acquisition parameters to the needed settings before embarking on detailed analysis in your software of choice.

The highest intensity part of the interferogram is called the centre burst. Explain the general shape of the interferogram. Why is the interferogram shifted? (hint: it should not be, consider playing with the 'Offset' setting) What would happen to the interferogram at higher (or lower) resolution?

In the interferogram, you were collecting the throughput signal of the source through the FTIR. Can you explain the general shape of the spectrum (hint: what is the IR source)? Why does this spectrum exhibit lower-intensity troughs? What is the useful spectral range of this FTIR system with the current source and optics? Although you will acquire data at all wavenumbers in the remainder of this lab, you need only perform the analyses on the system's useful spectral range. What are the relationships between wavenumber, wavelength and energy? What are the relationships between the interferometer resolution in the different units?

3. The effect of purging the apparatus:

At 4 cm⁻¹ resolution, acquire a spectrum without nitrogen flow. You will want to average several spectra for better SNR (how many?). Now gently flow N₂ gas through the FTIR and source units and let them purge for a while. Take a new spectrum after 5 min. of purge and another one 5 min. later (saving both, of course). What do you observe? Plot and save both the transmittance and absorbance of air over the useful spectral range. Identify as many peaks as you can. For the peaks of a given molecule, are the absorption peaks equidistant in energy? Can you identify the water peaks?

Continue purging the system with N₂ for the remainder of the lab.

4. Signal to noise ratio of the interferometer:

Acquire a signal at 4 cm⁻¹ resolution (possibly averaged). Determine the Signal to Noise (S/N) ratio over the useful spectral range. Repeat for a different resolution.

5. Throughput of the gas cell:

Install the gas cell and purge it too with N₂ making sure that the valve on the gas cell is open. Wait a sufficient amount of time for the system to be well purged. Acquire signal at 4 cm⁻¹ resolution and use the throughput spectrum from the last step as your normalization spectrum. Measure the optical throughput of the gas cell (which corresponds largely to the transparency of the windows). What is the transmittance and absorbance of this system? Is it transparent in the spectral range of interest for the study of the CO₂ vibrational absorption lines?

6. Absorption of CO₂ gas:

Replace the N₂ flowing through the gas cell with CO₂. Adjust the CO₂ pressure to be no more than a few psi - just enough to make sure there is flow through the cell; let the gases exchange over a period of 1 minute. **IMPORTANT:** shut the gas cell valve after 1 minute and fan the area with your labbook — CO₂ in sufficient quantities will cause headaches. Fortunately, our lab is large and fairly well ventilated.

Acquire a signal at 4 cm⁻¹ resolution. What are the transmittance and absorbance of CO₂? Try to identify the vibrational mode corresponding to each peak. Fit the lineshapes of the absorbance peaks. Are the peaks more Gaussian or Lorentzian in shape?

7. Absorption of air:

Let the cell fill with air and take data. Plot both air and CO₂ data on the same graph.

8. Use these data to measure the fraction of CO₂ in the atmosphere. Use absorption data given in Table 12.2.

12.6 References

1. Earl J. McCartney, *Absorption and Emission by Atmospheric Gases* (John Wiley & Sons, 1983).
2. Alois Fadini and Frank-Michael Schnepel, *Vibrational Spectroscopy* (Ellis Horwood Limited, 1989).
3. Spectra-Physics, *MIR 8000 Modular Infrared Fourier Transform Spectrometer* (Spectra-Physics, 2003).
4. J. Kauppinen and J. Partanen, *Fourier Transforms in Spectroscopy* (Wiley-VCH, 2001).
5. Peter R. Griffiths, James A. de Haseth, *Fourier Transform Infrared Spectrometry* (John Wiley and Sons, 1986).
6. HITRAN database www.cfa.harvard.edu/hitran/

Frequency (cm ⁻¹)	Absorption $a(\text{cm}^{-1})$
2260	0.3476
2272	0.5289
2284	0.4268
2296	1.8156
2308	6.7811
2320	22.5790
2332	49.6230
2344	32.6236
2356	51.3564
2368	51.8147
2380	7.1494
2392	0.0493
2404	2.0160E-05
2416	3.6899E-05
2428	1.5972E-05
2440	4.4422E-05

Table 12.2: Absorption of CO₂ at standard temperature and pressure (STP), convoluted with the lineshape of the laboratory spectrometer run with a resolution of 4 cm⁻¹. The exponential form is given, so the transmission $T = \exp(-acd)$ where c is the concentration with respect to 100% CO₂ at STP, and d is the pathlength. Original absorption line parameters are from the HITRAN database.

Experiment 13

Absorption Band-edge Thermometry of Semiconductors

13.1 Purpose

1. To explore several forms of thermometry.
2. To become familiar with some fundamental properties of semiconductors.
3. To understand and familiarize yourself with optical spectroscopy as a measuring tool.

13.2 Introduction

In this experiment, you will be characterizing the absorption edge of semiconductor samples at different temperatures. One application of this technique is the measurement of the process temperature of semiconductors under ultra-high vacuum where other methods fail [1,2]. Absorption bandedge thermometry was studied extensively at UBC, and has now been commercialized.

13.3 Theory

The Semiconductor Bandgap

Crystalline solids may be categorized as conductors or insulators depending on the distribution of electrons [3,4,5]. In a simple picture, the outer electrons in a metal, instead of remaining attached to their home ion, are delocalized over the entire crystal. Electrons in an insulator are more tightly bound. A semiconductor is both a poor conductor and a poor insulator.

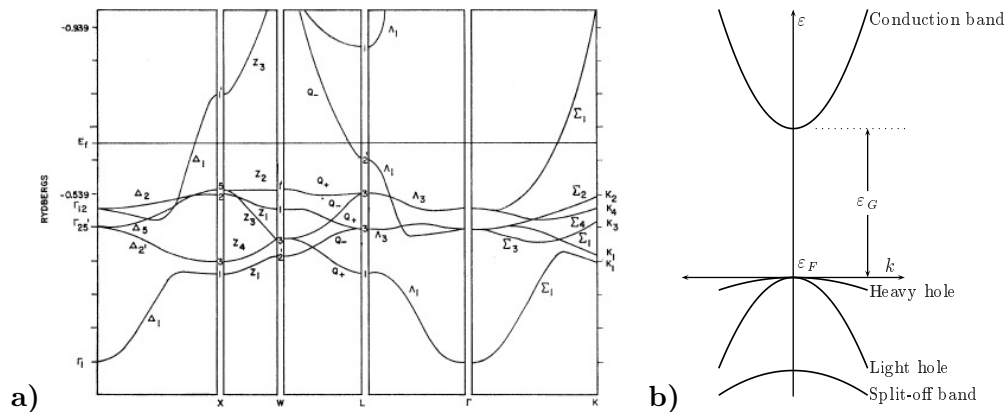


Figure 13.1: Band structure of different solids: **a)** Copper. **b)** Gallium arsenide (GaAs) near the Γ point (the origin in k -space) — labelled are the conduction band, two valence bands and the split-off band.

A more rigorous treatment requires considering electrons not in real space but in momentum (or wavevector) space, referred to as k -space, as well as quantum and statistical physics. Wavevector

space is the Fourier transform of real space, and states there are indexed by their crystal momentum $\vec{p} = \hbar\vec{k}$ instead of \vec{r} . In k -space, a solid is defined using band structure: a band describes energy levels $\varepsilon(\vec{k})$ where electrons are allowed, as shown by the curves in Fig. 13.1. These bands are combinations of orbitals on all atoms in the crystal, and can only accommodate as many electrons as could be accommodated in their component real-space orbitals.

The energy of the highest occupied electronic state at zero temperature is called the Fermi level, ε_F . If the Fermi energy falls in the middle of a band (i.e. the band is partially-filled) as in Fig. 13.1a, the crystal is metallic. When this occurs (e.g. band Σ_1 in the upper left), there is always a level slightly higher in energy for the last electron to excite into; hence, in an external field the electron will move and current will flow.

Fig. 13.1b shows part of the band structure of gallium arsenide (GaAs), a semiconductor. For this material, the Fermi level lies somewhere between the “valence” band (downward facing parabola) and the “conduction” band (upward facing parabola), and the highest-energy electron lies at the very top of the valence band. The gap between the valence and conduction bands is the forbidden energy gap, normally called the bandgap and labelled ε_g . There are no states at any momentum in this energy range. Under a moderate electric field, there are no allowed energy levels to move to, hence the material is insulating. For a pure GaAs crystal [4,6], the external field would have to exceed the energy of the bandgap in order to excite electrons to the conduction band and allow current to flow.

For the remainder of the discussion, we will only consider the band structure shown in Fig. 13.1b. As mentioned above, electrons could be excited from the valence band to the conduction band with a sufficiently strong electric field, but this can also be done with light. If a photon impinges on the crystal with an energy less than ε_g , then it cannot be absorbed and will pass unmolested, just as visible light goes through a window pane. However, if the energy of the photon exceeds ε_g , it can be absorbed by the material, exciting an electron from the valence band into the conduction band, and the material will be opaque to light of that particular color (this is why regular window glass protects us from ultraviolet light). Hence, an experiment using transmission of light can determine the bandgap of a material — the material would be completely transparent below ε_g and completely absorbing above ε_g , leading to a step function absorption spectrum.

This can be summarized as follows:

$$\begin{aligned} h\nu &\geq \varepsilon_g; & \alpha &\geq \alpha_g \\ h\nu &< \varepsilon_g; & \alpha &\rightarrow 0 \end{aligned} \tag{13.1}$$

where h is Planck’s constant, ν is the frequency of incident light, α is the optical absorption coefficient in cm^{-1} and α_g is the optical absorption coefficient at the band-gap energy. For GaAs, $\alpha_g = 8000\text{cm}^{-1}$ [7].

The preceding discussion is strictly rigorous for a perfect, infinite crystal at absolute zero. In this experiment, however, we will be dealing with real crystals which are finite and have imperfections, and the experiments will be done near room temperature. Both properties contribute to a broadening of the step function, leading to an absorption bandedge known as the Urbach edge [1,2].

The absorption in the Urbach region can be described by:

$$\alpha(h\nu) = \alpha_g e^{\frac{h\nu - \varepsilon_G}{\varepsilon_o}} \tag{13.2}$$

where ε_o is the characteristic energy of the Urbach edge, ε_G is the extrapolated optical bandgap energy, and α_g is again the optical absorption coefficient at the bandgap energy. Note that we

denote the Urbach edge optical bandgap with a capital G subscript to distinguish it from the other definition of the bandgap; in practice, we can consider the two quantities to be the same for the purposes of this laboratory. This equation is **only** valid for $h\nu < \varepsilon_G$; in practice, the region where $\alpha \sim 30 - 100\text{cm}^{-1}$ can be used to extrapolate for ε_G .

A full quantum mechanical treatment of optical absorption in direct bandgap semiconductor material gives the following relationship between α and $h\nu$:

$$\alpha h\nu \propto \sqrt{h\nu - \varepsilon_g} \quad (13.3)$$

Hence, a plot of $(\alpha h\nu)^2$ versus $h\nu$ should give an extrapolated value at $\alpha h\nu = 0$ that corresponds to the bandgap. This equation is **only** valid for $h\nu > \varepsilon_g$. In practice, this last method will work well when one can extract good values of α but will not work when α is obscured, for instance due to normalization or dark signal uncertainties. In summary, there are three methods that can be used to obtain a bandgap from optical absorption measurements.

In quantum theories of the Urbach edge for crystalline semiconductors, both ε_o and ε_G are proportional to the phonon population — phonons are quantized acoustic waves (vibrations of the crystal lattice). Using the Einstein model for phonons, the width of the Urbach edge is

$$\varepsilon_o = S_o k_B \theta_E \left[\frac{1+X}{2} + \frac{1}{e^{\frac{\theta_E}{T}} - 1} \right] \quad (13.4)$$

where the dimensionless parameter X is a measure of the structural disorder, θ_E is the Einstein temperature, S_o is a dimensionless constant related to the electron-phonon coupling, and k_B is the Boltzmann constant. X is expected to be zero for a perfect crystal. The temperature dependence of the band gap is given by

$$\varepsilon_G(T) = \varepsilon_G(0) - S_g k_B \theta_E \left[+ \frac{1}{e^{\frac{\theta_E}{T}} - 1} \right] \quad (13.5)$$

where S_g is a dimensionless coupling constant and $\varepsilon_G(0)$ is taken as the published band gap at liquid-He temperature.

Optical Absorption Measurements

In this experiment, the absorption coefficient will be extracted from optical transmission of light through the sample. The spectrum read by the computer is a convolution of the incident light intensity reaching the detector and the detector response. Fig. 13.2 shows a typical spectral response for a silicon detector. The signal $I(\lambda)$ read by the detector at wavelength λ , for light incident on a sample of thickness d with wavelength-dependent absorption coefficient α is given by

$$I(\lambda) = S(1 - R)I_o(\lambda)e^{-\alpha d} \quad (13.6)$$

where S is a dimensionless scattering factor, R is the reflectivity of the material and $I_o(\lambda)$ is the intensity of light incident on the sample. For semiconductors near the fundamental absorption edge, we can approximate the refractive index, n , to be wavelength independent; R is then

$$R = \left| \frac{n - 1}{n + 1} \right|^2 \quad (13.7)$$

The transmission of light through the sample is thus

$$T = \frac{I(\lambda)}{(1 - R)SI_o(\lambda)} = e^{-\alpha d} \quad (13.8)$$

and can be inverted to extract α when the thickness of the sample is known.

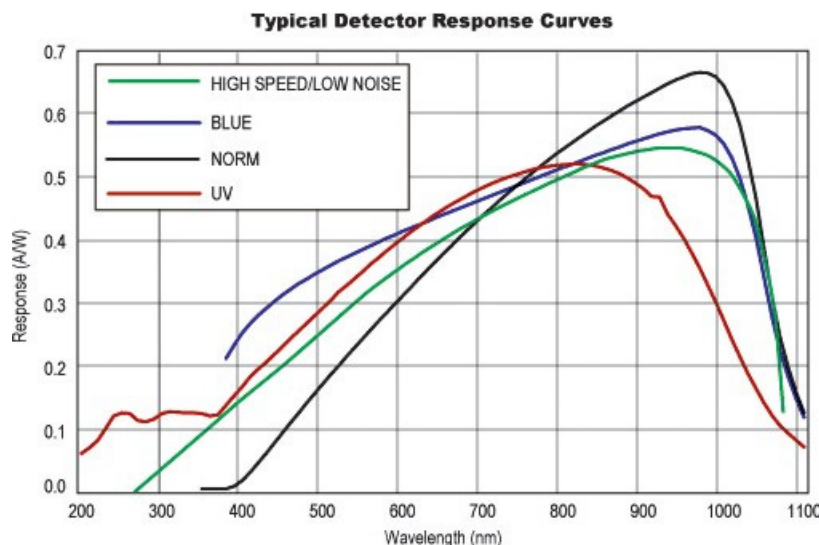


Figure 13.2: Silicon detector typical response.

Thermocouples

The theory of thermocouples is well covered in the Omega Corporation's practical temperature measurements publications [8,9]. These publications are available electronically [8] on the experiment computer as well as in the physical catalog [9] supplied with the experiment. The student is referred to section Z of the catalog for the theory of operation and the wiring diagrams.

13.4 Apparatus

The apparatus consists of a diffraction grating spectrometer with a CCD detector (Ocean Optics USB2000) connected to a computer by USB; a type K thermocouple and power resistor mounted on the copper sample mount for controlling the sample's temperature a halogen lamp; a variac to control the lamp intensity.

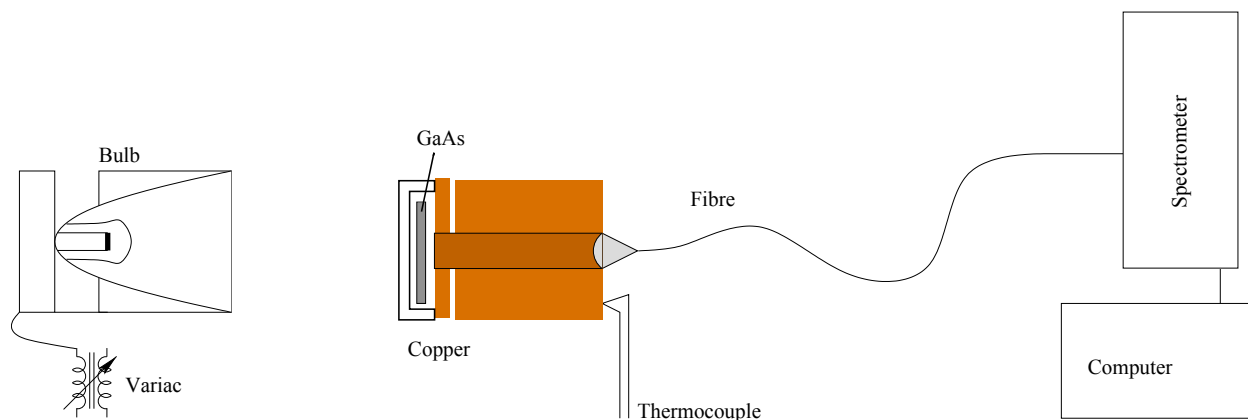


Figure 13.3: Schematic diagram of the apparatus.

Fig. 13.3 is a schematic diagram of the apparatus. The copper sample holder contains a hole in which the fibre optic's lens is mounted. Samples can be mounted to cover this hole. Samples are mounted in a copper mount and held in place with a plastic cover and four plastic screws. You should **not** need to remove the sample from its mount. To remove the sample from the spectrometer, simply unscrew the copper mount from the main housing.

13.5 Procedure

Note: it will be a good idea to consult some of the references given.

Task I — The Apparatus

1. Turn on the equipment. There is a desktop icon for the Ocean Optics spectrometer (SpectraSuite). You will want to look at the spectral response of the detector with and without incident light. Please save your data in `My_Documents\PHYS352\[Yourname]`. This can be set easily when saving your first spectrum.
2. What spectrum is detected without incoming light (i.e. dark signal)?
3. Qualitatively explain the spectrum obtained with incoming light. With directly incident light, what is the effect of the integration time? What is the effect of averaging over several curves?
4. There are 4 icons in the software labelled S, A, T, and I — explain what they stand for and how you can access the A, T and I functions. Hint: think of normalization and equations 13.6 to 13.8. Will normalization be required for your measurements? Why or why not?
5. Introduce a few material samples in front of the empty sample block (plastic, glass, hand,...) and look at the spectral response (you may need to adjust the integration time). Plot and explain your observations.
6. Explain the thermocouple circuit. What do you measure for room temperature?
7. What are the temperature precision and accuracy of this thermocouple? Are they temperature dependent? Hint: see part II of reference 8 or 9.

Task II — Bandgap of GaAs from Absorption Measurements

1. Measure the optical transmission through the GaAs sample (handle the sample with care and plastic tweezers). Extract its absorption coefficient. To measure the sample thickness, **do not** remove the sample from its holder, but measure the thickness of a second piece of GaAs provided.
2. For the sample provided, which has one unpolished side, scattering reduces the detected signal. How can you normalize its transmission to obtain reliable values of α ? Hint: consider what transmission you should expect for all values of α , which is wavelength dependent.
3. What is the bandgap of GaAs at room temperature? Is it what you expected? Which definition of the bandgap appears to give the best results? Why?
4. Repeat for different GaAs wafer temperatures. Does the temperature dependence behave as expected? Hint: refer to references 1 and 2.

13.6 References

1. Shane R. Johnson, *Optical Bandgap Thermometry In Molecular Beam Epitaxy*, Ph.D. thesis, UBC, 1995.
2. M. Beaudoin, A.J.G. DeVries, S.R. Johnson, H. Laman, and T. Tiedje, *Appl. Phys. Lett.* **70**, 3540 (1997).
3. See for instance: Charles Kittel, *Introduction to Solid State Physics* (Wiley, 2005).
4. K. Seeger, *Semiconductor Physics — An Introduction*, 8th Ed. (Springer-Verlag, 2002), particularly chapters 1 and 2 and sections 11-1 and 11-2.
5. For an advanced treatment (beyond the scope of this course) see: Neil W. Ashcroft and N. David Mermin, *Solid State Physics* (Saunders College, 1976).
6. To make semiconductors useful, impurities are incorporated (doped) into the crystal, in order to make them n-type (conduction by electrons in the conduction band) or p-type (conduction by “holes” or absence of electrons in the valence band). Consult references 1-2 for more information.
7. J.I. Pankove, *Phys. Rev.* **140**, A2059 (1965)
8. The PDF documents are named *Practical T meas part I...* and *Practical T meas part II...* and come from the Library Reference Edition CD.
9. *The Temperature Handbook*, <http://www.omega.com>

Experiment 14

Optical Pumping of Rubidium

14.1 Purpose

1. To become familiar with the occurrence and characteristics of optical pumping
2. To examine some atomic spectra, and understand atomic structure

14.2 Introduction

Optical pumping is a method of using photons to place or move atoms into a particular spin state. Sometimes this is referred to as spin polarizing a gas, as very efficient optical pumping can create a polarized sample, where all atoms are in the same spin state. This is useful, for example, in magnetic-resonance imaging, performing spectroscopy on a gas, or if one wanted to control the types of interactions that take place in an atomic ensemble. The techniques of modern optical pumping were introduced in the early 1950s, with a Nobel prize awarded in 1966 for the technique, and optical pumping is still widely used today in many modern physics labs.

14.3 Theory

The atom used in this experiment is Rubidium (an alkali metal) that has 37 protons and electrons. Like the other alkali metals, Rb has only a single valence electron, which lies in an s -orbital. Rb has two naturally occurring isotopes: ^{85}Rb and ^{87}Rb . While only ^{85}Rb is stable, the half-life of ^{87}Rb is over 49 billion years (for reference, the universe is estimated to be about 13.7 billion years old, as of the writing of this lab manual). You will investigate both isotopes in this lab.

In order to understand and investigate optical pumping, there are three main concepts that must be understood: 1) atomic structure, which will tell you which levels are involved in the optical pumping process, 2) photon absorption, which describes how photons interact with the Rb atoms, and 3) the polarization of light. This lab manual outlines each of these three topics, but it is strongly recommended that you look at some (or all) of the sources in the references section, and to read through the manual that comes with the apparatus.

Atomic Structure

Like many physical models, atomic structure starts with a fairly simple picture of the energy levels within an atom, and then makes small corrections to the model to account for additional terms or perturbations to the system. The key is that each successive correction or perturbation is on an energy scale that is much smaller than the energy scale of the unperturbed system.

Electronic Structure The starting point of atomic structure is the electronic configuration, where electrons fill orbital shells until all 37 electrons are placed:

$$1s^2 2s^2 2p^6 3s^2 3p^6 3d^{10} 4s^2 4p^6 5s^1 5p^0 \quad (14.1)$$

where the number represents n , the principal quantum number, and the letter represents ℓ , the electron orbital angular momentum. Each value of ℓ is represented by a number. That is, $\ell = 0$ is a s -orbital, $\ell = 1$ is a p -orbital, 2 is d , 3 is f , etc. You can remember this using the mnemonic *smart people don't fail geometry*. The $5p$ orbital represents the first available excited state for the electron. Since all the electrons in the inner shells are paired, Rb (and all the alkalis) can be modeled as though it was a simple hydrogenic system with a single valence electron.

Fine Structure One consideration that has not been included in the electronic structure model is that the electron itself has a spin, $S = 1/2$, and an associated magnetic dipole moment. This spin is important because it couples with the orbital angular momentum, L , and perturbs the energy of the system. Physically, in the frame of the electron, the positively charged nucleus appears to be moving, which induces a magnetic field. In turn, the electron spin interacts with the field, producing a (small) shift in energy. This additional term in the Hamiltonian has the form $\mathbf{L} \cdot \mathbf{S}$. We can define a new quantum number $\mathbf{J} = \mathbf{L} + \mathbf{S}$, where \mathbf{J} is the total angular momentum, and can take on values ranging from $L + S$ down to $|L - S|$ in integer steps, according to the rules of addition of angular momentum. Each state can be labelled by a new term symbol, $^{2S+1}L_J$ where S is the electron spin, L is the electron orbital and J is the total angular momentum. Since the ground state of Rb is a $5s$ state, $L = 0$ and therefore \mathbf{J} only takes on one value, $J = 1/2$. However, the first excited state is a $5p$ state, so $L = 1$ and \mathbf{J} can take on two values, either $J = 1/2$ or $J = 3/2$, see Figure 14.1. The transition from $^2S_{1/2} \rightarrow ^2P_{1/2}$ is called the D_1 transition, and from $^2S_{1/2} \rightarrow ^2P_{3/2}$ is called the D_2 transition. Although it is a little confusing, the S used in the term symbols which label the fine structure states correspond to the letter label for L (s,p,d,f etc.), and is distinct from the S in the $2S + 1$ term, which represents the electron spin. Note that the splitting between the two excited states is about 7 THz (we are giving the energy in frequency units, $E = h\nu$), which is small compared the energy difference between the $5s$ and $5p$ states, which is on the order of 380 THz.

Hyperfine Structure The nucleus has a spin as well, which is labeled with the quantum number I . Similar to fine structure, this nuclear spin couples with the total angular momentum, \mathbf{J} , which introduces a new term in the Hamiltonian that looks like $\mathbf{J} \cdot \mathbf{I}$. Likewise, we can define another new quantum number, $\mathbf{F} = \mathbf{J} + \mathbf{I}$, where \mathbf{F} can take on values ranging from $J + I$ down to $|J - I|$ in integer steps.

Up until this point, there hasn't been any distinction between the two different isotopes of Rb. Aside from a different number of neutrons, they also differ in the value of their nuclear spin. This means that each isotope has a different hyperfine structure. In the ground state, the splitting between hyperfine levels is on the order of a few GHz, and in the excited state the splitting is on the order of 100's of MHz, which is much smaller than the THz scale of fine structure splitting. You should work out the different hyperfine levels of Rb for yourself. As a check, Dan Steck has compiled an excellent reference document (see Section 14.5). In addition, the atomic structure for ^{87}Rb is shown in Figure 14.1.

Zeeman Effect In the absence of any external fields (for example, a magnetic field), each of the hyperfine levels is actually $2F + 1$ degenerate levels, which are labeled by M_F , the projection of \mathbf{F} along some quantization axis, where $-F \leq M_F \leq F$ in integer steps. An external magnetic field breaks this degeneracy as the magnetic dipole moment of the atom interacts with the magnetic field. In the case of a small magnetic field (if you are wondering what small means in this context

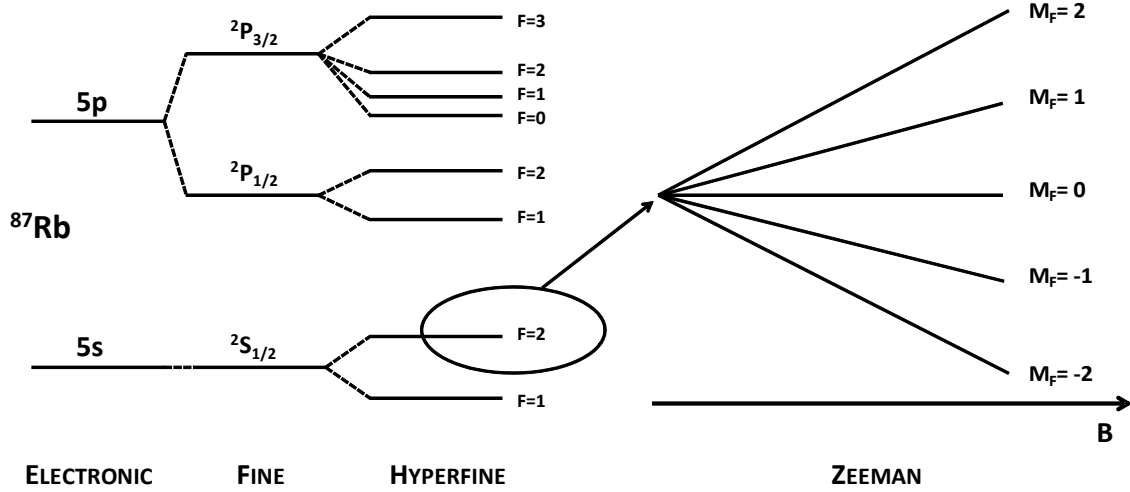


Figure 14.1: Atomic structure of ^{87}Rb ($I = 3/2$, showing electronic, fine and hyperfine structure. Also shown on the right is the small field Zeeman splitting as a function of magnetic field. Note that this sketch is not to scale.

- and you should be - keep reading... but you should do that anyway), the energy of each M_F level relative to energy in the absence of the magnetic field is,

$$E_Z = g_F \mu_B B M_F \quad (14.2)$$

where μ_B is the so-called Bohr magneton and,

$$g_F = g_J \frac{F(F+1) + J(J+1) - I(I+1)}{2F(F+1)} \quad (14.3)$$

where,

$$g_J = 1 + \frac{J(J+1) + S(S+1) - L(L+1)}{2J(J+1)} \quad (14.4)$$

Notice that for small (there's that word again) B the levels fan out with an equal spacing between adjacent M_F levels. Since the energy spacing increases with increasing magnetic field strength, you could conceivably make the Zeeman splitting as large as the hyperfine splitting (or bigger) if you applied a large enough field. This would break the assumption that each correction is small compared to the unperturbed system. To be clear: Eq. 14.2 is only valid when the magnetic field is small enough such that the Zeeman splitting is much less than the hyperfine splitting. You should work out approximately what field you would need to apply to break this condition, and keep this value in mind when you do this experiment. If you enter a regime where the magnetic field is not small (now you know what this means) then the energy difference between adjacent Zeeman levels will not be equal. You can investigate this effect in this lab.

Photon Absorption

If a photon incident on a Rb atom has the correct energy, such that the photon energy, $h\nu$, matches the energy difference between two atomic energy levels (and the lower energy level actually contains an electron), the atom can absorb the photon, and the electron is excited to the higher lying level.

However, there are particular rules which govern which transitions are allowed to occur. The most common type of transition is an electric dipole transition, which has the selection rules that,

$$\Delta F = 0, \pm 1 \quad \text{and} \quad \Delta M_F = 0, \pm 1 \quad (14.5)$$

with the exception that an electron in a $F = 0$ state cannot undergo a transition to another $F = 0$ state. The same selection rules apply to transitions between states with different L or different J quantum numbers.

In this lab, you might be able to imagine many different possible transitions that could occur, each a different energy scale. However, we only need to consider two. First, you will use optical light (in the near IR at 795 nm) to drive transitions on the D_1 line. Secondly, you will use an RF field with a frequency on the order of kHz or MHz. Since the splitting between different hyperfine levels (in the ground state) is on the order of several GHz, this radiation will only let you drive transitions where $\Delta F = 0$. That is, only between different Zeeman (M_F) levels, within the same hyperfine manifold. Whether the photon (either the optical or RF) drives a transition where $\Delta M_F = 0, +1, -1$ depends on the polarization of light.

Polarization

Consider an electric field vector (ie. light) travelling along the z-axis (in the positive direction). This electric field vector can have components along the x and y-axis, with a relative phase difference between the two components. There are three types of polarization we need to consider, and each type of polarization can drive transitions with specific ΔM_F values.

- **Linear Polarization** If the light is linearly polarized, the relative phase difference between the two components is zero. Light that is linear (π polarized) drives transitions where $\Delta M_F = 0$.
- **Right-Circular Polarization** If the light is RCP, the two components are equal in magnitude, with a relative phase of $\pi/2$, where the component along the x-axis lags behind the component along the y-axis. If you were to look at the electric field vector from the positive z-axis, it would trace out a helix in the clockwise direction (hence, right). RCP (σ^+ polarized) light will drive transitions where $\Delta M_F = 1$.
- **Left-Circular Polarization** If the light is LCP, the two components are equal in magnitude, with a relative phase of $\pi/2$, where the component along the y-axis lags behind the component along the x-axis. If you were to look at the electric field vector from the positive z-axis, it would trace out helix in the counterclockwise direction (hence, left). LCP (σ^- polarized) light will drive transitions where $\Delta M_F = -1$.

In the system in this experiment, the z-axis is defined by the quantization axis of the experiment. In this case, this is the direction of magnetic field, which is oriented along the direction of propagation of the light.

For optical pumping to work efficiently (see Section 14.3), the light needs to be either RCP or LCP. The light emitted from the Rb bulb used in this experiment does not have a well defined polarization. To polarize it, you will first pass it through a linear polarizer. Next, you pass it through a *quarter wave plate* (QWP). A QWP has two orthogonal axes, and is designed such that the index of refraction along one axis (the slow axis) will slow down the component of the electric

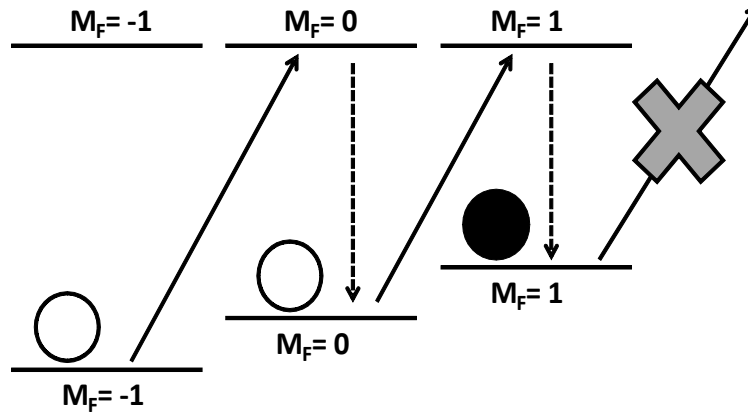


Figure 14.2: Cartoon diagram of optical pumping. In this example, both the ground (lower) and excited (upper) levels are $F = 1$ states. Solid lines represent absorption events with RCP light, where $\Delta M_F = 1$ and dashed lines represent the *average* decay event, where $\Delta M_F = 0$. Multiple absorption and decay events will lead the electrons to be pumped into the ground state with the largest M_F value. Notice that this final state is dark. That is, an electron cannot absorb any of the incident light because there is no excited state with $M_F = 2$.

field along that axis such that it exits the wave plate a quarter wave ($\pi/2$) out of phase relative to the electric field that transmitted along the other axis (the fast axis). This is exactly the phase shift we need to make our light LCP or RCP.

In this experiment, the optical light will either drive transitions with $\Delta M_F = +1$ or $\Delta M_F = -1$. It happens that the RF radiation is along an axis orthogonal to the magnetic field so it will always drive transitions with $\Delta M_F = \pm 1$. Of course, since the energy in the RF field is only large enough to drive transitions between different Zeeman levels, where $\Delta F = 0$, a transition with $\Delta M_F = 0$ wouldn't be very interesting, since the initial and final would be the same!

Optical Pumping

In this lab, we optically pump the Rb gas using the (optical) light driving the D_1 transition. That is, the light drives transitions between hyperfine levels in the $^2S_{1/2}$ manifold to another hyperfine level in the $^2P_{1/2}$ manifold (obeying, of course, the selection rules outlined above). The light will either drive transitions with $\Delta M_F = +1$ or -1 (depending on whether the light is RCP or LCP). However, when the electron decays from the excited state, the transition can have any of $\Delta M_F = 0, \pm 1$. This means that, *on average*, each decay event will have $\Delta M_F = 0$, while each absorption even will have (let's assume RCP light) $\Delta M_F = +1$. This will cause the electrons to be pumped to the ground state with the highest value of M_F (sometimes referred to as a stretched state), see Figure 14.2.

In a perfect experiment, all the atoms would end up in this final stretched state. In reality (and this lab) there are many other processes that act to undo the optical pumping (for example, collisions between Rb atoms can exchange angular momentum). Instead of putting all the atoms in the stretched state, the optical pumping light establishes a new equilibrium in the system where there are more atoms in the stretched state than there would be in the absence of the light.

The state that the electrons are optically pumped into should (ideally) be a dark state. That is, a state where the atom is no longer able to absorb a photon, even though the incident light has the right energy. If not, atoms in this state will continue to scatter light and possibly leave the state. How is it possible for a state to be dark? Selection rules! Go back to your sketch of the hyperfine levels in the ground and excited state for either isotope of Rb (and/or look at Figure 14.1) and see if you can find which state could be dark. Remember the selection rules that $\Delta F = 0, \pm 1$ and $\Delta M_F = +1$ or -1 depending on the polarization of the light.

In fact, since the state is dark, it creates the perfect signal to observe whether or not the sample is optically pumped. If more atoms are in the dark state, the more light is transmitted (i.e. not absorbed) in the cell. If fewer atoms are in the dark state, the less light is transmitted. Therefore, by measuring the intensity of the light after the cell, you can infer how well pumped the sample is.

Finally, the RF field drives transitions between different M_F states within the same hyperfine manifold (that is, within states with the same F). This field **can** drive transitions out of (and into) the dark state, which acts to reduce the number of atoms in the optically pumped dark state. In this experiment, you will set a particular frequency for the RF field, and vary the magnetic field strength inside the cell. At just the right magnetic field strength, the energy difference between Zeeman levels will equal the energy of the RF photons (see Eq. 14.2) and you will observe a loss of atoms from the dark state via a decrease in the optical light intensity transmitted through the cell.

14.4 Procedure

The details on how to run the experiment are well laid out in the manual for the apparatus that is found in the lab room. You should read the description of the experiment and apparatus in the manual carefully.

Task 1 - Measurement of the Nuclear Spins

Your goal is to measure the value of the nuclear spin (I) for both ^{85}Rb and ^{87}Rb . Recall, from Eq. 14.4 that the value of the nuclear spins influences the splitting of the Zeeman levels (as a function of magnetic field). You will measure the RF transition frequencies of each isotope as a function of magnetic field, from which you can infer g_F and I . This procedure roughly follows section 4B. **Low Field Resonances** in the experiment manual.

1. Turn on the apparatus and set the cell temperature to around 50°C . Although this needs to be the first thing you do when you want to run the experiment, it should also be the first thing you do when you get to the lab, because the Rb bulb and cell take a few minutes to warm up.
2. Install the optics in the experiment (see fig. 4A.1 of the experiment manual). You will need to install one plano-convex lens before the cell to collimate light from the Rb lamp and a second lens after the cell to focus the light onto a photodetector. You will also need to use a linear polarizer and a quarter wave plate to set the correct polarization of light before the cell. There is a second linear polarizer available that you can use before the detector to test how well you have set the circular polarization. You will also need to insert an interference filter before the cell, which ensures that only light that drives the D_1 transition enters the cell.

3. For this task, you will not need to use the Horizontal Field coils, so you should disconnect them so no current can run through them. You will only need to use the Horizontal Magnetic Field Sweep coils and Vertical Field coils. The “monitor” output for the sweep field should be connected to CH1 of the oscilloscope, and the detector amplitude output should be connected to CH2. It’s best if you trigger on CH1 (the magnetic field sweep) for this experiment.
4. In order to determine the current running through the sweep coils, there is a monitor output on the front panel of the apparatus. Since the current passes through a one ohm resistor, the voltage measured across the output is equal to the current in the coils. The coils are arranged in a Helmholtz configuration, and the field at the atoms is (approximately) given by:

$$B(\text{Gauss}) = 8.991 \times 10^{-3} \left(\frac{IN}{R} \right) \quad (14.6)$$

where I is the current, N is the number of turns of wire that make up the coils, and R is the mean radius. You can find the coil specifications in the experiment manual.

5. There is some background magnetic field present in the experiment. You need to minimize and measure the size of this field before you can take useful data. With no RF field applied from the function generator, vary the sweep horizontal magnetic field. (NB The switch sticks; you may have to toggle it to make sure it sweeps). You should see a dip occur in the light intensity, which occurs because of the Zeeman levels are degenerate (which acts to scramble the Zeeman states). Adjust the vertical field coils to minimize the width of this dip, and write down the current in the horizontal sweep field at the location of the dip. You will need this later to properly calibrate the magnetic field.
6. Apply an RF signal (say 150 kHz) to the RF coils, and set its amplitude to whatever value you want (just don’t choose the wrong value). Slowly sweep the horizontal magnetic field using the sweep coils searching for dips in the light intensity, which represent Zeeman resonances. Measure the current at which each resonance occurs. Once you have found a transition, adjust the RF amplitude to a value that optimizes the signal. For one choice of RF frequency, you should see two dips. Why? It’s also possible you might see some other much weaker dips. If so, turn down the RF amplitude (and think about why you saw these extra dips). If you can’t see any extra dips, try turning up the RF amplitude until you do (and think about why you saw these extra dips).
7. Measure the transition frequencies of each isotope as a function of the sweep coil current. You should take at least four or five points for each isotope.
8. Plot the transition frequency as a function of magnetic field. You will need to convert your recorded sweep coil current for each frequency to a magnetic field strength (be sure to account for the residual field you measured previously). Fit your data to extract g_F and I . What is the relationship between the transition frequency and the magnetic field? Is this what you expect? Why or why not?
9. Would this experiment have worked if you used a optical filter that passed light that drove the D_2 transition instead of the D_1 transition? Why or why not?

Task 2 - Choose Your Own Adventure

There are many other experiments that are possible on this apparatus. Take a look through Chapter 4 of the TeachSpin manual for the experiment, and do one of the other experiments. Some options include:

1. Rb Absorption as a function of cell temperature
2. Quadratic Zeeman effect
3. Transient / Dynamical effects

If you aren't sure which one sounds interesting, ask the instructor or TA and we can help you pick.

14.5 References

- 1 Eric D. Black, *Physics 77 Lab Manual: Optical Pumping*, available online <http://www.pma.caltech.edu/~ph77/labs/optical-pumping.pdf>
- 2 Daniel A. Steck, *Rubidium 85 D Line Data*, available online at <http://steck.us/alkalidata> (revision 2.1.5, 19 September 2012)
- 3 Daniel A. Steck, *Rubidium 87 D Line Data*, available online at <http://steck.us/alkalidata> (revision 2.1.5, 19 September 2012)
- 4 Daniel A. Steck, *Classical and Modern Optics*, available online at <http://steck.us/teaching> (revision 1.5.0, 13 June 2013)
- 5 David J. Griffiths, *Introduction to Quantum Mechanics*, 2nd ed. Pearson Prentice Hall, 2005.
- 6 Teachspin, *Optical Pumping of Rubidium OP1-A: Guide to the Experiment*, 2002.

Experiment 15

Water Waves

15.1 Purpose

To observe and measure the dispersive properties of water waves.

15.2 Theory

Consider an open water tank:

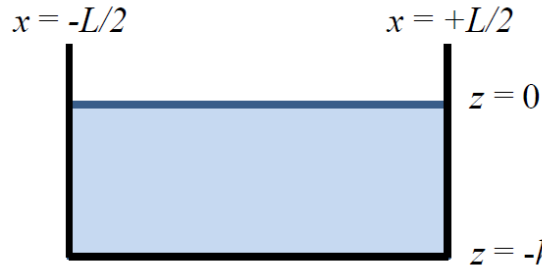


Figure 15.1: A rectangular open water tank.

Ignore for now motion in and out of the plane of the paper. The general form for the velocity potential ϕ for a travelling wave with 2D motion in this case is (see Landau and Lifshitz p.39):

$$\phi = [Ae^{kz} + Be^{-kz}]e^{i(kx \pm \omega t)} \quad (15.1)$$

Here k is the wavenumber ($2\pi/\lambda$). The particle velocities ($v = \nabla\phi$) are given by:

$$v_z = k[Ae^{kz} - Be^{-kz}]e^{i(kx \pm \omega t)} \quad (15.2)$$

$$v_x = ik[Ae^{kz} + Be^{-kz}]e^{i(kx \pm \omega t)} \quad (15.3)$$

For water in a tank, there are three boundary conditions:

1. The gauge pressure at the surface should be zero. Starting with the form of the velocity potential for water waves, this leads to:

$$\frac{\partial\phi}{\partial z} + \frac{1}{g} \left(\frac{\partial^2\phi}{\partial t^2} \right)_{z=0} = 0 \quad (15.4)$$

2. The vertical velocity at the bottom should be zero.

$$\left(\frac{\partial\phi}{\partial z} \right)_{z=-h} = 0 \quad (15.5)$$

3. The horizontal velocity at the two sides should be zero.

$$\left(\frac{\partial\phi}{\partial x}\right)_{x=\pm L/2} = 0 \quad (15.6)$$

Applying the first and second conditions to the general form of ϕ yields the dispersion relation:

$$\omega^2 = gk \tanh(kh) \quad (15.7)$$

Note that unlike light and sound, ω is not proportional to k , and so the wave speed is not constant, the phase velocity v_p differs from the group velocity v_g . Water waves are *dispersive*.

$$v_p = \omega/k; \quad v_g = d\omega/dk \quad (15.8)$$

Applying the second and third conditions gives a general solution for the wave motion at the surface and at depth. This formalism contains explanations for:

- How to go about extracting useful power out of ocean waves
- The complicated time-varying patterns seen in waves behind water craft (from ducks to supertankers)
- The awesome speed and destructive power of tsunamis

See:

- http://labman.phys.utk.edu/phys221core/modules/m12/Water_waves.html
- [https://en.wikipedia.org/wiki/Dispersion_\(water_waves\)](https://en.wikipedia.org/wiki/Dispersion_(water_waves))
- Simulation of the Indian Ocean tsunami of 2004:
<https://www.youtube.com/watch?v=YReIrrr0eqY>

Standing Waves

The physical tanks you have in the laboratory are small (50 cm \times 15 cm \times 5 cm) and the walls are highly reflective, so the opportunities for measuring travelling waves are limited. Mostly we will see standing waves.

For standing waves in the tank, we can assume that the amplitude of left-going travelling waves is the same as that for right-going waves. Hence the restrictions on frequency are the same as for acoustic waves in the tube open (or closed) at both ends:

$$kL = n\pi; \quad n = 1, 2, 3 \quad (15.9)$$

Apparatus

- Water tank (50 cm 15 cm 5 cm)
- Wave-maker with electromagnetically activated paddle
- Two QRD1113 position sensors
- DAQ system to read out the position sensors
- Basic DAQ code BareBonesDaq.m

Procedure

Fill the tank to a depth of about 10 cm. Position the two sensors somewhere along the length, with the tips a couple of mm above the water surface. The sensors will not be damaged but will not work if they are wet. Their output depends (not very linearly: look up the spec sheet) on the distance to the water surface.

The code BareBonesDAQ.m will read out the two sensors for however long you decide. It will display output vs. time graphs. Configure the code to produce frequency spectra (fast fourier transforms, or FFTs) of sensor outputs.

Use the paddle to make a wave, take the data, and find the frequencies of as many oscillation modes as you can see. A single pulse is sufficient to excite a variety of standing waves (a pulse of width Δt contains all frequencies up to $f = 1/\Delta t$)

Do it again for different depths.

Use these frequencies to make a plot of water wave speed (phase or group?) as a function of wavelength and depth.

Include in your report:

1. Properly labelled graphs with legends showing group and phase velocities for travelling water waves with depths of 1 cm, 10 cm and 100 cm. Put all the group velocities on one plot; ditto for the phase velocities.
2. Properly labelled graph with a legend showing the frequencies of the first ten standing waves, as a function of depth in a 50 cm long tank.

Bibliography

Landau and Lifshitz, Fluid Mechanics (available at <https://archive.org/details/FluidMechanics>)

Experiment 16

Acoustic Radiation

16.1 Purpose

To familiarize you with the coupling between mechanical vibration and sound radiation, and with the concepts of near- and far-field radiation.

16.2 Introduction

A tuning fork provides a simple example of vibrational resonance, and also of complex radiation patterns. The moving tines of the tuning fork produce high-pressure regions ahead and low-pressure behind. As there are two of them moving against each, there is plainly going to be a lot of interference going on, and it will be distance, angle, and frequency dependent. This is what you will investigate. Read Daniel Russell's paper listed in the bibliography below. In the process of doing this experiment, you will also learn how to establish and measure resonance behaviour using sweeping techniques and an accelerometer.

Apparatus

- Tuning fork, mounted on a stand with an electromagnetic shaker
- Small accelerometer
- Microphones mounted on a rail inside an acoustic isolation box
- Measurement Computing DAQ system, run by MATLAB code (start with BareBonesDaq.m)

NB The stand is heavy; please do not drop it, and especially not on your foot.

Resonance

1. The accelerometer consists of a micro-machined capacitor with a small mass on a flexible arm. The mass moves when undergoing acceleration and as a result, the capacitance changes. Internal circuitry on the chip produces a voltage proportional to the acceleration. Unlike some devices, it will measure a constant acceleration, producing a constant output. This makes calibration very easy, by turning it upside down in the Earth's gravitational field.

Plug the accelerometer into the DAQ box. To read this port, you will need to modify the code BareBonesDAQ.m (# 0).

Calibrate your accelerometer, and report its sensitivity in $V/(m/s^2)$.

2. Set up the electromagnet such that it excites the supermagnet on the side of the tuning fork in an optimal way, by adjusting the relative position of fork and electromagnet. Try not to knock

the supermagnet off. Make sure the fork is tight down on its base.

3. Using the function generator, find the fundamental resonance. Measure the amplitude of the acceleration of the accelerometer. Convert this number to a displacement amplitude of the top of the fork tines.

Angular distribution

1. Use the measured acceleration both to keep the fork at resonance (as it tends to wander off), and also to normalize the microphone measurements.

2. Set microphone 1 close (how close?) to the fork (near field). Set microphone 2 as far away as you can while still seeing a distinct signal from the fork (far field). Test at various angles of the fork. Make sure you are not saturating the DAQ system.

3. Measure the amplitude of sound versus angle of the tuning fork (as measured on the turntable). Make sure to rotate through as large an arc as the apparatus will allow. Choose angle steps such that the minima and maxima are clearly seen. Make sure to note each microphone's value of kr .

4. Plot angular distributions for both microphones on radar plots. Compare your results with the formulae in Russell's paper. Plot data and theory together. Note that Russell plots relative SPL in dB. In this case relative means:

$$L_p = 20 \log_{10} \left(\frac{p}{p_{max}} \right) \quad (16.1)$$

where p_{max} is the maximum amplitude in the angular distribution (defined to be 0 dB).

Bibliography

Daniel Russell, “**On the sound field radiated by a tuning fork**”, Am. J. Phys. 68 (2000) pp.1139-1145

Available at <http://www.acs.psu.edu/drussell/Publications/TuningFork.pdf>

Experiment 17

Acoustic Impedance

17.1 Purpose

To gain facility with the impedance tube, the standard method of measuring the acoustic properties of surfaces.

17.2 Introduction

See Rossing and Fletcher sections 6.2 and 8.3.

Acoustic impedance is the ratio of acoustic pressure to acoustic velocity or volume flow - which of these you choose depends on the application. There is a straightforward analogy here between acoustic and electrical impedance: pressure/voltage, velocity or flow/current. The expression of Newton's Second Law in the context of an acoustic wave relates pressure p to velocity u :

$$\rho \frac{\partial u}{\partial t} = -\nabla p \quad (17.1)$$

In the case of a plane wave with the following forms, the impedance z has a simple form:

$$p = p_0 e^{j(kx - \omega t)}; \quad u = u_0 e^{j(kx - \omega t)}; \quad z = \frac{p}{u} = \rho c \quad (17.2)$$

Note that the field of acoustics, by convention, uses the engineer's notation for the square root of minus one (j). For a plane wave in a free space pressure and velocity are in phase and their ratio is the real product of the density ρ and the speed of sound $c = \omega/k$. For spherical waves and waves in a tube with terminations, the impedance is complex and varies in space and time.

Consider a rigid hollow tube with a sound source at one end, a termination of some sort at the other, with the acoustic pressure measured by microphones at two points along its length (M1 and M2).

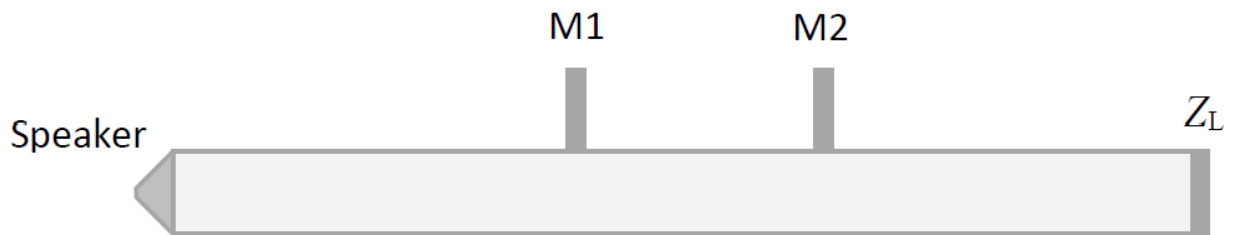


Figure 17.1: General arrangement of simple acoustic impedance tube.

The inner radius of the tube is a , the length L , and the two microphones are mounted at distances l_1 and l_2 from a speaker sealed in one end. At the other end is a sample of unknown acoustical impedance Z_L . In this case it makes sense to talk about impedance in terms of pressure

divided by volume flow rather than velocity. Thus the characteristic impedance of the tube is given by:

$$Z_0 = \frac{c}{S}, \quad S = \pi a^2. \quad (17.3)$$

If the speaker is delivering an acoustic signal of frequency $f = \omega/2\pi$ (whose wavelength is much longer than the radius of the tube) we can assume the pressure is a result of forward and backward-going plane waves.

$$p(x, t) = [Ae^{-jkx} + Be^{jkx}]e^{j\omega t} \quad (17.4)$$

Then the acoustic flow U in the tube can be written in terms Z_0 :

$$U(x, t) = (Ae^{-jkx} - Be^{jkx})/Z_0 \quad (17.5)$$

With a bit of algebra, and the assumption that the speaker end acts like a closed pipe we can find the reflection coefficient $r = B/A$ in terms of the ratio of the two microphone pressure signals, $H_{12} = p_2/p_1$, and two lengths $\Delta L = L - l_1$ and $s = l_2 - l_1$.

$$r = \frac{H_{12} - e^{-jks}}{e^{jks} - H_{12}} e^{2jk\Delta L} \quad (17.6)$$

$$Z_L = Z_0 \frac{1 + r}{1 - r} \quad (17.7)$$

To test the assumption about the speaker (which is actually delivering the acoustic signal through many small holes in a thick piece of brass), we can take data with a brass plug in the load end, and with the load end open. The brass plug is easy to model:

$$Z_L \gg Z_0, \quad r \approx 1 \quad (17.8)$$

The open end is less straightforward - p is small at this end but not zero. The standing wave does not stop here, it radiates to the outside world. We need an expression for the *radiation impedance* of the unflanged end of a pipe (why do you think a flanged pipe would be any different? See Rossing and Fletcher):

$$Z_L/Z_0 \approx 0.25(ka)^2 + 0.61jka \quad (ka \ll 1) \quad (17.9)$$

Otherwise, one can put in a material sample (architectural material, say) and measure its acoustic absorbing and reflecting qualities. Note there will be a change in ΔL when you insert a sample.

17.3 Equipment and Tasks

- Brass impedance tube with four electret microphones, a speaker and brass terminator
- Function generator
- Measurement Computing ADC
- DAQ computer
- Basic DAQ code BareBonesDaq.m

Use DAQ code to take sweep data with the microphones with the following end conditions:

- Brass termination
- Open end (unflanged)
- Various pieces of foam

The analysis above is predicated on two microphones being identical. You have four microphones that are not in reality identical; this makes a nice challenge and an opportunity for creativity. You will need to calibrate the microphones against each other, both in amplitude and phase (only relative amplitude and relative phase matter, as you don't know what is coming out of the speaker). Then make plots of H_{12} , Z_L/Z_0 and r (magnitude and phase, comparing data and theory for the impedances you know (brass termination, unflanged open pipe) for pairs of microphones.

When you feel confident you understand the system, measure materials whose impedance you don't know.

Bibliography

T. D. Rossing and N. Fletcher, **“Principles of Vibration and Sound”**, (Springer) 1994.